Dissertation
submitted to the
Combined Faculties for the Natural Sciences and for Mathematics
of the Ruperto-Carola University of Heidelberg, Germany
for the degree of
Doctor of Natural Sciences

presented by
Dipl.-Phys. Benedict von Harling
born in Celle
Oral examination: 16th October 2008

Throat Cosmology

Referees: **Prof. Dr. Arthur Hebecker**
Prof. Dr. Michael G. Schmidt

Throat-Kosmologie — Zusammenfassung: In dieser Arbeit untersuchen wir „Throats" im frühen, heißen Universum. Throats sind ein häufiges Merkmal in der „Landscape" der Typ-IIB-Stringtheorie. Wenn ein Throat während der kosmologischen Entwicklung aufgeheizt ist, wird nach und nach Energie zu anderen Throats oder dem Standardmodell transferiert. Wir berechnen die Transferrate von Wärmeenergie und die Zerfallsrate von im Throat lokalisierten Kaluza-Klein-Moden in einem zehndimensionalen Model. Dazu benutzen wir die duale Beschreibung der Throats durch Eichtheorien. Wir diskutieren Modifikationen der Zerfallsrate, die in Flusskompaktifizierungen und für Klebanov-Strassler-Throats auftreten, und betonen die Rolle von tachyonischen Skalaren in solchen Throats für die Vermittlung von Zerfällen von Kaluza-Klein-Moden. Unsere Resultate sind auch anwendbar auf den Energietransfer vom aufgeheizten Standardmodell zu Throats. Wir bestimmen die daraus resultierende derzeitige Energiedichte in Throats in Abhängigkeit von den Infrarotskalen der Throats und der „Reheating-Temperatur". Die Kaluza-Klein-Moden in den Throats zerfallen in andere Sektoren mit einer stark unterdrückten Rate. Falls ihre Lebensdauer länger als das Alter des Universums ist, sind sie ein interessanter Kandidat für die Dunkle Materie. Wir zeigen, daß Throats mit Infrarotskalen im Bereich von 10^5 GeV bis 10^{10} GeV die Dunkle Materie erklären können, wenn die Reheating-Temperatur $10^{10} - 10^{11}$ GeV war. Wir finden zahlreiche Szenarien, in denen diese Form der Dunklen Materie ausreichend langlebig ist, aber in denen Zerfälle zum Standardmodell trotzdem durch Beobachtung von Gammastrahlung entdeckt werden können.

Throat Cosmology — Abstract: In this thesis, we study throats in the early, hot universe. Throats are a common feature of the landscape of type IIB string theory. If a throat is heated during cosmological evolution, energy is subsequently transferred to other throats and to the standard model. We calculate the heat transfer rate and the decay rate of throat-localized Kaluza-Klein states in a ten-dimensional model. For the calculation, we employ the dual description of the throats in terms of gauge theories. We discuss modifications of the decay rate which arise in flux compactifications and for Klebanov-Strassler throats and emphasize the role of tachyonic scalars in such throats in mediating decays of Kaluza-Klein modes. Our results are also applicable to the energy transfer from the heated standard model to throats. We determine the resulting energy density in throats at our epoch in dependence of their infrared scales and of the reheating temperature. The Kaluza-Klein modes in the throats decay to other sectors with a highly suppressed rate. If their lifetime is longer than the age of the universe, they are an interesting dark matter candidate. We show that, if the reheating temperature was $10^{10} - 10^{11}$ GeV, throats with infrared scales in the range of 10^5 GeV to 10^{10} GeV can account for the observed dark matter. We identify several scenarios where this type of dark matter is sufficiently stable but where decays to the standard model can be discovered via gamma-ray observations.

Contents

Chapter 1

Introduction

1.1 String theory, flux and throats

The standard model of particle physics is remarkably successful in that it correctly predicts the outcome of a large number of experiments. It is a certain type of quantum field theory, a theoretical framework which results from the unification of quantum mechanics and special relativity. Yet there are several reasons to believe that this theory is only an approximation which is valid at comparatively low energies and that it has to be replaced by a more fundamental theory at energies larger than that. In particular, there is a combination of the velocity of light, Newton's constant and Planck's constant which has the dimension of energy. For processes with this Planck energy, gravity can no longer be neglected in standard model interactions and a theory of quantum gravity is required. Such a unification of general relativity with quantum field theory is still a major open issue in fundamental physics.

A candidate for this unification is string theory in which the pointlike particles of quantum field theory are replaced by tiny one-dimensional objects. When viewed from large distances or, equivalently, at small energies, these strings behave like pointlike particles. String theory reduces to quantum field theory at such low energies. For processes at energies close to the Planck scale, on the other hand, the fact that strings have a finite extent becomes important and quantum field theory is no longer a good approximation.

The quantization of a classical string theory leads to a spectrum of particles with various properties which correspond to different excitations of the string. In particular, the spectrum contains a particle which behaves like the graviton, the quantum of the gravitational field. String theory therefore provides a quantum theory of gravity. In addition, gauge fields and particles which are charged under the corresponding gauge groups appear naturally in the spectra of quantized strings. For the appropriate gauge group and particle spectrum, the standard model could thus follow as the low-energy limit of a particular string theory. Since the graviton is contained in the same spectrum, such a string realization of the standard model would mean a unification of gravity with

the other known interactions. However, a completely satisfactory realization has not been constructed so far.

The consistent quantization of string theory requires additional space dimensions. To explain why these extra dimensions have escaped detection so far, one assumes that they are curled up into a tiny space. The extra dimensions are said to be compactified. At large distances or, equivalently, low energies, our world then still seems to have only three space dimensions. Although such extra dimensions are in principle an interesting model building tool, the different ways in which they can be curled up lead to a large variety of low-energy theories which follow from a given string theory.

This variety is even larger since additional choices can be made which influence the low-energy theory. In certain string theories, open strings are confined to hyperplanes in the higher-dimensional space. These hyperplanes are called Dp-branes, where p refers to the number of space dimensions in which the plane is extended. After quantization of the open strings, one finds a supersymmetric gauge theory which lives on the world-volume of the D-brane. There are various possibilities to embed these objects into a given compactification. The particular embedding of the D-branes determines the gauge theory which lives on their world-volume. In particular, it may be possible to realize the standard model on D-branes. On the other hand, there is a large number of other gauge theories which can be obtained in that way.

The spectrum of string theories contains differential form fields which are generalizations of the Maxwell field of electrodynamics. The D-branes act as sources for these form fields and can therefore be viewed as higher-dimensional generalizations of the pointlike sources of electrodynamics. The latter sources lead to electric flux through a sphere which surrounds them. Similarly, in the aforementioned embeddings into a compactification, the D-branes source form field flux which threads certain compact submanifolds or cycles in the compact space. This flux can, however, be switched on even in absence of any D-brane sources. Due to the nontrivial topology of the compact space, such a configuration remains stable. This is similar to the Dirac monopole that can be viewed as a configuration of magnetic flux that is topologically stable because a point has been removed from space. Furthermore, as is the case for the Dirac monopole, the form field flux is quantized.

Typical compact spaces that one considers have a large number of cycles. Through each of theses cycles, one can have a certain number of flux. Combined with the different possibilities for the compact space and the number and embeddings of D-branes, this leads to a huge number of compactified solutions of string theory. There are probably by far more vacua in this so-called landscape than there are particles in the visible universe. In principle, there are only five consistent versions of string theory without any tunable parameters but the landscape unfortunately introduces a large indeterminacy. In particular, there may be many solutions which look like the standard model at low energies but which are very different from each other at high energies.

Flux is, on the other hand, interesting for model-building purposes. The size of cycles in a given compact space is initially unfixed. From a four-dimensional viewpoint, these unfixed cycles lead to massless scalar fields which are called moduli. The existence

of such fields, however, would violate the equivalence principle in a measurable way and is therefore excluded. The flux through a given cycle, on the other hand, has a certain energy density. From a four-dimensional viewpoint, the potential energy will therefore depend on the sizes of the cycles. Thus, flux can lead to their stabilization. The moduli then become massive and are no longer a phenomenological problem.

Since it has an energy density, the flux backreacts on the geometry. This backreaction can lead to so-called warped regions in the compact space. In these regions, there is a strong gravitational potential along certain directions. As is well known from general relativity, the deeper in such a gravitational potential a given physical process takes place, the more does it appear redshifted for a fixed observer. Due to this fact, large hierarchies can be generated in string compactifications with flux.

More precisely, as Randall and Sundrum have shown [1, 2], the four-dimensional graviton can be localized in a warped geometry. This graviton is a Kaluza-Klein mode of the higher-dimensional graviton and it therefore has a certain profile along the compactified dimensions. Randall and Sundrum considered the five-dimensional anti-de-Sitter space. At fixed positions along the fifth dimension of this spacetime, the geometry is four-dimensional Minkowski space. The prefactor of the Minkowski metric, however, depends exponentially on the position along the fifth dimension. Accordingly, energy scales are exponentially redshifted or blueshifted if one moves along this extra dimension. Randall and Sundrum chopped this space off on two sides in such a way that they obtained a finite slice of anti-de-Sitter space along the fifth dimension. The boundaries of this slice are two copies of Minkowski space which are called the ultraviolet brane and the infrared brane[1], respectively. Remarkably, the profile of the four-dimensional graviton in this geometry turns out to be localized near the ultraviolet brane. Gravity is therefore blueshifted compared to processes which are localized towards the infrared brane. This fact allows for the generation of large hierarchies relative to the Planck scale. In particular, if the standard model is realized on the infrared brane and the redshift between the two branes corresponds to the hierarchy between the Planck scale and the electroweak scale, this setup is a solution to the hierarchy problem of the standard model.[2]

It was shown by Giddings, Kachru and Polchinski [3] that the Randall-Sundrum model can be realized in flux compactifications of type IIB string theory. The backreaction of the flux on the geometry can lead to the formation of a so-called Klebanov-Strassler throat [4] which plays the role of the slice of anti-de-Sitter space in the Randall-Sundrum model. The geometry of this warped region is smoothly terminated in the infrared and thereby provides a realization of the infrared brane in the Randall-Sundrum model. Furthermore, in the compactification proposed by Giddings et al., the ultraviolet part of the Klebanov-Strassler throat is smoothly embedded into the compact space. The unwarped part of the compact space thus plays the role of the ultraviolet brane in the Randall-Sundrum model.

[1] These branes should not be confused with D-branes from string theory. Both types of branes have in common that they are hyperplanes in a higher-dimensional space.

[2] In the setup that we have described, this is actually not yet the case. A mechanism is needed which stabilizes this geometry without too much fine-tuning. Such mechanisms are known.

1.2 String theory and cosmology

It is expected that, in most vacua in the string theory landscape, the strings are only slightly larger than the four-dimensional Planck length.[3] The energies, which are necessary to resolve this length scale and thus to test string theory directly are many orders of magnitude larger than the energies achieved in accelerators so far. It is therefore impossible to test string theory directly in the near future and it may in fact never be possible.

It is thus important to conceive other, indirect tests of string theory. Since rather high energies have been reached in the early universe, it is natural to consider cosmology for this purpose. String physics may have led to observable signatures in several ways. As is well known, many observations in cosmology imply a phase of inflation shortly after the big bang. A possible string realization of such a phase is by means of two D-branes which move slowly towards each other. Another realization employs moduli with a sufficiently shallow potential. These inflationary mechanisms lead to certain predictions for the anisotropies in the cosmic microwave background and can thus be tested by experiments. However, tests of this kind have to be interpreted carefully since in most cases other and in particular field-theoretic realizations lead to similar signatures.

The energy density of the universe becomes extremely diluted during inflation and the universe has to be reheated when inflation ends. Relics like topological defects may be produced at this stage. For instance, during reheating after brane-antibrane inflation in a Klebanov-Strassler throat, a network of cosmic strings is formed. These cosmic strings influence the cosmic microwave background and may in addition be detected by gravitational wave experiments. Note, however, that the detection of cosmic strings would again be no clear signal of string theory since they can also arise in field theories.

Other relics like heavy particles may be produced by the reheating mechanism and by thermal reactions in the hot standard model plasma. For instance, Kaluza-Klein modes which are localized in a throat can be sufficiently light to be produced during reheating. As we have discussed, energy scales of processes which are localized in warped regions are redshifted. Similarly, Kaluza-Klein modes whose wave functions are localized in a throat have redshifted and thus rather light masses. The decay of relics which are produced in that way to standard model fields at later stages of the cosmological evolution may have led to observable signatures. On the other hand, if the relics are sufficiently stable, they can provide a new explanation of the observed dark matter.

1.3 Throats in the early universe

A Klebanov-Strassler throat can be formed if flux threads the cycles of a so-called conifold region (more precisely, of a deformed conifold) in a compact Calabi-Yau space.

[3] Exceptions are compactifications with a large volume and setups in which the standard model is localized in a strongly warped region. String effects become important at much lower energies in these setups.

It is expected that typical Calabi-Yaus can have a large number of these conifold regions. In the landscape of type IIB string theory vacua, flux is distributed over the cycles of the Calabi-Yau in various ways. It is then not surprising that in many cases the backreaction of the flux leads to a Klebanov-Strassler throat. These throats are indeed expected to be a common feature of the type IIB landscape. It is therefore interesting to consider possible observable consequences of throats in cosmology.

In the early, hot universe, these throats may have been heated to a certain temperature. If the temperature of a Klebanov-Strassler throat is larger than a certain critical energy scale, the backreaction of the thermal plasma on the geometry can no longer be neglected and leads to the formation of a black hole horizon which replaces the infrared end of the throat. Such a black hole horizon emits Hawking radiation. Due to the warping of the Klebanov-Strassler throat, this radiation has to tunnel through an effective energy barrier before it can reach the unwarped part of the compact space or other throats. Nevertheless, energy will be transferred to other throats with a certain rate. This heat transfer rate is an important quantity for the cosmology of throats.

In the first part of this thesis, based on our publication [5] (with Arthur Hebecker and Tatsuya Noguchi), we calculate this rate in a simple setup: Two throats with geometry $\mathrm{AdS}_5 \times \mathrm{S}^5$ which are embedded into a six-dimensional torus. As opposed to a Klebanov-Strassler throat, these throats are infinite in the infrared direction. If a throat of this type is heated, the backreaction of the thermal plasma leads to an AdS-Schwarzschild geometry. The heat transfer rate from such a heated throat to another throat is determined by the tunneling probability of the Hawking radiation. However, to determine this probability, we have to solve a multi-dimensional tunneling problem. Since this is quite difficult, we choose a different approach.

Consider a stack with a large number of D3-branes which is embedded into flat ten-dimensional space. The D3-branes have a certain energy density and can therefore backreact on the geometry. Taking this backreaction into account leads to a background solution of type IIB supergravity which is known as a black three-brane. Close to this object, the geometry is deformed to $\mathrm{AdS}_5 \times \mathrm{S}^5$, whereas far away it smoothly goes over to flat space. The crucial point is that, in this description, the D3-brane stack has disappeared and is replaced by a curved geometry. The black three-brane is therefore an *alternative* description of the D3-brane stack in flat space. This correspondence is the very basis of the AdS/CFT duality: By taking the low-energy limit in both descriptions, one is led to a duality between string theory in the $\mathrm{AdS}_5 \times \mathrm{S}^5$ region of the black three-brane and the world-volume theory, a $\mathrm{U}(N)$ gauge theory with $\mathcal{N} = 4$ supersymmetry, on the D3-brane stack.

In order to test the correspondence between a black three-brane and a D3-brane stack, one can probe both objects with particles and compare the corresponding absorption cross sections. Due to the warping, there is again an effective energy barrier which separates the throat region from the asymptotically flat region of a black three-brane. The absorption cross section of a particle, which is incident on the brane from the asymptotically flat region, is determined by the corresponding tunneling probability. The world-volume theory on the D3-brane stack, on the other hand, couples to

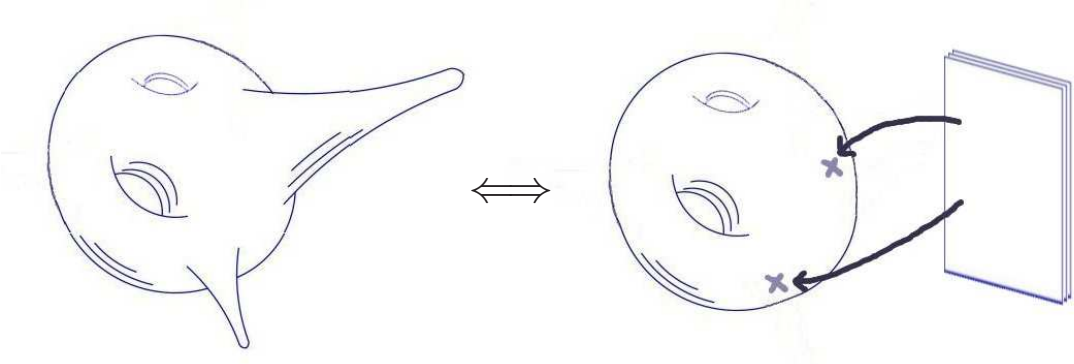

Figure 1.1: *Warped regions or throats in a compact space can equivalently be described by D-brane stacks. The four-dimensional world-volume of these D-branes is aligned along the four uncompactified dimensions. The D-branes are therefore pointlike in the extra-dimensional compact space.*

supergravity in the embedding flat space. The absorption of a particle by a D3-brane stack is due to these couplings. The corresponding calculations are particularly simple for the absorption of a dilaton. Remarkably, the resulting absorption cross sections by a D3-brane stack and by a black three-brane agree exactly.[4]

Heat transfer between two throats is due to tunneling and absorption of Hawking radiation. Since the absorption cross sections agree, we can replace the two $\mathrm{AdS}_5 \times \mathrm{S}^5$ throats in our setup by two equivalent D3-brane stacks. In particular, the heated throat is replaced by a stack with a heated world-volume gauge theory. Both stacks are coupled to each other by supergravity fields in the embedding torus. If we perform a Kaluza-Klein expansion of these supergravity fields, we obtain a purely four-dimensional description of our setup: A heated gauge theory which is coupled to another gauge theory by a tower of Kaluza-Klein modes. This four-dimensional description is much easier to analyse than the initial ten-dimensional setup with two throats in a torus. The heat transfer rate between the two throats is the same as the corresponding rate between the two gauge theories. The calculation of the latter is a straightforward exercise in quantum field theory.

A Klebanov-Strassler throat can be understood as the result of the backreaction of D3-branes and fractional D3-branes which are placed on a conifold singularity. Such a throat can therefore equivalently be described by a D-brane stack (cf. Fig. 1.1). In this description, the supergravity dynamics in the throat region is replaced by the dynamics of the world-volume gauge theory. We will correspondingly refer to these two descriptions as the gravity picture and the gauge theory picture, respectively.

[4]It turns out that, if the geometry due to the backreaction is weakly curved and the description in terms of an $\mathrm{AdS}_5 \times \mathrm{S}^5$ throat is applicable, the world-volume theory on the D3-brane stack is strongly coupled. For the aforementioned comparison, however, the absorption process of a dilaton by a D3-brane stack is calculated only at tree-level. The fact that the resulting absorption cross section nevertheless agrees with the absorption cross section by a black three-brane is explained by a nonrenormalization theorem in the $\mathcal{N} = 4$ supersymmetric $\mathrm{U}(N)$ gauge theory.

The Klebanov-Strassler throat is finite in the infrared direction. In the dual gauge theory, this is reflected by the existence of a confinement scale. The gauge theory therefore has massive glueball states which correspond to the Kaluza-Klein modes in the throat. During cosmological evolution, the energy density in a throat or, equivalently, in the dual gauge theory is diluted by the expansion of the universe. If this energy density reaches the confinement scale, a phase transition takes place and a gas of glueballs is formed. Similarly, the black hole horizon in the throat is replaced by the infrared end of that throat during the phase transition. The glueballs or Kaluza-Klein modes which are formed during the phase transition can decay to other throats or gauge sectors. The corresponding decay rate is again important for the cosmology of throats.

As before, we calculate this rate in the gauge theory picture instead of the gravity picture. In this description, the glueball decays to a Kaluza-Klein mode of supergravity in the embedding space which in turn decays to gauge fields on another brane stack. However, since the glueball is a nonperturbative object, the vertex between a glueball on a brane stack and supergravity fields in the embedding space can not be read off from any Lagrangian. To determine this vertex, we calculate the decay rate in a simple example: The decay of a dilaton from the throat region of a black three-brane to the asymptotically flat region. We can then determine the decay vertex of a glueball on the equivalent brane stack by the requirement that the decay rate be reproduced from the gauge theory picture. Once we have this vertex, it is again a straightforward exercise in quantum field theory to calculate the decay rate of a glueball or a Kaluza-Klein mode to another sector. We compare certain limiting cases of this decay rate with results from calculations in the gravity picture.

The heat transfer rate that we derive is applicable to more general geometries than our simplified setup with two $\mathrm{AdS}_5 \times \mathrm{S}^5$ throats in a torus. In particular, we can consider a different geometry for the embedding compact space. That the parametric dependence of the heat transfer rate does not change is particularly easy to see if the distance between the throats is of the order of the size of the embedding space. We find that the heat transfer rate is then dominated by the mediation by zero-modes of supergravity fields in the embedding space. The wave function of these lowest Kaluza-Klein modes, however, does not depend on the geometry of the embedding space. Similarly, our result stays correct for more general throat geometries such as Klebanov-Strassler throats. Moreover, our results can also be applied to small stacks of D-branes. If the standard model is realized on a small number of D-branes, we can determine the rate of heat transfer to a throat.

For the decay rate in flux compactifications, on the other hand, modifications of our result can arise. Certain moduli, which are massless in our simplified setup and which mediate decays, become very massive due to the flux. This fact can lead to a suppression of the decay rate. In addition, the decay rate of Kaluza-Klein modes in a Klebanov-Strassler throat is in general difficult to determine. The equations of motion of these modes are involved because the flux in such a throat mixes field fluctuations in a complicated way. In order to determine the glueball vertex as discussed above, we would have to solve these equations of motion. On the other hand, we find that the glueballs in a given gauge sector (dual to a throat) can decay to a certain lightest glueball with

the emission of a graviton. This process is similar to the decay of a hadron into a lighter hadron with the emission of a photon. These decays typically happen on cosmologically short timescales. From the point of view of cosmology, it is then sufficient to analyse decays to other sectors only for these lightest glueballs or the corresponding lightest Kaluza-Klein modes. We show that there is a flat direction for the supergravity fields in the Klebanov-Strassler throat. The field which parameterizes this flat direction has the same equation of motion as the dilaton in an $AdS_5 \times S^5$ throat and therefore couples to supergravity in the embedding space with the previously derived vertex. We then argue that the lightest Kaluza-Klein mode mixes with this flat direction and thus also couples with the previously derived vertex. Taking this fact and the suppression due to the flux-stabilization of moduli into account, we can determine the decay rate of this Kaluza-Klein mode.

A stronger decay vertex arises if the Kaluza-Klein mode mixes with a tachyon in the Klebanov-Strassler throat. The reason is that the wave function of a tachyon, i.e. a scalar with a negative mass squared, is less suppressed than the wave function of a dilaton if one moves in the ultraviolet direction in the throat. A tachyon therefore couples with a stronger vertex to supergravity fields in the embedding space. On the other hand, there is a compensating effect. In anti-de-Sitter space, scalars with negative mass squared down to the so-called Breitenlohner-Freedman bound [6] do not lead to instabilities. In a Randall-Sundrum model, or a string realization thereof, however, a tachyon must have a large mass on the ultraviolet brane in order to avoid tachyonic Kaluza-Klein modes. This mass is similar to the aforementioned mass of mediating fields in flux compactifications and again leads to a suppression of the decay rate. In order to determine the relative importance of the enhancing effect and the suppressing effect, we calculate the decay rate of Kaluza-Klein modes of a tachyon between two throats in a five-dimensional model. To this end, we approximate one throat by a Randall-Sundrum model. The other throat is then dual to a gauge theory which lives on the ultraviolet brane of the Randall-Sundrum model. The decay rate of Kaluza-Klein modes between the two throats can be calculated as the decay rate of Kaluza-Klein modes in the Randall-Sundrum model to gauge fields on the ultraviolet brane. The corresponding part of the thesis is based on [7] (with Sebastian Halter and Arthur Hebecker).

1.4 Dark matter in throats

The glueball decay rates that we find are highly suppressed. If the mean lifetime of the glueballs is larger than the age of the universe, these particles are an interesting dark matter candidate. Furthermore, a small fraction of these glueballs decays to the standard model already at our epoch and can lead to interesting observable signals. In the second part of this thesis, based on our publication [8] (with Arthur Hebecker), we study this new dark matter candidate.

For definiteness, we assume that the standard model is realized on some D-branes in the unwarped part of a compact space which also has throat regions. The standard model and possibly the throats are heated by the reheating mechanism after inflations ends.

If the throats were heated to the same temperature as the standard model, however, they would lead to too much dark radiation during big bang nucleosynthesis and/or would overclose the universe. Accordingly, the reheating mechanism has to interact more weakly with the throats than with the standard model. The resulting abundance of Kaluza-Klein dark matter depends on the model at hand. In order to provide a model-independent lower bound on this abundance, we assume that the throats receive no energy from the reheating process. Even under this minimal assumption, energy is deposited in a given throat due to heat transfer from the standard model.

The resulting energy density in the throat is diluted by the expansion of the universe. In order to calculate the abundance of glueballs at our epoch, we have to determine the scaling behaviour of this energy density with the expansion of the universe. This analysis is easiest in the gauge theory picture. As we will show, if the energy density in a given gauge sector was above the confinement scale after reheating, the gauge theory thermalizes. The energy density then scales like radiation until a confinement phase transition takes place. Afterwards, it scales like matter.

The situation is different if the energy density was never above the critical energy density for a confinement phase transition. The energy density is produced by the annihilation of standard model particles into some gauge theory states. This is similar to the annihilation of an electron with a positron into a quark and an antiquark. In QCD, this process leads to two jets which subsequently hadronize. The particles, which are produced in that way, are ultrarelativistic and would scale like radiation with the expansion of the universe. As we will discuss in more detail, there are no jets in the strongly coupled gauge theories which are dual to throats. Instead, after hadronization, the energy is completely in the form of slow glueballs. These particles then immediately scale like matter. This fact partially balances a large suppression of the heat transfer rate by four powers of the four-dimensional Planck scale that we find. In particular, the energy density in the corresponding throats can have the right magnitude to account for the observed dark matter already for moderately high reheating temperatures.

More precisely, we find that throats with infrared scales between $10^5\,\mathrm{GeV}$ and $10^{11}\,\mathrm{GeV}$ can account for the observed dark matter if the reheating temperature was approximately $10^{10} - 10^{11}\,\mathrm{GeV}$. The lifetime of Kaluza-Klein modes in these throats or, equivalently, of glueballs can be made considerably longer than the age of the universe. Nevertheless, for certain choices of parameters, glueball decays to the standard model can lead to interesting observable signatures. In particular, these decays produce hadrons which in turn decay to relatively soft photons. These photons contribute to the diffuse γ-ray background at low energies and may be detected by experiments like GLAST. In addition, certain glueballs species can decay directly into a pair of photons. Decays of this type in the halo of our galaxy lead to a sharp line in the γ-ray spectrum at high energies. This line may be observed by experiments like HESS.

Since throats are expected to be a common feature in the landscape of type IIB vacua, it is interesting to analyse scenarios with a large number of throats. To this end, we use the estimate of the expected number of throats in dependence of their infrared scales from Ref. [9]. The decay rates that we find depend strongly on the mass

of the glueballs. In scenarios with a large number of throats, it is therefore possible that glueballs from certain sectors decay already at early epochs while other glueballs are sufficiently stable to account for the observed dark matter. Decays to the standard model at early epochs can influence primordial nucleosynthesis and are therefore severely constrained. We check in a specific example that the corresponding bounds can be fulfilled.

1.5 Organization of the thesis

This thesis is organized as follows. In Chapters 2 and 3, we review several aspects of throats and their dual gauge theories that are relevant for this thesis. We begin in Chapter 2 by recapitulating the Randall-Sundrum models. We then introduce black-three branes and D3-branes and review a calculation showing that these branes are just two descriptions of the same object. We discuss the AdS/CFT conjecture and how it can be motivated by taking the low-energy limit of the black 3-brane and the equivalent D3-brane stack. We also introduce the Klebanov-Strassler throat and review the high-temperature phase of throats and their dual gauge theories. In Chapter 3, we first recapitulate how the Randall-Sundrum II model can be obtain from string theory. We then revisit the string realizations of the Randall-Sundrum I model which can arise in flux compactifications. Finally, we conclude Chapter 3 with a discussion of the statistical probability of throats in the landscape of flux vacua.

In Chapter 4, we first present a motivation for the central topic of Chapters 4 to 7: The transfer of energy in different forms between throats in the early universe. We then review a calculation of the decay rate of Kaluza-Klein modes between throats in a simple five-dimensional geometry. We also present two other ways to derive this decay rate, one way being based on our paper [5]. In Chapter 5, following again [5], we derive the energy loss rate of a heated throat to another throat in a simple ten-dimensional model. This calculation is performed by modelling both throats by equivalent stacks of D-branes. It is then straightforward to derive the heat transfer rate by summing over the contributions of bulk Kaluza-Klein modes coupling to both D-brane stacks. We also present a cross-check in which we compare the heat loss of a throat and an equivalent D-brane stack to flat space.

In Chapter 6, which is still based on [5], we describe an analogous calculation for the decay rate of Kaluza-Klein modes localized in one throat to fields in a distant throat. In the gauge theory picture, the decaying Kaluza-Klein modes are represented by glueballs. Thus, we first derive the effective vertex for the coupling of these glueballs to bulk fields. After that, the calculation proceeds analogously to that in the previous chapter. Finally, we compare certain limiting cases of our result with calculations in the gravity picture and with formulae from the literature.

Modifications to our results from Chapters 5 and 6, that arise in setups which are more realistic than our simple ten-dimensional model, are discussed in Chapter 7. This chapter contains results from our papers [5], [7] and [8]. We first argue that our

heat transfer rate is applicable to other geometries of the throats and the embedding compact space. The decay rate of Kaluza-Klein modes from a Klebanov-Strassler throat, on the other hand, is in general difficult to determine. We discuss several aspects of the Kaluza-Klein spectrum of such a throat and then show that all Kaluza-Klein modes decay quickly to a lightest scalar state and its superpartner. As we argue, these Kaluza-Klein modes decay again with the vertex from Chapter 6. Taking a suppression due to flux-induced masses into account, we derive the decay rate of the lightest scalar Kaluza-Klein mode and its superpartner. On the other hand, we find that Kaluza-Klein modes mixing with tachyons in a Klebanov-Strassler throat decay with a stronger vertex than that from Chapter 6. Finally, we discuss the energy transfer between throats and the standard model.

Glueballs as a dark matter candidate are studied in Chapters 8 and 9. We describe the thermal production of this form of dark matter in Chapter 8. Using the heat transfer rate from Chapter 5, we determine the energy density deposited in a throat by the heated standard model. We discuss how the initially created gauge theory states hadronize and in which situations the gauge theory thermalizes. Taking the resulting scaling of the energy density with the expansion of the universe into account, we calculate the late-time abundance of glueballs as a function of the reheating temperature and the confinement scale of the gauge theory.

Cosmological scenarios are discussed in Chapter 9. First, we analyse scenarios with a single throat. We find that a moderately long throat gives a promising dark matter candidate which may allow for a discovery by new γ-ray experiments. Then, we consider scenarios with a large number of throats, using results on the distribution of multi-throat configurations reviewed in Chapter 3. We find that a throat in the required range of lengths is in many cases present. We also discuss some issues in scenarios with low-scale supersymmetry breaking and the relation of our dark matter scenario to earlier work in the literature.

Our conclusions are given in Chapter 10. Some calculations are relegated to appendices: The Kaluza-Klein decomposition of the graviton and a tachyon in a Randall-Sundrum model is determined in Appendices A and B, respectively. In Appendix C, an integral is evaluated which is needed in Chapters 5 and 6. Finally, Appendix D discusses a process which takes place after the confinement phase transition of gauge theories dual to finite throats.

Finally, let us fix some notations and conventions. Throughout this thesis, we use the 'mostly-plus' signature for the metrics. Our notation for the form fields of type IIB supergravity is e.g. as in [3]. We denote the (reduced) Planck scale in d dimensions by M_d, the string scale by M_s and the string coupling by g_s. The symbol $\sim$ that we will use frequently signifies equality up to $\mathcal{O}(1)$ prefactors, whereas the symbols $\approx$ and $\simeq$ are reserved for results which hold to a higher precision.

Chapter 2

Warped geometries and dual gauge theories

In this chapter, we will review several aspects of warped geometries. This will fix our notation and will also provide results that will be needed in later chapters. There are in particular two reasons for the enormous interest in these geometries in recent years: As Randall and Sundrum have shown, AdS-spaces allow for the generation of large hierarchies of scales. Moreover, Maldacena has argued that string theory on AdS_5 times some compact manifold is dual to a gauge theory. More exhaustive reviews of these subjects can be found e.g. in [10–12].

2.1 The Randall-Sundrum models

We will now review the Randall-Sundrum (RS) models [1,2] which will play an important role in this thesis. In particular, the RSI model [1] offers a possible solution to the hierarchy problem. However, we should clarify at this point that we will not be concerned with the hierarchy problem later in this thesis. Instead, we will more generally be interested in the generation of large hierarchies in geometries of the RS type.

We consider a 5-dimensional theory and take the 5th dimension to be compactified on an $S^1/\mathbb{Z}_2$ orbifold of length ℓ. Thus, the following equivalence relations hold for the 5th coordinate y:

$$y \sim y + 2\,\ell \qquad y \sim -y\,. \tag{2.1}$$

We denote the coordinates of the 4 uncompactified dimensions by x. Points in spacetime which remain fixed under the orbifold $\mathbb{Z}_2$-action $y \to -y$ form $(3+1)$-dimensional hypersurfaces which are located at $y = 0$ and $y = \ell$. These hypersurfaces, which form the boundaries of the 5th dimension, are called the ultraviolet (UV) brane and the infrared (IR) brane, respectively. The branes can support (3+1)-dimensional field theories. We denote the corresponding Lagrangian on the UV brane by $\mathcal{L}_{\mathrm{UV}}$ and the Langrangian on the IR brane by $\mathcal{L}_{\mathrm{IR}}$, respectively. Furthermore, the branes can have certain tensions V_{UV} and V_{IR}. Taking also a 5-dimensional cosmological constant Λ into account, the action

of the theory is given by

$$S \;=\; \int d^4x \int_{-\ell}^{\ell} dy\, \sqrt{g}\, \Big(2M_5^3\, \mathcal{R} - \Lambda + \delta(y)\, (\mathcal{L}_{\rm UV} - V_{\rm UV}) + \delta(y-\ell)\, (\mathcal{L}_{\rm IR} - V_{\rm IR}) \Big) \,. \quad (2.2)$$

Here, M_5 is the 5-dimensional Planck mass. We look for solutions of the Einstein equations that satisfy an ansatz of the form

$$ds^2 \;=\; e^{-2A(y)}\, \eta_{\mu\nu} dx^\mu dx^\nu + dy^2 \,. \quad (2.3)$$

Using this ansatz, the Einstein equations which follow from the action Eq. (2.2) reduce to

$$A'^2 \;=\; \frac{-\Lambda}{24\, M_5^3} \quad (2.4)$$

$$A'' \;=\; \frac{1}{12 M_5^3} \Big(V_{\rm UV} \delta(y) + V_{\rm IR} \delta(y-\ell) \Big) \,. \quad (2.5)$$

A solution to Eq. (2.4) which respects the orbifold symmetry $y \to -y$ is

$$A(y) \;=\; k\, |y| \,, \quad \text{where} \quad k \;\equiv\; \sqrt{\frac{-\Lambda}{24 M_5^3}} \,. \quad (2.6)$$

This solution is meaningful only if the 5d cosmological constant is negative, $\Lambda < 0$. The geometry in between the two branes accordingly is a slice of 5-dimensional anti-de-Sitter space (AdS_5). The curvature scale of this geometry is given by k. We can therefore trust our solution only if $k \ll M_5$. Keeping in mind that $y \sim y + 2\ell$, Eq. (2.6) also solves Eq. (2.5) if

$$V_{\rm UV} \;=\; -V_{\rm IR} \;=\; \sqrt{-\Lambda\, 24 M_5^3} \,. \quad (2.7)$$

This is a tuning of two parameters and is required in order to get a static solution with 4d Poincaré symmetry. A fine-tuning of parameters in a proposed solution to the hierarchy problem may seem strange. A detailed analysis shows (see e.g. [11] for a pedagogical discussion) that one tuning is necessary to get a flat potential for the scalar field which parameterizes the length of the 5th dimension (the radion). Otherwise, in absence of a stabilization mechanism for the radion, the 5th dimension would either collapse or decompactify. By stabilizing the radion (which is anyway required in a phenomenologically viable theory), this tuning is no longer necessary. The remaining tuning corresponds to a vanishing 4d cosmological constant and is common to other solutions to the hierarchy problem.

To discuss the effective 4d gravity theory from the point of view of brane observers, we promote the background metric $\eta_{\mu\nu}$ in Eq. (2.3) to a dynamical field $g^{(4)}_{\mu\nu}$. The 4d Ricci scalar $\mathcal{R}^{(4)}$ constructed from $g^{(4)}_{\mu\nu}$ is contained in the 5d Ricci scalar $\mathcal{R}$:

$$2M_5^3 \int d^5x\, \sqrt{g}\, \mathcal{R} \quad \subset \quad 2M_4^2 \int d^4x\, \sqrt{g^{(4)}}\, \mathcal{R}^{(4)} \,, \quad (2.8)$$

$$\text{where} \quad M_4^2 \;=\; M_5^3 \int_{-\ell}^{\ell} dy\, e^{-2k|y|} \;=\; \frac{M_5^3}{k} \left(1 - e^{-2k\ell} \right) \,. \quad (2.9)$$

From the last equation, we see that the 4d Planck mass M_4 hardly depends on the size ℓ of the extra dimension. In particular, it stays finite in the limit $\ell \to \infty$. This suggests that we can recover 4d gravity (with small corrections) on the UV brane even with an infinite 5th dimension. This was analysed in great detail in [2,13,14]. The corresponding setup, in which the IR brane is sent to infinity, is known as the RSII model. The setup in which the IR brane is kept, on the other hand, is called the RSI model.

The Kaluza-Klein (KK) expansion of gravity in a RS model is discussed in Appendix A. In particular, one finds that the wavefunction of the 4d graviton is localized near the UV brane. The massive KK modes, on the other hand, are localized in the IR and their couplings to the UV brane are strongly suppressed. These KK modes therefore give only small corrections to 4d gravity on the UV brane even if the IR brane is sent to infinity. If the IR brane is kept, on the other hand, the masses m_n of the KK modes are quantized in units of the warped AdS scale:

$$m_n \sim n\, m_{\text{IR}}\,, \qquad \text{where } m_{\text{IR}} \equiv e^{-k\ell}k \text{ and } n \in \mathbb{N}\,. \tag{2.10}$$

Next, we consider the field theory which is confined to the IR brane in a RSI model in more detail. From Eq. (2.2), the relevant part of the action is

$$\int d^4x \sqrt{g^{\text{IR}}}\, \mathcal{L}_{\text{IR}}\left(g^{\text{IR}}_{\mu\nu}, \phi, m\right)\,. \tag{2.11}$$

Here, ϕ and m collectively denote any fields and mass scales which may appear in the action and g^{IR} is the induced metric on the IR brane. Using Eqs. (2.3) and (2.6), we have

$$g^{\text{IR}}_{\mu\nu} = g_{\mu\nu}(x, y=\ell) = e^{-2k\ell} g^{(4)}_{\mu\nu}\,. \tag{2.12}$$

The crucial point is that the action on the IR brane, Eq. (2.11), is given in terms of the metric g^{IR} which is rescaled by a factor $e^{-2k\ell}$. The gravity part of the action, Eq. (2.8), on the other hand, depends on the unrescaled metric $g^{(4)}$. To compare the scales M_4 and m in Eqs. (2.8) and (2.11), we have to agree on one metric to be used in both actions. For the moment, we choose $g^{(4)}$ to be this metric. Rewriting Eq. (2.11) in terms of $g^{(4)}$ by using Eq. (2.12) brings factors of $e^{-2k\ell}$ into the action. These factors can be absorbed into field redefinitions and the mass parameters. Thus, the action is invariant except for the mass parameters which transform as

$$m \longrightarrow e^{-k\ell}\, m\,. \tag{2.13}$$

The mass scales which appear in the Lagrangian using $g^{(4)}$ as reference metric are rescaled by a factor of $e^{-k\ell}$! In particular, for $k\ell \simeq 35$, a mass of the order of the Planck scale is scaled down to the TeV scale. Note however that, to solve the hierarchy problem, a mechanism is required which stabilizes the branes at the right distance (i.e. $k\ell \simeq 35$) without too much fine-tuning. An example of such a mechanism is due to Goldberger and Wise [15].

Alternatively, we can use g^{IR} as the reference metric in Eqs. (2.8) and (2.11). In this case, we get a factor of $e^{2k\ell}$ into the action in Eq. (2.8). Absorbing this factor into the

4d Planck scale, we have

$$M_4^2 \;=\; \frac{M_5^3}{k}\left(e^{2k\ell}-1\right)\,. \tag{2.14}$$

The mass scales m in the action Eq. (2.11), on the other hand, are not rescaled. From this viewpoint, we can have the 5d Planck scale and the AdS scale in the TeV range and still get a sufficiently large 4d Planck scale. According to Eq. (2.14), the resulting hierarchy is again given by $e^{k\ell}$. In the following, however, we use the definition of scales corresponding to Eqs. (2.9) and (2.13).

2.2 D3-branes and black 3-branes

String realizations of the RS models exist which we will discuss in Chapter 3. In these constructions, D-branes and supergravity branes play an important role. Furthermore, these objects are also the starting point from which one can motivate the AdS/CFT conjecture.

We consider type IIB string theory. A D3-brane is a $(3+1)$-dimensional hyperplane in 10-dimensional space on which open strings end. At low energies, the open strings give rise to a field theory which is confined to the world-volume of the brane. For a D3-brane which is embedded into 10d Minkowski space, it is straightforward to guess this field theory: A D-brane preserves 1/2 of the $\mathcal{N}=2$ supersymmetry of type IIB string theory in the bulk [16]. The field theory on the 4d world-volume of the brane thus has $\mathcal{N}=4$ supersymmetry. Furthermore, oscillations of a D3-brane in the 6 directions transverse to its world-volume lead to 6 scalar fields.[1] Now, 6 scalars are contained in an $\mathcal{N}=4$ vector multiplet. Accordingly, the world-volume theory on a D3-brane is the $\mathcal{N}=4$ supersymmetric U(1) gauge theory.

More precisely, a D3-brane and its interactions with supergravity fields in the embedding space is governed by the so-called DBI action. It reads

$$S_{\text{DBI}} \;=\; -\,T_3\int d^4x\sqrt{-\det\left(G_{\alpha\beta}+e^{-\phi/2}\left(B_{\alpha\beta}+F_{\alpha\beta}\right)\right)}\,,$$
$$\text{where}\quad G_{\alpha\beta} \;=\; \frac{\partial X^M}{\partial x^\alpha}\,\frac{\partial X^N}{x^\beta}\,g_{MN} \tag{2.15}$$

is the pullback of the 10d metric g_{MN} to the 4d brane world-volume parametrized by x^α ($\alpha=0\ldots3$) and the $X^M(x^\alpha)$ ($M=0\ldots9$) describe the embedding of the brane into 10d space. Similarly, $B_{\alpha\beta}$ is the pullback of the NS 2-form B_2, whereas ϕ is the dilaton. The field strength of the U(1) gauge boson is denoted by $F_{\alpha\beta}$. We have not written out fermionic contributions to the action as well as interactions with RR-form fields. Furthermore, $T_3=\sqrt{\pi}M_{10}^4$ is the tension of a D3-brane, where M_{10} is the 10d Planck scale. Note that, here and below, we work in the 10d Einstein frame. Using the

[1] These scalar fields are the Goldstone bosons due to broken Lorentz invariance in the transverse directions [17, 18].

static gauge $X^\alpha = x^\alpha$ ($\alpha = 0 \ldots 3$), an expansion of Eq. (2.15) in a 10d Minkowski background gives

$$S_{\text{DBI}} = T_3 \int d^4x \left(1 - \frac{1}{4} e^{-\phi} F_{\alpha\beta}^2 - \frac{1}{2} \partial^\alpha X^m \partial_\alpha X_m + \text{interactions}\right) , \tag{2.16}$$

where the X^m ($m = 4 \ldots 9$) describe oscillations of the brane. We have written out the interaction of the dilaton with the gauge field strength because it will be needed later on.

A D3-brane is charged under the RR 4-form C_4 and thus sources a unit of the corresponding flux. The resulting repulsion of two D3-branes due to this charge is precisely cancelled by the mutual attraction due to gravity. Thus, one can place N D3-branes on top of each other. The world-volume theory on this D3-brane stack is a $\mathcal{N} = 4$ U(N) gauge theory.

As can be seen from the first term in Eq. (2.16), the tension T_3 of a D3-brane acts as a localized cosmological constant. Therefore, D3-branes backreact on the geometry. Assuming for the moment that the resulting curvature is weak, the backreaction can be described by the low energy limit of type IIB string theory, type IIB supergravity. The corresponding solution is called a black 3-brane. It has the metric [19]

$$ds^2 = H^{-1/2}(r)\, \eta_{\mu\nu} dx^\mu dx^\nu + H^{1/2}(r) \left[dr^2 + r^2 d\Omega_5^2\right] ,$$
$$\text{where} \qquad H(r) = 1 + \frac{R^4}{r^4} , \tag{2.17}$$

R is a curvature scale and $d\Omega_5^2$ is the line element of a 5-sphere. Furthermore, the 5-form field strength F_5 of the RR 4-form C_4 has an r-dependent vacuum expectation value whereas the axion C and the dilaton ϕ are constant.

The geometry in Eq. (2.17) can be understood as the result from the backreaction of a D3-brane stack at $r = 0$. A natural question then is: What has happened to the D3-brane stack? In the limit $r \ll R$, Eq. (2.17) takes the form

$$ds^2 = \frac{r^2}{R^2} \eta_{\mu\nu} dx^\mu dx^\nu + \frac{R^2}{r^2} dr^2 + R^2 d\Omega_5^2 . \tag{2.18}$$

After a coordinate transformation to $y \equiv -k^{-1} \ln[kr]$, where $k \equiv R^{-1}$, the metric reads

$$ds^2 = e^{-2ky} \eta_{\mu\nu} dx^\mu dx^\nu + dy^2 + R^2 d\Omega_5^2 . \tag{2.19}$$

As we have discussed in Section 2.1, the first two terms in this metric determine the AdS_5 geometry (cf. Eqs. (2.3) and (2.6)) with curvature scale $k = R^{-1}$. The third term describes an S^5 of radius R. The geometry of the brane in the region $r \ll R$ thus is $AdS_5 \times S^5$. Using the above relation between the coordinates r and y, we see that $r \to 0$ corresponds to $y \to \infty$. Thus, instead of the initial D3-brane stack, one encounters an infinitely deep throat region if one moves towards smaller r. The black 3-brane is therefore believed to give an *alternative* description of D3-branes: The dynamics of

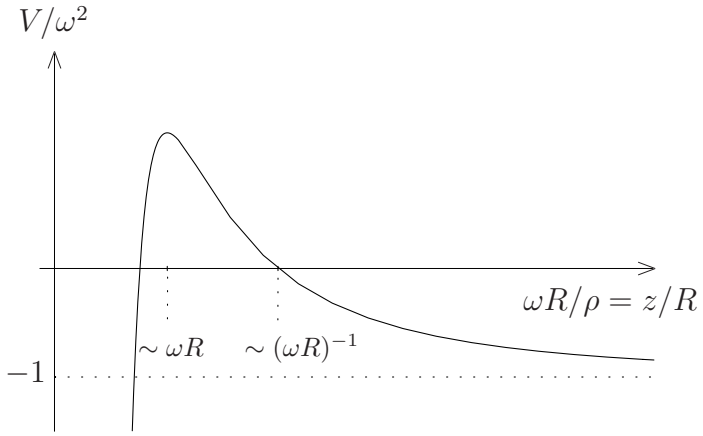

Figure 2.1: *Potential in the effective Schrödinger equation for the dilaton in a throat*

open strings on a D3-brane is replaced by closed string dynamics in the black 3-brane background.

The curvature scale R due to the backreaction of N D3-branes (or, equivalently, due to N units of 5-form flux through S^5) is

$$R^4 \sim N M_{10}^{-4} \sim N g_s M_s^{-4}, \tag{2.20}$$

where M_s is the string scale and $g_s = e^{\langle\phi\rangle}$ is the string coupling. A description in terms of classical supergravity is valid if $R \gg M_{10}^{-1}$ and $R \gg M_s^{-1}$. These conditions are fulfilled if $N \gg 1$ and $N g_s \gg 1$. The Yang-Mills coupling $g_{\rm YM}$ is related to the string coupling g_s by $g_{\rm YM}^2 = g_s$. Therefore, when the description in terms of a black 3-brane is applicable, the gauge theory on the corresponding stack of D3-branes is at large 't Hooft coupling $\lambda \equiv g_{\rm YM}^2 N$ and perturbation theory breaks down. When the gauge theory is in the perturbative regime $\lambda < 1$, on the other hand, the supergravity description is no longer valid.

In the limit $r \gg R$, the function H in the metric Eq. (2.17) is approximately 1 and the geometry is 10d Minkowski space. This corresponds to the fact that the geometry is due to the backreaction of a D3-brane stack in 10d Minkowski space. In particular, similar to the D3-brane, we can think of the black 3-brane as a localized object embedded into flat space.

2.3 Absorption of a dilaton by a brane

To check whether D3-branes and black 3-branes are really just two descriptions of the same object is in general difficult, as we have seen in the last section: If one description is weakly coupled, the other one is strongly coupled and vice versa. We will now describe a calculation [20] which nevertheless allows such a check.

Consider a dilaton ϕ which is incident on a black 3-brane. Its equation of motion is the Laplace equation in the background geometry given by Eq. (2.17):

$$\partial_M \left(\sqrt{g} g^{MN} \partial_N \phi\right) = 0\,. \tag{2.21}$$

Performing an expansion into eigenwaves of the angular Laplacian on S^5, the equation of motion of an incident dilaton with energy ω reads

$$\left(\rho^{-5}\frac{d}{d\rho}\rho^5\frac{d}{d\rho} + 1 + \frac{(\omega R)^4}{\rho^4} - \frac{l(l+4)}{\rho^2}\right)\phi^{(l)} \;=\; 0\,. \tag{2.22}$$

Here, $\rho \equiv \omega r$ and l determines the eigenvalues of the angular Laplacian. Introducing a new coordinate $z \equiv R^2/r$ and substituting $\psi \equiv z^{-3/2}\phi$, this can be written as

$$-\frac{d^2}{dz^2}\,\psi^{(l)} \;+\; \left(\frac{15/4 + l(l+4)}{z^2} - \frac{\omega^2 R^4}{z^4} - \omega^2\right)\psi^{(l)} \;=\; 0\,. \tag{2.23}$$

This has the form of a Schrödinger equation with a potential which is given by the term in brackets. A schematic plot of this potential is shown in Fig. 2.1. As one can see, a wave coming from the asymptotically flat region ($z \to 0$ corresponding to $\rho \to \infty$) has to tunnel through an effective barrier to reach the inner region ($z \to \infty$ corresponding to $\rho \to 0$).[2]

We will now solve Eq. (2.23) by applying the so-called matching technique: For $z \gg \omega R^2$ corresponding to $\rho \ll 1$, the term $\omega^2 R^4/z^4$ in Eq. (2.23) can be ignored. An approximate solution in this region is given by

$$\phi^{(l)} \;=\; \rho^{-2}\left[J_{2+l}\Big(\frac{(\omega R)^2}{\rho}\Big) + iY_{2+l}\Big(\frac{(\omega R)^2}{\rho}\Big)\right]\,. \tag{2.24}$$

Here, J and Y are Bessel functions and the linear combination corresponds to an incoming wave in the direction of small ρ. This can be seen from the asymptotic forms of the Bessel functions for large arguments: Eq. (2.24) approximately is $\psi^{(l)} \propto \rho^{-3/2} e^{i(\omega R)^2/\rho}$ for $\rho \ll (\omega R)^2$. Another way of writing Eq. (2.22) is by substituting $\tilde{\psi} \equiv \rho^{5/2}\phi$:

$$\left(\frac{d^2}{d\rho^2} - \frac{15/4 + l(l+4)}{\rho^2} + 1 + \frac{(\omega R)^4}{\rho^4}\right)\tilde{\psi}^{(l)} \;=\; 0\,. \tag{2.25}$$

For $\rho \gg (\omega R)^2$, the term $(\omega R)^4/\rho^4$ can be ignored and an approximate solution in this region is

$$\phi^{(l)} \;=\; \rho^{-2}\left[A\,J_{2+l}(\rho) + B\,Y_{2+l}(\rho)\right]\,. \tag{2.26}$$

The regions of validity of Eqs. (2.24) and (2.26) overlap for

$$\omega R \ll 1\,. \tag{2.27}$$

[2] As we will see in Section 6.3, by using cartesian coordinates for the directions transverse to the brane, one again gets a Schrödinger-like equation. However, in this case there is no barrier an incoming wave would have to tunnel through. Instead, the reflection of a large part of the incoming wave is due to the steepness of the potential well.

We restrict ourselves to this case from now on. Using the asymptotic forms of the Bessel functions for small arguments, we can then match both solutions in the overlapping region $(\omega R)^2 \ll \rho \ll 1$. This fixes the constants A and B in Eq. (2.26) and we find, to lowest order in ωR and up to numerical prefactors:

$$A \;\sim\; (\omega R)^{-4-2l} \tag{2.28}$$

$$B \;=\; 0\,. \tag{2.29}$$

The absorption probability $\mathcal{P}$ of a dilaton by a black 3-brane follows from the ratio of the flux at $\rho = 0$ and $\rho = \infty$. Using Eqs. (2.24) and (2.26), we have

$$\mathcal{P} \;\simeq\; A^{-2} \;\sim\; (\omega R)^{8+4l}\,. \tag{2.30}$$

In $(6+1)$ dimensions (where we mean the 6 dimensions transverse to the world-volume of the 3-brane), the relation between the absorption probability $\mathcal{P}$ and the absorption cross section σ is $\sigma \sim \mathcal{P}/\omega^5$, again neglecting numerical prefactors. The absorption cross section per 4d world-volume of the 3-brane thus is

$$\sigma \;\sim\; \omega^{3+4l}\, R^{8+4l}\,. \tag{2.31}$$

Alternatively, we can consider the decay of a dilaton onto an equivalent stack of D3-branes. The kinetic term of the dilaton from the type IIB supergravity action is

$$S_{\rm IIB} \;\supset\; -\frac{M_{10}^8}{4}\int d^{10}x\sqrt{g}(\partial\phi)^2\,. \tag{2.32}$$

The dilaton couples to the operator $F^2_{\alpha\beta}$ on a single D3-brane according to Eq. (2.16). Canonically normalizing the kinetic terms of the dilaton and the fields X^i and allowing for brane fluctuations, we get [20]

$$S \supset \frac{M_{10}^{-4}}{2^{3/2}}\left[\int d^4x\,\phi(x,\langle\vec{X}\rangle)\,F^2_{\alpha\beta} + \sum_{l=1}^{\infty}\int d^4x \frac{M_{10}^{-2l}}{l!\pi^{l/4}}\,(\partial_{i_1}\cdots\partial_{i_l}\phi)\,X^{i_1}\cdots X^{i_l}\,F^2_{\alpha\beta}\right], \tag{2.33}$$

where $\langle\vec{X}\rangle$ is the position of the brane. The coupling of a dilaton s-wave to the world-volume theory is due to the first term in Eq. (2.33), whereas higher partial waves couple via the other terms. In additon, there are couplings of the dilaton to fermionic terms which we can neglect for an order of magnitude estimate. The absorption cross section of the l-th partial wave by a single D3-brane follows from the vertices in Eq. (2.33) as

$$\sigma \;\sim\; M_{10}^{-8-4l}\omega^{3+4l}\,, \tag{2.34}$$

up to numerical prefactors. For a stack of N D3-branes, the absorption cross section has an extra factor of $\sim N^{2+l}$ since the gauge fields and the fields X^i are in the adjoint representation of the U(N) world-volume gauge theory.[3] Using Eq. (2.20), we then have

$$\sigma \;\sim\; \omega^{3+4l}\, R^{8+4l}\,. \tag{2.35}$$

[3]For N D3-branes, one has traces over U(N) indices in the DBI action and accordingly in Eq. (2.33). For example, the $(l=1)$-vertex has the structure $X^I_J F^J_K F^K_I$, where I, J, K are U(N) indices. The three summations lead to a factor $\sim N^3$.

This is the same result as in Eq. (2.31)! Thus, we have found the same parametric dependence of the dilaton absorption cross section for a black 3-brane and a D3-brane stack. We have ignored numerical prefactors in our calculation. Remarkably, even these prefactors turn out to agree exactly [20–22]. This is evidence that black 3-branes and D3-branes are just two descriptions of the same object.

Taking a closer look, the exact agreement of the absorption cross sections from both calculations comes as a surprise. The absorption cross section for the black 3-brane actually is a perturbative expansion in ωR (cf. Eq. (2.27)). Corrections to Eq. (2.31) in higher orders of ωR are the only possible corrections in the limit of classical supergravity (i.e. for large N and large λ, cf. Section 2.2).[4] The gauge theory on the corresponding D3-brane stack, on the other hand, has a large 't Hooft coupling λ. The absorption cross section therefore has the general form

$$\sigma \sim \omega^3 R^8 \left(1 + b_1 \lambda + b_2 \lambda^2 + \dots\right) + \text{higher orders in } \omega R\,, \tag{2.36}$$

where we have taken $l = 0$ for simplicity. If the coefficients b_i in Eq. (2.36) were nonvanishing, the results from the calculations for the black 3-brane and the D3-brane stack would disagree. It was shown [25], though, that all the coefficients b_i are zero due to a nonrenormalization theorem in 4d $\mathcal{N} = 4$ super-Yang-Mills theory.[5]

2.4 The Maldacena or AdS/CFT conjecture

As before, let us consider a black 3-brane and an equivalent stack of D3-branes. We want to analyse the low-energy limit while keeping the parameters M_s, g_s and N fixed.[6] In the black 3-brane background, two kinds of excitations can have arbitrarily low energies (when measured by a fixed observer): There are massless closed string states in the asymptotically flat region. These states give rise to type IIB supergravity in 10d Minkowski space. In addition, there are closed string states (not necessarily massless) in the throat region at smaller and smaller r (cf. Section 2.1). These states form type IIB string theory on $\mathrm{AdS}_5 \times \mathrm{S}^5$. Interactions between the two types of excitations vanish in the low-energy limit. For example, the absorption cross section of a dilaton which is incident on the brane from the asymptotically flat region, Eq. (2.31), goes to zero for $\omega \to 0$. In turn, states which are localized at smaller and smaller r find it more and more difficult to climb the gravitational potential to escape to the asymptotically flat region. Thus, we end up with two decoupled theories in the low-energy limit: Type IIB supergravity in flat space plus type IIB string theory on $\mathrm{AdS}_5 \times \mathrm{S}^5$.

For the D3-brane stack, it is more convenient to keep the energy fixed and to take the limit $M_s \to \infty$ instead. Since we keep g_s fixed, this means that also

[4] For an s-wave process, these corrections were calculated to higher orders in ωR in [23, 24].

[5] Actually, this was shown for the absorption cross section of a graviton polarized parallel to the D3-brane stack. A similar nonrenormalization theorem is expected to hold also for the dilaton absorption process.

[6] In this section, we follow closely the analysis in [10].

$M_{10} \sim g_s^{-1/4} M_s \to \infty$. Interactions between the gauge theory on the stack and the theory in the surrounding flat space vanish in this limit. This can be seen, for example, from Eq. (2.33) which gives the leading interactions between the dilaton and the gauge field strength. Since string corrections vanish for $M_s \to \infty$, the theory in the surrounding 10d Minkowski space is type IIB supergravity. Moreover, higher derivative terms from the DBI action also vanish in this limit as can be seen from an expansion of Eq. (2.15) (see e.g. [23]). The remaining theory on the D3-brane stack is the pure $\mathcal{N} = 4$ U(N) gauge theory which is a conformal field theory (CFT). Thus, we again have two decoupled theories in the low-energy limit (or, equivalently, for $M_s \to \infty$): Type IIB supergravity in flat space and $\mathcal{N} = 4$ U(N) super-Yang-Mills.

In summary, we find two decoupled theories in the low-energy limit of the black 3-brane as well as the D3-brane stack. The fact that one theory is the same for both types of branes (namely type IIB supergravity in flat space) led Maldacena to the conjecture [26] that also the other two theories are identical. The (Maldacena or AdS/CFT) conjecture thus is that type IIB string theory on $\mathrm{AdS}_5 \times \mathrm{S}^5$ is the same as (or dual to) $\mathcal{N} = 4$ SU(N) super-Yang-Mills in 4d Minkowski space.[7]

As an immediate test of the correspondence, one can compare the symmetries on both sides. The isometry group of AdS_5 and the conformal group in 4d Minkowski space are both SO(4, 2). In particular, a translation along the radial coordinate of AdS_5 maps to a conformal transformation on the gauge theory side. The radial coordinate of AdS_5 can therefore be viewed as the dual of the renormalization scale of the gauge theory.[8] The gauge theory has an SU(4) R-symmetry which can be identified with the isometry group SO(6) of S^5. Furthermore, one can show that even the supergroups which contain the aforementioned bosonic symmetries agree.

More generally, it is believed that other theories on AdS_5 which include gravity are as well dual to a CFT in 4d Minkowski space. In particular, one can consider the RS models in the light of the AdS/CFT duality. In the RSII model, AdS_5 is cut off in the UV by a brane (cf. Section 2.1). Since the radial coordinate of AdS_5 is dual to the renormalization scale, the RSII model is dual to a CFT which has a cutoff at a certain UV scale. Furthermore, due to the cutoff, the RSII model has a normalizable 4d graviton. One therefore expects that the dual CFT is coupled to 4d gravity as well. Let us describe a test of this correspondence. To this end, one calculates corrections to the 4d Newton potential on both sides of the duality. On the RSII side, these corrections are due to the exchange of KK modes between two test particles and result in a leading correction which goes like distance^{-3}. On the CFT side, on the other hand, one considers the coupling of the energy-momentum tensor T of the CFT to the 4d graviton. The graviton propagator is corrected by insertions of the 2-point function $\langle TT \rangle$. Even though the CFT is strongly coupled, this 2-point function is fully determined by conformal

[7] Up to some $\mathbb{Z}_N$ identifications, U(N) is SU(N)×U(1). The U(1) factor is related to the center of mass motion of the branes. On the black 3-brane side, it corresponds to certain low-energy modes which live in the transition region between the throat and flat space. These modes and the U(1) can be omitted from the correspondence (see e.g. [10]).

[8] Of course, since the gauge theory is conformal and AdS_5 is homogenous in the radial direction, both sides of the duality are invariant under such a transformation.

invariance. The leading insertion again results in a distance^{-3}-correction to the Newton potential [27].

In the RSI model, the AdS_5 space is additionally cut off in the IR by another brane. The dual theory correspondingly has a certain IR scale at which the conformal symmetry is broken (see e.g. [28]). Below this scale, we expect a discrete spectrum of particle-like states to which we refer as glueballs. This spectrum simply corresponds to the tower of KK modes in the RSI model. The latter fact can be used to determine the masses of glueballs from a KK expansion.

2.5 The Klebanov-Strassler throat

Up to now, we have considered D3-branes (and their backreaction) in 10d Minkowski space. Another interesting option for the embedding space is a product of 4d Minkowski space and the conifold. The latter is a 6-dimensional submanifold of $\mathbb{C}^4$ defined by the equation

$$z_1^2 + z_2^2 + z_3^2 + z_4^2 \;=\; 0\,. \tag{2.37}$$

One can show that this space is a cone[9] over the 5-dimensional manifold $T^{1,1} \equiv (\mathrm{SU}(2)\times\mathrm{SU}(2))/\mathrm{U}(1)$. It has a singularity at $(z_1, z_2, z_3, z_4) = 0$ [29]. The metric can be written as

$$ds^2 \;=\; dr^2 \;+\; r^2 d\Omega^2_{T^{1,1}}\,, \tag{2.38}$$

where $d\Omega^2_{T^{1,1}}$ is the line element on $T^{1,1}$. The space is Ricci-flat and an explicit Calabi-Yau metric is known [29] but will not be needed in the following. We place a large number N of parallel D3-branes, which are aligned along 4d Minkowski space, on the singularity of the conifold. The metric due to their backreaction is

$$ds^2 \;=\; H^{-1/2}(r)\,\eta_{\mu\nu}dx^\mu dx^\nu \;+\; H^{1/2}(r)\,\left[dr^2 + r^2 d\Omega^2_{T^{1,1}}\right]\,,$$
$$\text{where} \qquad H(r) \;=\; 1 + \frac{R^4}{r^4} \tag{2.39}$$

and R is given in Eq. (2.20). The gauge theory on the world-volume of the D3-brane stack was determined in [30]: It is a conformal $\mathcal{N} = 1$ $\mathrm{SU}(N)\times\mathrm{SU}(N)$ super-Yang-Mills with some chiral superfields and a certain superpotential. Studying the low-energy limit, we are led to a duality between this gauge theory and string theory on the small-r part of Eq. (2.39), which is $AdS_5\times T^{1,1}$.

It is interesting to look for nonconformal theories. To this end, one can place a certain number of fractional D3-branes on the conifold singularity in addition to D3-branes [31]. Topologically, $T^{1,1}$ is $S^3\times S^2$. Fractional D3-branes are D5-branes which are wrapped over the 2-cycle of $T^{1,1}$. Each fractional D3-brane sources a unit of F_3-flux through the 3-cycle of $T^{1,1}$, where F_3 is the field strength of the RR 2-form C_2.[10] This

[9] This can be seen from the fact that Eq. (2.37) is invariant under $z_i \to t z_i$ for real t.

[10] Our notation for the form-fields of type IIB supergravity is e.g. as in [3].

flux causes the 5-form flux through $T^{1,1}$ to depend on the radial coordinate r [31, 32]:

$$N_{\text{eff}}(r) \sim N + g_s M^2 \ln(r/r_0) . \tag{2.40}$$

Here, N and M are the numbers of D3-branes and fractional D3-branes, respectively, r_0 determines a UV scale and we have suppressed an $\mathcal{O}(1)$ factor in the second term.

The fluxes backreact on the geometry and this backreaction produces a so-called Klebanov-Strassler (KS) throat [4]: Sufficiently far away from the conifold singularity, the metric again has the form given in Eq. (2.39). Furthermore, the curvature scale R is fully specified by the number of 5-form flux N_{eff} as in Eq. (2.20) and the warp factor thus is

$$H(r) = 1 + \frac{R_{\text{UV}}^4 + R_{\text{IR}}^4 \ln(r/r_0)}{r^4} = 1 + \frac{R_{\text{IR}}^4 \ln(r/r_s)}{r^4} . \tag{2.41}$$

Here, R_{UV} and R_{IR} are, respectively, the AdS radius at the UV scale defined above and at an IR scale whose meaning will become clear in a moment. The AdS radii are determined by the corresponding numbers of 5-form flux $N_{\text{UV}} = N_{\text{eff}}(r_0) = N$ and $N_{\text{IR}} \sim g_s M^2$ (cf. Eq. (2.20)).

Comparing Eqs. (2.17) and (2.41) for small r, we see that the warping of the KS throat deviates logarithmically from AdS warping. Due to the relation between the radial coordinate r and the renormalization scale of the dual gauge theory, we conclude that the latter is no longer conformal. Indeed, the dual gauge theory, which has again $\mathcal{N} = 1$ supersymmetry, has running gauge couplings and performs a so-called duality cascade: The rank of the gauge group, which is $\text{SU}(N+M)\times\text{SU}(N)$ in the UV, is repeatedly reduced by a series of Seiberg duality transformations along the renormalization group flow towards the IR.

Close to $r = r_s$, the warp factor Eq. (2.41) vanishes and the metric becomes singular. This singularity is unphysical and can be removed if one replaces the conifold by the so-called deformed conifold [4]. The latter is a submanifold in $\mathbb{C}^4$ defined by the modified equation

$$z_1^2 + z_2^2 + z_3^2 + z_4^2 = \epsilon . \tag{2.42}$$

Due to the small constant ϵ, the singularity is replaced by a finite S^3 at the bottom of the deformed conifold. The KS throat is thus finite. This fact corresponds to the existence of a confinement scale in the dual gauge theory. Indeed, the duality cascade is stopped at a certain IR scale and the remaining gauge group confines.

2.6 Heated branes, throats and gauge theories

The black 3-branes that we have considered in Section 2.2 are also known as extremal 3-branes because they fulfill a BPS condition. A generalization are the non-extremal 3-branes with background metric

$$ds^2 = H^{-1/2}(r) \left[-f(r)\, dt^2 + dx^i dx_i\right] + H^{1/2}(r) \left[f^{-1}(r)\, dr^2 + r^2 d\Omega_5^2\right] ,$$
$$\text{where} \qquad f(r) = 1 + \frac{r_0^4}{r^4} \tag{2.43}$$

and the warp factor $H(r)$ is as before. This brane has a black hole horizon at $r = r_0$ which in turn has a certain Hawking temperature. This brane is therefore dual to a stack of D3-branes on which the world-volume gauge theory is heated to the same temperature (see [33]). Absorption calculations in order to test this correspondence where performed in [34]. The results for the D-brane stack (at zeroth order in the 't Hooft coupling λ but taking finite-temperature effects into account) and the non-extremal 3-brane have the form

$$\sigma_T \sim \sigma_0 \, f\Big(\frac{\omega}{T}\Big) \,. \tag{2.44}$$

Here, ω is the energy of the incident dilaton and T is the Hawking temperature. Furthermore, $\sigma_0 \sim \omega^3 R^8$ is the absorption cross section by an extremal 3-brane which was determined in Section 2.3. It was found in [34] that the function f differs for the 3-brane and the D-brane stack. This is not surprising: The fact that the zeroth order (in λ) calculation gave the correct result in Section 2.3 was due to a nonrenormalization theorem in 4d $\mathcal{N} = 4$ super-Yang-Mills theory. Such a nonrenormalization theorem is usually related to supersymmetry. At nonzero temperature, however, supersymmetry is broken and we cannot expect the nonrenormalization theorem to hold any more.

As in Section 2.4, we can study the low-energy limits of the non-extremal 3-brane and the heated D3-brane stack. In that way, we are led to a duality between string theory in the small r part of Eq. (2.43), the so-called AdS-Schwarzschild space, and the $\mathcal{N} = 4$ SU(N) gauge theory at nonzero temperature [35].

It is also interesting to analyze theories with IR cutoff or confinement scale at nonzero temperature. A simple example is provided by the RSI model and its dual gauge theory. The low-temperature phase can be described by a gas of KK modes or glueballs. From the gauge theory point of view it is clear that, if we raise the temperature above the confinement scale, the gauge theory undergoes a deconfinement phase transition. As we have discussed above, this deconfined phase is dual to an AdS-Schwarzschild geometry. In this phase, the IR brane is thus replaced by a Schwarzschild horizon. In turn, if the theory is cooled below the confinement scale, a confinement phase transition takes place. The corresponding transition between AdS-Schwarzschild and AdS_5 with IR cutoff was analyzed in [36]: It is first order and involves the nucleation of bubbles of the IR brane phase from the Schwarzschild horizon. Similarly, if the KS throat is heated above its critical temperature, it develops a horizon. The corresponding supergravity solution was found in [37]. The phase transition between this phase and the KS throat was studied in [38] using the full 10d geometry and in [39] using a 5d model of the KS throat developed in [40].

Chapter 3

String realizations of the Randall-Sundrum model

In this chapter, we will continue our review of material that will be relevant for this thesis. We will modify the geometries from the last chapter in order to obtain approximate RS models. The resulting solutions are examples of flux compactifications of type IIB string theory. In particular, we will see that approximate RS models are quite common in the landscape of type IIB flux vacua. More exhaustive reviews can be found e.g. in [41–43].

3.1 The Verlinde compactification

In the small-r region, the geometry of black 3-branes is $AdS_5 \times S^5$. These objects are therefore an interesting building block for a string realization of the RS model. Black 3-branes are not terminated at large r, however, but go over to 10d Minkowski space. In order to obtain an (approximate) RS model, we have to add an UV cutoff to this geometry. To this end, we consider an orientifold of type IIB string theory on a 6-torus T^6 [44]. This compactification has 64 O3-planes which are located at all the half-way points of the T^6. The charge of an O3-plane is $-1/4$ times that of a D3-brane. To fulfill the tadpole cancellation (or vanishing charge) condition, we place 16 D3-branes into the orientifold.[1] If these D3-branes are on top of each other, their backreaction on the geometry creates an $AdS_5 \times S^5$ throat which is glued into the torus [44]. To see this, recall that a black 3-brane, which is dual to a D3-brane stack, can approximately be viewed as a localized object which is embedded into flat space. The diameter of this object is given by the AdS scale. As long as the size L of the torus is larger than this diameter R, it should be possible to glue the black 3-brane into the torus. Moreover, even though the number of D3-branes is not very large, there is still a parameter range in which we can trust the supergravity approximation. Using Eq. (2.20) with $N = 16$

[1] More precisely, there are 32 D3-branes in the T^6. These are pairwise identified under the orientifold $\mathbb{Z}_2$-action.

and inserting the omitted numerical prefactor, we have to require that

$$g_s \gg \frac{1}{64\,\pi}\,. \tag{3.1}$$

In principle, we also have to take the backreaction of the O3-planes into account (see [44]). For simplicity, we will neglect it in the following. The metric is then given by[2]

$$ds^2 = H(\vec{x}_\perp)^{-1/2}\,\eta_{\mu\nu}\,dx^\mu_{\shortparallel}dx^\nu_{\shortparallel} + H(\vec{x}_\perp)^{1/2}\,dx^{\,i}_\perp dx_{\perp\,i}\,,$$
$$\text{where} \qquad H(\vec{x}_\perp) \,=\, 1+\sum_{\vec{n}\in\mathbb{Z}^6}\frac{R^4}{|\vec{x}_\perp-\vec{A}+\vec{n}L|^4}\,. \tag{3.2}$$

The coordinates along the 4 uncompactified dimensions are denoted by $x_{\shortparallel}$, the $x_\perp$ refer to coordinates in the torus and $\vec{A}$ is the position of the D3-brane stack. The sum in the warp factor H is due to mirror effects in the torus. In particular, we see that close to the D3-brane stack, i.e. for small $r=|\vec{x}_\perp-\vec{A}|$, the space is indeed $\mathrm{AdS}_5\times\mathrm{S}^5$. At large r, on the other hand, the space is cut off by the compactness of the torus.

We thus have obtained an approximate RSII model from string theory. The torus plays the role of the UV brane, whereas the $\mathrm{AdS}^5\times\mathrm{S}^5$ throat replaces the slice of AdS_5. As in the RSII model, we expect a normalizable 4d graviton. The 4d Einstein-Hilbert action is contained in the 10d action:

$$M_{10}^8\int d^{10}x\,\sqrt{g_{10}}\,\mathcal{R}_{10} \,\supset\, M_4^2\int d^4x_{\shortparallel}\sqrt{g_4}\,\mathcal{R}_4\,,$$
$$\text{where} \qquad M_4^2 \,=\, M_{10}^8\int_{T^6}d^6x_\perp\,H(\vec{x}_\perp) \,\sim\, M_{10}^8\,L^6\,. \tag{3.3}$$

We have used Eq. (3.2) and the fact that $L>R$ as discussed above. The integral thus yields a finite result and the 4d graviton is indeed normalizable.

3.2 Flux compactifications à la GKP

In the UV, the geometry of a KS throat (i.e. the small-r part of the geometry in Eqs. (2.39) and (2.41)) is approximately $\mathrm{AdS}_5\times\mathrm{T}^{1,1}$, whereas it is smoothly terminated in the IR. The KS throat is therefore an interesting building block for a string realization of the RSI model. A way to add a smooth UV cutoff to this geometry was found in a seminal paper by Giddings, Kachru and Polchinski (GKP) [3]:

Many Calabi-Yau manifolds develop conifold singularities at certain points in their moduli space. Close to this singularity, the manifold is then described by Eq. (2.37). More precisely, we consider an orientifold of such a Calabi-Yau and place N D3-branes and M fractional D3-branes on the conifold singularity. The tadpole cancellation (or vanishing charge) condition requires negative-charge objects somewhere in the rest of

[2]The backreaction of O3-planes leads to additional terms in the function $H(\vec{x}_\perp)$.

the compact space. These can be provided e.g. by some O3-planes. The backreaction of the D-branes on the geometry creates a KS throat and this yields a string realization of the RSI model: The IR end of the throat plays the role of the IR brane in the RSI model. Since the throat is embedded into the Calabi-Yau orientifold, it is also terminated in the UV. The (rest of the) Calabi-Yau orientifold thus corresponds to the UV brane of the RSI model.

The KS throat in this setup can equivalently be understood as a result of the backreaction of 3-form fluxes on a deformed conifold. This can be seen as follows: Each fractional D3-brane sources a units of F_3-flux through the 3-cycle of the $T^{1,1}$. This flux together with the F_5-flux from the D3-branes acts as a source for B_2. Moreover, the F_5-flux can be absorbed into B_2 (see [32]). Altogether, this leads to a certain number of H_3-flux (recall that $H_3 = dB_2$) through another 3-cycle which consists of the 2-cycle of the $T^{1,1}$ and the radial direction.[3] Since we consider a deformed conifold which is embedded into a compact space, this submanifold is indeed compact. Denoting the two 3-cycles by A and B, we have

$$\begin{aligned} \left(\frac{M_s}{2\pi}\right)^2 \int_A F_3 \;&=\; M \\ \left(\frac{M_s}{2\pi}\right)^2 \int_B H_3 \;&=\; -K\,. \end{aligned} \tag{3.4}$$

In order to determine the resulting hierarchy, we analyse the setup from a 4d viewpoint. A compactification of type IIB supergravity on a Calabi-Yau orientifold leads to an $\mathcal{N} = 1$ supersymmetric low-energy theory. Certain flux choices may also break this amount of supersymmetry but we restrict ourselves to a supersymmetric setup for simplicity. From the 4d perspective, the blow-up parameter ϵ in the defining equation of the deformed conifold, Eq. (2.42), is promoted to a 4d scalar field $z(x)$. Without fluxes, this scalar is massless and as such is an example of a modulus in string compactifications. The fluxes enter into a superpotential of the Gukov-Vafa-Witten type [3, 45]:

$$W \;=\; \int G_3 \wedge \Omega \;=\; \left(\frac{2\pi}{M_s}\right)^2 \left(M \int_B \Omega - K\,\tau \int_A \Omega \right)\,. \tag{3.5}$$

Here, $\tau = C + ie^{-\phi}$ is the axio-dilaton, $G_3 = F_3 - \tau H_3$ and Ω is the holomorphic 3-form. It is a well-known result [46] that[4]

$$\int_A \Omega \;=\; z \quad \text{and} \quad \int_B \Omega \;=\; \mathcal{G}(z) \;\equiv\; \frac{z}{2\pi i} \ln z \;+\; \text{holomorphic}\,. \tag{3.6}$$

As we will see in a moment, the holomorphic terms are not important for a leading-order analysis. For a supersymmetric vacuum, we have to require that $D_z W = 0$, where $D_z = \partial_z + (\partial_z \mathcal{K})$ is the Kähler covariant derivative and $\mathcal{K}$ is the Kähler potential:

$$0 \;=\; D_z W \;\propto M \partial_z \mathcal{G} - K\tau + \partial_z \mathcal{K}\,(M\mathcal{G} - K\tau z) \;\sim\; \frac{M}{2\pi i} \ln z - i\frac{K}{g_s}\,. \tag{3.7}$$

[3] This cycle is the Poincaré dual of the 3-cycle of the $T^{1,1}$.

[4] The first equation is usually taken as a definition for the modulus z. We have already defined z in a different way, namely via Eq. (2.42) (recall that $\epsilon \to z$).

For the last result, we have assumed that $K \gg g_s$ and that z is exponentially small. Solving for z, we see that the latter assumption can be justified if M is not too large:

$$z \sim e^{-2\pi K/Mg_s} . \tag{3.8}$$

In order to estimate the generated hierarchy between the UV end, where the throat goes over to the embedding Calabi-Yau orientifold, and the IR end, we can neglect the logarithmic running of the AdS scale R in a KS throat. Deep in the throat, the warp factor Eq. (2.41) is $H(r) \simeq (R/r)^4$. As we have seen in Section 2.1, 4d energy scales of processes which are located at a certain distance r in the throat are rescaled by a factor of $h^{-1} \equiv H(r)^{-1/4} \simeq r/R$ (cf. Eq. (2.13)). Due to the deformation of the conifold, the S^3 inside the $T^{1,1}$ does not shrink to zero size at the tip (as for the singular conifold) but it only shrinks to a certain radius r_c. The throat is then terminated in the IR at this value of the radial coordinate r. From the explicit supergravity solution from [4], we know that the size of the S^3 at the bottom of the KS throat is $r_c \sim z^{1/3}R$. The hierarchy between the unwarped part of the compact space and the bottom of the KS throat thus is

$$h \sim e^{2\pi K/3Mg_s} . \tag{3.9}$$

To give an example: For $K = 9$, $M = 5$ and $g_s = 0.1$, we find $h \sim 10^{16}$, the hierarchy between the Planck scale and the electroweak scale.

We see from the result in Eq. (3.8) that the (complex-structure) modulus $z(x)$ is stabilized by the 3-form flux. More generally, it was shown in [3] that the other complex-structure moduli of the Calabi-Yau orientifold can be stabilized as well by using 3-form flux. In addition, it is possible to fix the dilaton at a small value (as we have assumed in deriving Eq. (3.8)).

For completeness, let us mention that it is not possible to stabilize the Kähler moduli along the lines of [3]: They remain flat directions of the scalar potential. This flatness is due to a cancellation in the scalar potential which in turn results from the form of the tree-level Kähler potential (which is of the so-called no-scale type). Perturbative corrections to the Kähler potential may lead to the stabilization of the Kähler moduli (see e.g. [47] and references therein).[5] Alternatively, non-perturbative corrections to the superpotential may depend on the Kähler moduli. This fact was employed in the seminal work by Kachru, Kallosh, Linde and Trivedi (KKLT) to construct stabilized de Sitter vacua [48]: Using D3-instantons or gaugino condensation on D7-branes, the universal Kähler modulus can indeed be stabilized but the resulting vacuum has a negative cosmological constant. This vacuum can be uplifted by adding an anti-D3-brane in a warped region. By varying the length of this throat, the contribution of the brane to the vacuum energy can be fine-tuned in order to yield a vacuum with a small, positive cosmological constant. Although this vacuum is only metastable, its lifetime can be shown to be considerably larger than the age of the universe.

[5] Recall that the Kähler potential, as opposed to the superpotential, is not protected from perturbative corrections.

3.3 Statistics

Calabi-Yau manifolds can have a large number of 3-cycles. Through each of these 3-cycles, one can have some 3-form flux as in Eq. (3.4). The resulting variety of different flux configurations on different Calabi-Yau orientifolds is known as the landscape of type IIB flux vacua. The large number of vacua ($\sim 10^{500}$ in some estimates) in this type of constructions makes them amenable to statistical analysis [49]. In particular, given a Calabi-Yau orientifold, one can ask for the number of vacua in which the complex-structure moduli (and the dilaton) are stabilized at a particular value. In [50, 51], it was shown how to calculate this number from the metric on the corresponding moduli space.

We will particularly be interested in the number of vacua which have strongly warped regions. Such throats are formed if the modulus z, which controls the size of the 3-cycle at the tip of a conifold, is stabilized by flux at an exponentially small value. Here, $z = 0$ corresponds to a situation with a vanishing 3-cycle and a singularity at the tip of the conifold. For a Calabi-Yau orientifold with a single conifold singularity, the number of vacua with $|z| < |z_*|$ was found to be [51]

$$\mathcal{N} \propto \frac{1}{\log(1/|z_*|)} \,. \tag{3.10}$$

Let us consider a more general Calabi-Yau orientifold. We denote the number of 3-cycles by K. The moduli space will contain regions in which certain 3-cycles shrink to zero size. In these regions, a singularity develops in the Calabi-Yau orientifold. In [9], it was argued that often, presumably even for an $\mathcal{O}(1)$ fraction, these singularities are conifold singularities. Let us choose coordinates on moduli space such that these conifold singularities arise for $z_i = 0$ with $i = 1 \ldots K$. It was furthermore argued in [9] that the probability that a randomly chosen vacuum is near $z_j = 0$ for some j will have the same parametric dependence as Eq. (3.10). If we assume that the probabilities are uncorrelated, we can calculate the expected number of 3-cycles which are smaller than some value $|z_*|$. Using also the relation between moduli coordinates z and generated hierarchy h ($h \sim z^{-1/3}$ as we have found at the end of Section 3.2), the expected number of throats with a hierarchy larger than some h_* follows as [9]

$$\bar{n}(h > h_*) \,=\, \frac{K}{3c \log h_*} \,. \tag{3.11}$$

Here, c is an unknown constant of order 1 which is related to the normalization of the aforementioned probabilities.

Chapter 4

Energy transfer between throats

4.1 A motivation: Reheating after brane-antibrane inflation

We will now discuss a motivation for the topics which will be analysed in subsequent chapters. A different application of the results from these chapters will be presented in Chapters 8 and 9.

Branes allow for an interesting realization of the inflationary scenario [52]. Two branes, which are initially separated in the extra dimensions and which exert an attractive force on each other, will move towards each other. From a 4d viewpoint, the relative distance between these branes is a scalar field which rolls down a potential. If this potential is sufficiently flat, the brane motion can lead to slow-roll inflation.

A string theory realization of this idea is provided by a D3-brane and an anti-D3-brane which are aligned along the noncompact dimensions [53, 54].[1] Unfortunately, for branes in flat extra dimensions, the potential is usually too steep to achieve slow-roll inflation with enough e-foldings. The potential is much flatter if the branes instead move in a warped region [55]. More precisely, we consider a KS throat in a flux compactification as in Section 3.2. We place the anti-D3-brane at the tip of the KS throat. It will approximately remain fixed at this position due to the background fluxes. As a result of the warping, the potential between the brane and the antibrane is very flat. If the D3-brane starts far away from the tip, slow-roll inflation with a sufficient number of e-foldings is thus possible.

Inflation ends when the brane comes close to the antibrane. The subsequent annihilation of the branes produces a large amount of KK modes which are localized in the throat.[2] If the standard model is realized on some D-branes in that same throat, the

[1] Recall that two D3-branes exert no force on each other, hence the anti-D3-brane.

[2] More precisely, an open string tachyon develops at substringy distances [56] whose condensation produces a large amount of massive, closed string states [57]. The final phase of brane-antibrane inflation is thus similar to the waterfall regime of hybrid inflation. The massive string states in turn decay quickly

KK modes decay to standard model fields and thereby lead to the reheating of the visible sector. There are reasons, though, to prefer that the standard model and inflation are realized in different throats. Most importantly, in order to reproduce the observed amplitude of density fluctuations, the throat in which inflation takes place should have an IR scale of the order of 10^{14} GeV [55]. If the standard model lives in such a throat, a solution of the hierarchy problem à la RS is not possible.

The KK modes in the inflation throat, however, have only very weak couplings to the rest of the compact manifold. Namely, due to the warping, they have to climb a potential well before they can reach the unwarped part or other throats. It is therefore not immediately clear whether reheating will be successful if the standard model is not realized in the inflation throat. A detailed analysis in a series of papers [58–62] has shown that, at least for a certain range of parameters, viable reheating is possible.

Obviously, a crucial quantity in this respect is the decay rate of KK modes from one throat to another throat. The energy density of KK modes is diluted by the expansion of the universe. The reheating temperature of the standard model therefore depends on this decay rate. It was calculated in a 5d model in [63] and we will review this calculation in the next section. In Chapter 5, we will present a calculation of the decay rate in a 10d model.

4.2 The tunneling calculation using a 5d model

We consider a Calabi-Yau orientifold with two strongly warped regions. We do not need to specify the precise form of these throats, but we assume that they are finite and reasonably well approximated by a slice of AdS_5 times some compact 5d manifold $\mathcal{M}$. The prime example certainly is a KS throat. For simplicity, we also assume that both throats have the same AdS scale R. The size L of the embedding manifold is larger than this AdS scale, $L \gtrsim R$, since otherwise the throats could not be glued into the manifold. If the embedding manifold is of minimal size, $L \sim R$, KK modes with masses $m_n \ll R^{-1}$ cannot resolve its precise geometry. We can then describe the embedding manifold by the UV brane in a RS model. A setup with two such throats can correspondingly be approximated by two RSI models which are glued together at a common UV brane (cf. Fig. 4.1) times the compact manifold $\mathcal{M}$. The metric for this setup (ignoring $\mathcal{M}$) is given by Eqs. (2.3) and (2.6) but the 5th coordinate y now runs from $y_1 < 0$ to $y_2 > 0$ and negative and positive coordinate values are no longer identified. We want to determine the transition rate of KK modes from one throat to the other throat. For simplicity, we consider only KK modes of the 4d graviton and restrict ourselves to s-waves with respect to the compact manifold $\mathcal{M}$. A convenient parameterization for these spin-2 fluctuations is

$$ds^2 \;=\; e^{-2k|y|}\,\left(\eta_{\mu\nu} + h_{\mu\nu}(x,y)\right)\,dx^\mu dx^\nu + dy^2\,, \tag{4.1}$$

where $k = R^{-1}$ is the inverse AdS radius.

to massless string states, respectively to KK modes of the corresponding supergravity fields.

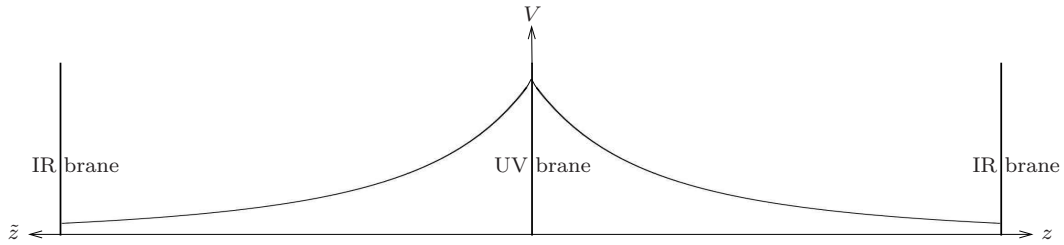

Figure 4.1: *Two throats in a compact space approximated by two RSI models which are glued together at a common UV brane. A KK mode in one throat has to tunnel through an effective energy barrier before it can decay to the other throat.*

The linearized equation of motion for the fluctuation $h_{\mu\nu}$ is a Laplace equation [64, 65]

$$\partial_M \left(\sqrt{g} g^{MN} \partial_N h_{\mu\nu}\right) = 0\,, \tag{4.2}$$

where g^{MN} is the background metric. We consider eigenstates of the 4d d'Alembertian,

$$h_{\mu\nu}(x,y) \;=\; \epsilon_{\mu\nu}\, e^{ipx}\, \psi(y)\,, \tag{4.3}$$

where $\epsilon_{\mu\nu}$ is a polarization tensor, $p^2 = -m^2$ and m is the 4d mass of the mode. We focus on the first throat (i.e. $y < 0$) for the moment and introduce a new (dimensionless) coordinate $z \equiv k^{-1} e^{k|y|}$ and a rescaled field $\chi \equiv z^{-3/2}\psi$ in this throat. Using Eq. (4.3) in Eq. (4.2), the equation of motion can be written as

$$-\frac{d^2}{dz^2}\,\chi(z) + \frac{15}{4z^2}\,\chi(z) = m^2\,\chi(z)\,. \tag{4.4}$$

This is a Schrödinger equation with a potential which is given by the second term on the l.h.-side and which we have plotted, together with the corresponding potential for the second throat, in Fig. 4.1.[3] As one can see, a light mode has to tunnel through an effective energy barrier before it can reach the other throat. The mode has to fulfill certain boundary conditions at the IR branes and the UV brane. Note, however, that we do not take the boundary conditions on the IR branes into account. It was shown in [59] that, at least for orbifold boundary conditions, the results from the following calculation are not changed up to $\mathcal{O}(1)$ prefactors by the IR boundary conditions.

The equation of motion can be solved in terms of Bessel functions. Going back to the unrescaled field, we have

$$\psi(z) \;=\; A\,(mz)^2\, H_2^+(mz) + B\,(mz)^2\, H_2^-(mz)\;. \tag{4.5}$$

For later convenience, we have written the solution in terms of Hankel functions $H_2^\pm = J_2 \pm i Y_2$, where J_2 and Y_2 are Bessel functions. The constants A and B will be determined in a moment.

Next, we introduce a new coordinate $\tilde{z}$ for the second throat (i.e. for $y > 0$) and denote the unrescaled field and the rescaled field in that throat by $\tilde{\psi}$ and $\tilde{\chi}$, respectively.

[3] As expected, Eq. (4.4) is the same as Eq. (2.23) for $l = 0$, up to the term proportional to z^{-4}.

We have

$$\tilde{\psi}(\tilde{z}) \;=\; \tilde{A}\,(m\tilde{z})^2\,H_2^+(m\tilde{z}) + \tilde{B}\,(m\tilde{z})^2\,H_2^-(m\tilde{z})\;. \tag{4.6}$$

We want to determine the transition (or tunneling) probability of a mode from the first throat to the second throat. Accordingly, we consider a wave which is incoming in the second throat. This corresponds to $\tilde{A} = 1$ and $\tilde{B} = 0$. To see this, note first that the mass of the tunneling KK mode is quantized in units of $m_{\rm IR} = e^{-k\ell_1}k$ according to Eq. (2.10), where ℓ_1 is the length of the first throat. We assume that the second throat is longer than that, i.e. $\ell_2 > \ell_1$. Near the IR brane of the second throat we then have $m\tilde{z} \gg 1$ and can use the asymptotic forms of the Bessel functions for large arguments. We find $\tilde{\psi} \propto \tilde{z}^{3/2}e^{im\tilde{z}}$ which is an incoming wave as one can see from the time-dependence in Eq. (4.3).

We determine the constants A and B from the requirement that both solutions, Eqs. (4.5) and (4.6), as well as their first derivatives match smoothly at $z = \tilde{z} = R$, corresponding to $y = 0$.[4] That is, we have to require that $\psi(R) = \tilde{\psi}(R)$ and $\psi'(R) = -\tilde{\psi}'(R)$.[5] Since $mR \ll 1$ (cf. Eq. (2.10)), we can use the asymptotic forms of the Bessel functions for small arguments:

$$\psi(z) \;\sim\; (A+B)\,(mz)^4 + i\,(B-A)\left(1+(mz)^2\right) + \ldots \tag{4.7}$$

$$\tilde{\psi}(\tilde{z}) \;\sim\; (m\tilde{z})^4 - i\,\left(1+(m\tilde{z})^2\right) + \ldots \tag{4.8}$$

The ellipsis represent higher order corrections and we have neglected numerical prefactors. The tunneling probability $\mathcal{P}$ is given by the ratio of amplitudes of the outgoing wave in the first throat and the incoming wave in the second throat. Thus, we have to calculate $\mathcal{P} \sim |\tilde{A}/B|^2 = |1/B|^2$. Matching and solving for B, we find [63]

$$\mathcal{P} \;\sim\; (mR)^4\;. \tag{4.9}$$

A mode that is initially localized in the first throat is described by a wave packet in that throat. This wave packet can be decomposed into two sets of modes which move in the IR direction and in the UV direction, respectively. If the barrier on the UV side were impenetrable, the modes would be reflected entirely. However, since a small fraction of the incoming flux is able to penetrate the barrier, the wave leaks out of the throat. A wave packet initially localized in the throat will thus decohere. The incoming flux at the barrier $j_{\rm in}$ and the tunneling probability $\mathcal{P}$ determine the decay rate Γ:

$$\Gamma \;=\; j_{\rm in}\mathcal{P}\,. \tag{4.10}$$

To determine Γ, we need solutions to Eq. (4.4) describing waves which are reflected back and forth between the UV barrier and the IR end of the throat. From these we can calculate the incoming flux $j_{\rm in}$. For $z \gg m^{-1}$, we can neglect the last term in the

[4]Note that there is no jump in the first derivative at $y = 0$ if the fluctuation is parametrized as in Eq. (4.1). This follows from Eq. (4.2).

[5]The minus sign is due to the fact that both coordinates, z as well as $\tilde{z}$, grow in the directions away from the UV brane.

potential in Eq. (4.4), keeping only the constant term. In this limit, the solution is simply given by plane waves:

$$\chi(z) \simeq A \cos mz + B \sin mz \,. \tag{4.11}$$

The approximation is valid for $z_{\rm IR} \geq z \gg m^{-1} \sim z_{\rm IR}/n$, where $z_{\rm IR} = k^{-1} e^{k\ell_1} = m_{\rm IR}^{-1}$ is the position of the IR brane and we have used Eq. (2.10). If n is not too small, the mode is well approximated by a plane wave in a large portion of the throat. Deviations from this form for $z \lesssim m^{-1}$ are due to reflection at and tunneling through the effective barrier.

To calculate $j_{\rm in}$ from Eq. (4.11), we have to determine the normalization of the solution in physical terms. As a simplification, we consider a complex scalar and a plane wave moving around an S^1 parametrized by $z \in [0, z_{\rm IR})$. Going to the rest frame with respect to momenta parallel to the brane and reinstating time dependence, we have

$$\chi(z) = \mathcal{N}\, e^{im(z+t)} \tag{4.12}$$

for the plane wave moving towards the UV barrier. To determine the normalization constant $\mathcal{N}$, we use the standard charge density for a Klein-Gordon particle, $j^0 = \mathrm{Im}(\chi^* \partial_t \chi)$. It has to be normalized according to

$$1 = \int_0^{z_{\rm IR}} dz\, j^0 \quad \Rightarrow \quad \mathcal{N} = \frac{1}{\sqrt{m z_{\rm IR}}} \,. \tag{4.13}$$

The flux is then given by $j_{\rm in} = j^z = \mathrm{Im}(\chi^* \partial_z \chi)$. Using the solution of Eq. (4.12) with the normalization of Eq. (4.13), we find

$$j_{\rm in} = \frac{1}{z_{\rm IR}} = m_{\rm IR} \,. \tag{4.14}$$

Using this result and Eq. (4.9), the decay rate of a graviton KK mode follows from Eq. (4.10) as [63]

$$\Gamma \sim m_{\rm IR} (mR)^4 \,. \tag{4.15}$$

4.3 Two other ways to derive the decay rate

We will now derive the decay rate Eq. (4.15) of KK modes between two throats in a different way. Similar to the last section, we assume that the AdS scale of the first throat is of the same order as the size of the embedding manifold, $R_1 \sim L$, and that this throat can well be approximated by a RSI model times a compact manifold $\mathcal{M}$. We restrict ourselves to KK modes of the graviton and to an s-wave with respect to the compact manifold $\mathcal{M}$. Let us furthermore assume that the second throat has the geometry $\mathrm{AdS}_5 \times \mathrm{S}^5$. In this case, it can equally well be described by a stack of D3-branes. Its AdS scale R_2 cannot be larger than the size L of the embedding manifold, and since we have assumed that $L \sim R_1$, we have $R_1 \gtrsim R_2$. The corresponding number

N_2 of D3-branes follows from Eq. (2.20) as $N_2 \sim M_{10}^4 R_2^4$. Now, when viewed from the first throat, the U(N_2) gauge theory on the stack of N_2 D3-branes resides on the UV brane. Therefore, the graviton KK modes in this throat couple directly to the energy-momentum tensor of the gauge theory.

The KK expansion of the graviton in a RS model is reviewed in Appendix A. In particular, the coupling of the KK modes $h_{\mu\nu}^{(n)}$ to the energy-momentum tensor $T^{\mu\nu}$ on the UV brane is given in Eq. (A.12):[6]

$$S \supset \frac{g_n}{M_{10}^4 R_1^3} \int d^4x \, h_{\mu\nu}^{(n)} \, T^{\mu\nu} \, . \tag{4.16}$$

We have used Eq. (3.3) and the fact that $L \sim R_1$. The coupling constants g_n are given in Eq. (A.13),

$$g_n \sim \sqrt{m_n m_{\text{IR}}} \, R_1 \, , \tag{4.17}$$

where we have used $k = R_1^{-1}$ as well as Eq. (2.10) for the masses m_n of the KK modes and the IR scale m_{IR}.

Using Eqs. (4.16) and (4.17), the decay of graviton KK modes into the second throat can be calculated as a decay into gauge fields.[7] By the standard formula, the decay rate of a graviton KK mode into one species of gauge fields is

$$\Gamma \sim \frac{m_n^4 m_{\text{IR}}}{M_{10}^8 R_1^4} \, . \tag{4.18}$$

There are N_2^2 gauge fields in the adjoint representation of U(N_2). Summing and using Eq. (2.20), the total decay rate follows:

$$\Gamma \sim \frac{R_2^8}{R_1^4} \, m_n^4 \, m_{\text{IR}} \, . \tag{4.19}$$

For $R_1 \sim R_2$, Eq. (4.19) gives the same result as Eq. (4.15), including the factor of m_{IR}! Note that this decay process is just the reverse of the energy loss by the heated UV brane considered e.g. in [68, 69].

There is yet another way to derive Eq. (4.15), which is due to Ref. [70]. To this end, one considers a KK expansion in the geometry with two throats. As in the last section, one models this geometry by two RS models with AdS scale R which are glued together

[6] The usual orbifold boundary conditions were taken for the derivation of coupling strengths and masses of graviton KK modes. It is not immediately clear whether the same boundary conditions follow from a reduction to 5d of a 10d geometry since the effective theory is defined on an interval instead of an $S^1/\mathbb{Z}_2$ orbifold. However, one can rederive the RS model on an interval if one takes Gibbons-Hawking terms [66] at the IR and the UV brane into account. Varying with respect to the metric yields a condition similar to the Israel junction condition, to be evaluated only at one side of the brane. Inserting the background metric, one finds the relation between the cosmological constants on the brane and in the bulk as well as the usual boundary conditions for the fluctuations (see e.g. [67] for a derivation of the Israel junction condition using Gibbons-Hawking terms).

[7] There are also decays into the fermions and scalars in the gauge theory. However, the corresponding decay rates have the same order of magnitude as the decay rate into gauge fields.

at a common UV brane. As before, it is assumed that the second throat is much longer than the first throat. It turns out [70] that the amplitudes of KK modes are sizeable in the first throat only around certain resonance peaks. These peaks occur for the discrete set of masses m_n which would follow from a KK expansion in the first throat if that throat would be taken as an isolated system. The width of the peaks is

$$\delta m_n \sim m_n^5 R^4 \,. \tag{4.20}$$

Now, consider a mode which is created in the first throat. This mode can be viewed as a wave packet which is fully localized in that throat, i.e. whose amplitude vanishes in the second throat. The spread in frequencies of this wave packet is roughly given by the width δm_n of the amplitude peaks. Due to the different time evolution of the constituent modes, the wave packet decoheres after a time $t_{\rm dec}$ and the amplitude no longer vanishes in the second throat. This is the analogue of the KK mode decay that we have discussed before. The decoherence time can be estimated as $t_{\rm dec} \sim \delta m_n^{-1}$. Thus, in this approach the decay rate follows as

$$\Gamma \sim \delta m_n \sim m_n^5 R^4 \,. \tag{4.21}$$

For the light modes, $m_n \sim m_{\rm IR}$, this once again is the same result as Eq. (4.15).

Chapter 5

Heat transfer between throats from a 10d perspective

5.1 Preliminaries

For the calculations in the last chapter, we have assumed that the size L of the embedding manifold is of the same order of magnitude as the AdS scales R of the throats. Of course, this is not always the case. In the following, we will determine the rates of heat transfer for larger embedding manifolds. In this case, a 5d model is no longer sufficient and we have to take the full 10d geometry into account. To this end, we consider two throats which are separated at distance A and which are embedded into a compact manifold of size L (cf. Fig. 5.1).

We will perform the calculation for a simple example – two semi-infinite $\mathrm{AdS}_5 \times \mathrm{S}^5$ throats embedded in a 6-dimensional torus. This is similar to the Verlinde compactification discussed in Section 3.1. As it stands, though, our model is not a consistent compactification since negative-charge objects are needed to fulfill the tadpole cancellation condition. However, in the course of our calculation we will argue that including these and other objects (e.g. further D-branes) as well as using a different embedding manifold and a different throat geometry only leads to $\mathcal{O}(1)$ corrections.

The calculation of the heat transfer rate between these two throats turns out to be a multi-dimensional tunneling problem. Since such a problem is difficult to solve, we choose a different approach: As we have discussed in Section 2.2, $\mathrm{AdS}_5 \times \mathrm{S}^5$ throats are the near-horizon geometries of black 3-branes which in turn correspond to stacks of D3-branes.[1] Due to this fact, instead of the aforementioned geometry with throats, we can equally well consider a torus with two D3-brane stacks.

In this picture, the heat transfer from throat to throat is rephrased as heat transfer between the two world-volume gauge theories. This reduces the problem to the calcula-

[1] Recall that the number N of branes in each stack is related to the S^5 radius R of the corresponding throat by Eq. (2.20).

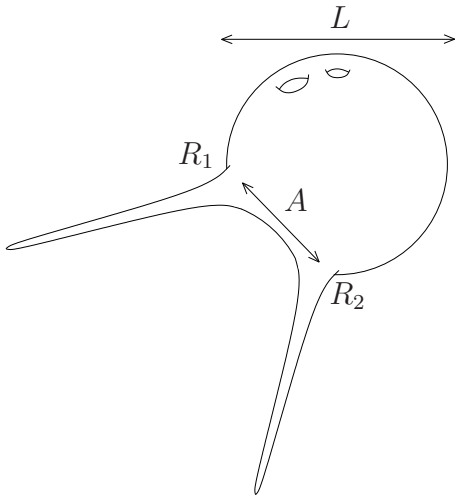

Figure 5.1: *Two throats with AdS radii R_1 and R_2 separated at distance A inside a Calabi-Yau orientifold of total size L.*

tion of simple processes in quantum field theory. To see this, consider a throat which is heated to a certain temperature T. As we have discussed in Section 2.6, such a throat is the near-horizon geometry of a non-extremal black 3-brane which is dual to a D3-brane stack with a heated world-volume gauge theory. The latter is coupled to the world-volume theory on the second brane stack (corresponding to the second throat) by the supergravity fields in the embedding space. Heat transfer between the two throats then is, in this picture, due to processes of the type shown in Fig. 5.2, where fields in the thermal plasma on one brane stack scatter into fields on the other brane stack.

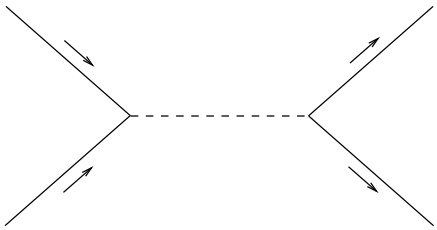

Figure 5.2: *Feynman diagram for the scattering of fields on one brane stack into fields on another brane stack.*

We will now calculate this heat transfer rate from a heated throat to another throat. An application of the result will be presented in Section 8.2. The decay rate of KK modes between two throats, which generalizes the results from the last chapter, will be determined in Chapter 6, using similar methods. We will restrict our calculation to the mediation by the dilaton, the RR scalar and the graviton polarized parallel to the branes. In the gravity picture these three fields satisfy the same wave equation [21]. Correspondingly, in the gauge theory picture their effect in mediating heat transfer is parametrically the same.[2] Hence, we can further restrict our calculation to one of the

[2]This can also be inferred from the relevant part of the DBI action, which couples them to the

three fields, which we take to be the dilaton. In particular, we will not consider the effect of fermions living in the embedding manifold. In fact, in [71] the absorption cross section of dilatinos by 3-branes was calculated and found to agree with the result for the dilaton. Therefore, we expect the fermions to give parametrically the same contribution as the fields that we consider.

Recall from Section 2.2 that the (low-energy) world-volume theory on N parallel D3-branes is $\mathcal{N} = 4$ U(N) super Yang-Mills. Its field content is given by the field strength $F_{\alpha\beta}$ in the adjoint representation, six adjoint scalars X^i corresponding to the positions of the branes, and fermionic superpartners. The relevant couplings between the dilaton ϕ and the world-volume theory are given in Eq. (2.33):

$$S \supset \frac{M_{10}^{-4}}{2^{3/2}} \left[\int d^4x \, \phi(x, \langle \vec{X} \rangle) \, F_{\alpha\beta}^2 + \sum_{l=1}^{\infty} \int d^4x \frac{M_{10}^{-2l}}{l! \pi^{l/4}} \left(\partial_{i_1} \cdots \partial_{i_l} \phi \right) X^{i_1} \cdots X^{i_l} \, F_{\alpha\beta}^2 \right]. \quad (5.1)$$

Here, $\langle \vec{X} \rangle$ is the position of the brane stack. The dilaton ϕ and the X^i are defined such that their kinetic terms are canonically normalized. We ignore couplings to fermions, since they are proportional to the fermionic equations of motion and thus give no contributions to S-matrix elements [21]. Direct couplings between the dilaton ϕ and the scalars X^i are absent. Moreover, as can be seen from Eq. (5.1), couplings involving the X^i as well as $F_{\alpha\beta}$ are suppressed by extra factors of M_{10}^{-2l} and can therefore be ignored.

5.2 Energy loss rate to flat 10d space

Before we proceed, we should check whether a calculation in terms of weakly coupled gauge fields is a good approximation in the strongly coupled regime of the gauge theory. At zero temperature, this is adequate due to the nonrenormalization theorem discussed at the end of Section 2.3. However, the gauge theory is at finite temperature, which breaks supersymmetry. With supersymmetry being broken, this nonrenormalization theorem cannot be expected to hold and it is not immediately clear why to trust our calculation. Therefore, we analyse a simple example in both the gauge theory and the gravity picture and compare the results. Namely, we consider a heated stack of D3-branes in flat 10d space which is dual to a non-extremal black 3-brane and calculate the energy loss rate in both pictures.

We model the heated, strongly-coupled gauge theory on the D3-brane stack by a thermal plasma of free fields. In principle, one would have to use finite temperature field theory for the calculation of the energy loss rate. However, as we are only interested in the correct order of magnitude, we can perform a zero-temperature calculation using a thermal particle distribution in the initial state. Following from Eq. (5.1), the cross section for scattering of two gauge bosons into one dilaton is

$$\sigma \sim \frac{s^3}{M_{10}^8} \quad (5.2)$$

world-volume theories on the D3-branes.

up to $\mathcal{O}(1)$ prefactors, where $\sqrt{s}$ is the energy of the gauge bosons in the center of mass frame. From Eq. (5.2), we can calculate the rate of energy loss per world-volume of the branes induced by this scattering process. This is done by thermally averaging the product of cross section and lost energy, in analogy to the standard calculations of reaction rates in a hot plasma [68, 72]:

$$\dot{\rho} = \frac{1}{2} \int d^3k_1 \, d^3k_2 \; f(\omega_1) \, f(\omega_2) \, \sigma v \, (\omega_1 + \omega_2) \, . \tag{5.3}$$

Here

$$f(\omega) = \frac{1}{4\pi^3 (e^{\omega/T} - 1)} \tag{5.4}$$

is the distribution function for the gauge bosons, v is the relative velocity of the colliding particles, and T is the temperature of the heated gauge theory. Inserting Eq. (5.2) into Eq. (5.3), we get the energy loss rate due to scattering of one gauge boson species. To get the total energy loss rate, we have to sum over all species and polarizations. In a U(N) gauge theory there are N^2 gauge bosons. Thus, there is an extra factor of $2N^2$ coming from the summation. Using Eq. (2.20) and neglecting prefactors of order one coming from the integration in Eq. (5.3), we get

$$\dot{\rho} \sim R^8 \, T^{13} \, , \tag{5.5}$$

where R is the AdS scale of the corresponding black 3-brane.

Energy loss from the non-extremal black 3-brane is due to Hawking radiation emitted by its black hole horizon. The corresponding rate per brane world-volume $\dot{\rho}$ is given by a generalization of the Hawking formula (see e.g. [10]). If we restrict ourselves to the dilaton, we get

$$\dot{\rho} = \int \frac{d^9k}{(2\pi)^9} \, \frac{v \, \omega \, \sigma_T(\omega)}{e^{\omega/T} - 1} \, , \tag{5.6}$$

where v is the velocity of the emitted particles and T is the Hawking temperature of the horizon. The absorption cross section of a dilaton by a non-extremal black 3-brane is given in Eq. (2.44): $\sigma_T \sim \sigma_0 \, f(\omega/T)$, where $\sigma_0 \sim \omega^3 R^8$ is the absorption cross section at zero temperature and f is some function. Using this result and performing the integral, we have

$$\dot{\rho} \sim R^8 \, T^{13} \, . \tag{5.7}$$

Here we have neglected prefactors of order one which come in particular from the integration over $f(\omega/T)$.

Both results for the energy loss rate, Eqs. (5.5) and (5.7), agree up to $\mathcal{O}(1)$ factors. Accordingly, a weak-coupling calculation in the gauge theory picture gives the right order of magnitude. The crucial ingredient is the fact that the absorption cross section σ_T of a dilaton by a non-extremal black 3-brane differs from the zero-temperature absorption cross section σ_0 only by a function of $\lambda \equiv \omega/T$. By gauge/gravity duality, this means that the gauge boson-dilaton vertex is corrected by a function of λ at non-zero temperature.[3] Accordingly, the cross section for the process in Fig. 5.2 that we will

[3] This is also the case if one takes finite-temperature effects properly into account on the gauge theory side.

calculate assuming weak coupling and zero temperature has to be corrected by a function of λ. However, inserting the corrected cross section into Eq. (5.3) and performing the integral will just give a different $\mathcal{O}(1)$ prefactor, which we ignore anyway.

5.3 Heat transfer rate to a different throat

Let us now calculate the cross section for the process in Fig. 5.2. To this end, we need the KK expansion of the dilaton in a 6d torus,

$$\phi(x, \langle\vec{X}\rangle) = \sum_{\vec{n}\in\mathbb{Z}^6} \frac{1}{L^3}\, e^{2\pi i \vec{n}\langle\vec{X}\rangle/L}\, \Phi_{\vec{n}}(x)\,, \tag{5.8}$$

where L is the size of the torus and the expression is already evaluated at the position $\langle\vec{X}\rangle$ of one brane stack. The mass of the $\vec{n}$th KK mode is $m_{\vec{n}} = 2\pi|\vec{n}|/L$. Inserting Eq. (5.8) into Eq. (5.1), one sees that the vertex for the $\vec{n}$th KK mode in Fig. 5.2 is

$$\sim \frac{s}{M_{10}^4\, L^3}\, e^{2\pi i \vec{n}\langle\vec{X}\rangle/L}\,. \tag{5.9}$$

Here the energy in the center of mass frame of the gauge bosons is denoted by $\sqrt{s}$. Let $\langle\vec{X}_1\rangle$ and $\langle\vec{X}_2\rangle$ be the positions of the two brane stacks inside the T^6. If we denote the relative distance of the stacks by $\vec{A} \equiv \langle\vec{X}_2\rangle - \langle\vec{X}_1\rangle$ and introduce the shorthand $\vec{a} \equiv 2\pi\vec{A}/L$, the matrix element corresponding to the process in Fig. 5.2 is given by

$$\mathcal{M} \sim \frac{s^2}{M_{10}^8\, L^6} \sum_{\vec{n}\in\mathbb{Z}^6} \frac{e^{i\vec{n}\vec{a}}}{s - m_{\vec{n}}^2 + i\epsilon}\,. \tag{5.10}$$

We have ignored prefactors of order one. For phenomenological purposes, we can safely assume $\sqrt{s} < L^{-1}$. Namely, since the energy $\sqrt{s}$ of the colliding gauge bosons is determined by the temperature T of the heated gauge theory, this corresponds to $T < L^{-1}$. If this were not the case, the gauge theory would heat up the compact manifold and the geometrical picture would be lost. Following from $\sqrt{s} < L^{-1}$, one has $s < m_n^2$ for $n > 0$ and the contribution of the energy $\sqrt{s}$ in the propagator can be neglected for all but the zero mode. Thus, Eq. (5.10) simplifies to

$$\mathcal{M} \sim \frac{s^2}{M_{10}^8\, L^4} \sum_{\vec{n}\in\mathbb{Z}^6}{}' \frac{e^{i\vec{n}\vec{a}}}{\vec{n}^2} + \frac{s}{M_{10}^8\, L^6}\,, \tag{5.11}$$

where the prime denotes exclusion of $\vec{n} = \vec{0}$ in the sum. Since the 4d Planck scale is determined by $M_4^2 \simeq M_{10}^8 L^6$, the last term in Eq. (5.11) simply reflects the fact that the zero mode interacts with gravitational strength. The sum, which would be UV divergent in absence of the exponential factor, is dominated by terms with large $\vec{n}$. It can therefore be approximated by an integral:

$$\int d^6n\, \frac{e^{i\vec{n}\vec{a}}}{\vec{n}^2} \sim \frac{1}{a^4}\,. \tag{5.12}$$

The r.h. side of Eq. (5.12) results from the fact that the exponential function oscillates quickly for $|\vec{n}| \gtrsim a^{-1}$ ($a \equiv |\vec{a}|$), effectively cutting off the integral.[4] More precisely, we evaluate a similar but more general integral, which we will need in Section 6.2, in Appendix C. Equation (5.12) follows from this integral in a particular limit, which is displayed in Eq. (6.16).

Inserting Eq. (5.12) into Eq. (5.11), we find

$$\mathcal{M} \sim \frac{s^2}{M_{10}^8 A^4} + \frac{s}{M_{10}^8 L^6}\,, \tag{5.13}$$

where $A \equiv |\vec{A}|$. For an order-of-magnitude calculation, we can neglect the interference term in $|\mathcal{M}|^2$. The cross section for the process in Fig. 5.2 then reads

$$\sigma \sim \frac{s^3}{M_{10}^{16} A^8} + \frac{s}{M_{10}^{16} L^{12}} \qquad \text{for} \qquad \sqrt{s} < L^{-1}\,. \tag{5.14}$$

Inserting this cross section into Eq. (5.3), we get the energy loss rate due to scattering of one particle species into another particle species. To get the total energy loss rate, we have to sum over all initial and final state species and polarizations. Let us denote with N_1 and N_2 the number of colors of the heated gauge theory and the gauge theory that is being heated, respectively. The summation then gives extra factors of $2N_1^2$ and $2N_2^2$ and we get, again neglecting prefactors of order one coming from the integration in Eq. (5.3),

$$\dot{\rho} \sim \frac{N_1^2 N_2^2}{M_{10}^{16} A^8}\, T^{13} + \frac{N_1^2 N_2^2}{M_{10}^{16} L^{12}}\, T^9\,. \tag{5.15}$$

Using Eq. (2.20), this can be written in a slightly more compact form. Denoting by R_1 and R_2 the AdS scales of the corresponding throats, we arrive at the main result of this chapter:

$$\dot{\rho} \sim \frac{R_1^8 R_2^8}{A^8}\, T^{13} + \frac{R_1^8 R_2^8}{L^{12}}\, T^9\,. \tag{5.16}$$

The applicability of this heat transfer rate to more general throat geometries and embedding manifolds will be discussed in Section 7.1.

[4] One can see in particular that the sum in Eq. (5.11) is effectively cut off before the geometry of the throats becomes relevant, justifying our flat-space approximation.

Chapter 6

Decay of KK modes between throats from a 10d perspective

6.1 The glueball decay vertex

We will now calculate the decay rate of KK modes which localized in one throat to a different throat. We will thus determine the same quantity as in Chapter 4. This time, though, we will perform the calculation for the 10d setup from the last chapter, two $AdS_5 \times S^5$ throats in a 6-dimensional torus. Again, we will use the dual gauge theory picture and consider D3-brane stacks instead of the $AdS_5 \times S^5$ throats.

In this picture, we have to calculate the decay rate of glueballs on one brane stack into two gauge fields on another brane stack. The Feynman diagram for this process is shown in Fig. 6.1. Due to the nonrenormalization theorem described in the introduction, we do not have to care whether the decay products will arrange into one or more glueballs. The vertex for this part of the diagram is simply the one already derived in Eq. (5.9). However, the other vertex between a dilaton and a glueball can not so easily be read off from the Lagrangian. Therefore, we first calculate the decay rate for a simpler situation in the gravity picture. From this we determine the vertex by demanding that this decay rate agree with the gauge theory picture.

Namely, we consider a single $AdS_5 \times S^5$ throat which is embedded into flat 10d space. As we have discussed in Section 2.2, this is the geometry of an extremal black 3-brane. Excitations in the throat region of this 3-brane correspond to excitations in the dual gauge theory. The state dual to a glueball on a D-brane stack is therefore a wave packet which is localized in the throat. Due to the different time evolution of its constituent modes, this wave packet will decohere after a certain time (cf. Section 4.3). Hence, excitations will show up in the asymptotically flat region as well. This is the analogue of the decay of a glueball on a D-brane stack to supergravity fields in the embedding flat space.[1]

[1] As opposed to the 'derivation' of the AdS/CFT conjecture in Section 2.4, we keep M_s and M_{10} finite. In this case, the asymptotically flat region does not decouple from the throat region of a black 3-

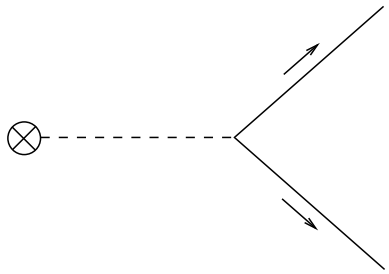

Figure 6.1: *Feynman diagram for the decay of a glueball in one throat into fields in another throat.*

Thus, we want to determine the decay rate of a dilaton which is localized in the throat into flat space. To this end, we assume the throat to be sharply cut off somewhere in the IR. Such an $AdS_5 \times S^5$ throat with an IR cutoff might not exist as a solution to supergravity, but it can serve as a simple toy model capturing the relevant information. In Chapter 7, we will show how to extend our results to realistic finite throats such as the KS throat. On the gauge theory side, the cutoff corresponds to a deformation by a relevant operator, in which case the gauge theory has a discrete set of glueball states.

The tunneling probability $\mathcal{P}$ of a wave from the throat to the asymptotically flat space is given in Eq. (2.30) (see also [62]). Although this result has been derived for a throat which is infinite in the IR direction, we can still use it for a finite throat, as long as the mass m of the wave is not too small. To see this, consider the dilaton equation of motion in Schrödinger form, Eq. (2.23) with $\omega = m$. In the region $z \gg m^{-1}$, the constant term in the potential is dominant and the equation is approximately solved by plane waves:

$$\psi(z) \simeq A \cos mz + B \sin mz \,. \tag{6.1}$$

We denote the position of the IR cutoff of the throat by $z_{\rm IR}$. The boundary condition for ψ or its first derivative at $z_{\rm IR}$ lead to a quantization of the mass in units of $m_{\rm IR} \equiv z_{\rm IR}^{-1}$ such that $m \sim n\, m_{\rm IR}$ with n an integer.

The approximation by a plane wave is valid in the region $z_{\rm IR} \geq z \gg m^{-1} \sim z_{\rm IR}/n$, where we have used the mass quantization condition. As long as n is sufficiently larger than 1, the wave is a plain wave (in the parametrization of Eq. (2.23)) in a large portion of the throat. This plain wave tunnels to the asymptotically flat space with the probability given in Eq. (2.30). Moreover, the analysis at the end of Section 4.2 applies to this situation as well. The relation of the tunneling probability to the decay rate is

brane. Excitations in the two regions will thus mix with each other. This reflects the fact that, since we do not send M_{10} to infinity, the gauge theory will interact with the supergravity fields in the embedding space (cf. Eq. (2.33)).

thus given by Eqs. (4.10) and (4.14) and the decay rate follows as

$$\Gamma \sim m_{\rm IR}(mR)^{8+4l}\,. \tag{6.2}$$

Now that we have the decay rate in the gravity picture, we need to define a vertex V in the gauge theory picture which reproduces this result. We model the coupling by a term

$$\mathcal{L}_{\rm 10d} \;\supset\; V\,\delta^{(6)}(\vec{X}-\langle\vec{X}\rangle)\,\phi(x,\langle\vec{X}\rangle)\,\mathcal{G}(x) \tag{6.3}$$

in the 10d Lagrangian, where $\mathcal{G}$ denotes the glueball state with canonically normalized 4d kinetic term. Compactifying the 6 dimensions perpendicular to the brane on a torus of size L for the moment and using the KK mode decomposition of Eq. (5.8), we get the effective 4d Lagrangian

$$\mathcal{L}_{\rm 4d} \;\supset\; \sum_{\vec{n}\in\mathbb{Z}^6}\left(-\frac{1}{2}\partial_\mu\Phi_{\vec{n}}\,\partial^\mu\Phi_{\vec{n}}-\frac{1}{2}m_{\vec{n}}^2\,\Phi_{\vec{n}}^2+e^{2\pi i\vec{n}\langle\vec{X}\rangle/L}\,\frac{V}{L^3}\,\Phi_{\vec{n}}(x)\,\mathcal{G}(x)\right)\,. \tag{6.4}$$

From this, the total decay rate of a glueball into KK modes of the dilaton follows:

$$\Gamma=\frac{1}{2\omega_i}\frac{1}{L^6}\sum_{\vec{n}\in\mathbb{Z}^6}\int\frac{d^3p_f}{(2\pi)^3}\,\frac{1}{2\omega_f}\,(2\pi)^4\,\delta^{(4)}(p_f-p_i)\,|V|^2\,. \tag{6.5}$$

In this formula, $p_f=p_{f_\parallel}$ is a 4-vector characterizing the momentum of the final-state dilaton parallel to the brane, while ω_i and ω_f are the energies of the initial and final state. The 4-momentum of the decaying glueball is denoted by p_i. Introducing the dilaton momentum in the compact dimensions as $\vec{p}_{f_\perp}=2\pi\,\vec{n}/L$, we can replace the sum by an integral when we go back to $L\to\infty$:

$$\frac{1}{L^6}\sum_{\vec{n}\in\mathbb{Z}^6}\;\longrightarrow\;\int\frac{d^6p_{f_\perp}}{(2\pi)^6}\,. \tag{6.6}$$

The decay rate of a glueball into a dilaton is then given by

$$\Gamma=\frac{1}{2\omega_i}\int\frac{d^6p_{f_\perp}}{(2\pi)^6}\frac{d^3p_{f_\parallel}}{(2\pi)^3}\,\frac{1}{2\omega_f}\,(2\pi)^4\,\delta^{(4)}(p_{f_\parallel}-p_i)\,|V|^2\,. \tag{6.7}$$

Since the dilaton is massless, $\omega_f=\sqrt{|\vec{p}_{f_\perp}|^2+|\vec{p}_{f_\parallel}|^2}$. Going to the rest frame of the glueball, $\vec{p}_i=0$, and performing the momentum integrations, we arrive at

$$\Gamma=\frac{1}{2\omega_i}\int\frac{d^6p_{f_\perp}}{(2\pi)^6}\,\frac{1}{2\omega_f}\,(2\pi)\,\delta(\omega_f-\omega_i)\,|V|^2\sim\omega_i^3\,|V|^2\,, \tag{6.8}$$

where we have used $\omega_f=|\vec{p}_{f_\perp}|$ and neglected prefactors of order one. In its rest frame, ω_i is simply the mass m of the glueball. Comparing with Eq. (6.2), we get

$$V\sim\sqrt{m_{\rm IR}m}\;\;m^{2+2l}R^{4+2l}\,. \tag{6.9}$$

6.2 Decay rate calculation in the gauge theory picture

With the effective vertex V at hand, calculating the decay rate of one glueball into gauge fields living on a different brane stack is straightforward. Following from Eqs. (6.4) and (6.9), the vertex between a glueball and a KK mode of the dilaton is

$$\frac{V}{L^3}\, e^{2\pi i \vec{n}\langle \vec{X}\rangle/L}\,. \tag{6.10}$$

The other vertex in the diagram is still given by Eq. (5.9). Summing over all intermediate KK modes, we arrive at an expression very similar to Eq. (5.10):

$$\mathcal{M} \sim \frac{\sqrt{m_{\rm IR} m}\,(mR)^{4+2l}}{M_{10}^4\, L^6} \sum_{\vec{n}\in\mathbb{Z}^6} \frac{e^{i\vec{n}\vec{a}}}{m^2 - m_{\vec{n}}^2 + i\epsilon}\,. \tag{6.11}$$

Compared to Eq. (5.10), the only difference is the prefactor and the substitution of the energy $\sqrt{s}$ of the colliding gauge bosons by the mass m of the glueball.

We will analyse Eq. (6.11) in two different regimes, namely for $m^{-1} > L$ and for $m^{-1} \ll L$. The former case is the most interesting one from a phenomenological viewpoint. As we have argued in Chapter 5, we can assume that the reheating temperature $T_{\rm RH}$ in early cosmology is smaller than L^{-1}. Accordingly, the mass m of any relic KK modes is also restricted by $m < L^{-1}$. The latter case, on the other hand, can be easily analysed in the gravity picture as well. We will perform this cross-check in Section 6.3.

For $m^{-1} > L$, we can make the same simplifications as in Eq. (5.11) and use Eq. (5.12) for the sum. The decay rate of a glueball into a pair of gauge bosons follows from the standard 4d formula:

$$\Gamma \sim m^{-1} |\mathcal{M}|^2\,. \tag{6.12}$$

To get the total decay rate, we have to sum over the N^2 final state gauge bosons. If we denote by R_1 and R_2 the AdS scale of the throat containing the initial and the final state, respectively, and use Eq. (2.20), we find

$$\begin{aligned}\Gamma \quad &\sim \quad \frac{N_1^{2+l} N_2^2}{M_{10}^{16+4l} A^8}\, m_{\rm IR}\, m^{8+4l} + \frac{N_1^{2+l} N_2^2}{M_{10}^{16+4l} L^{12}}\, m_{\rm IR}\, m^{4+4l} \\ &\sim \quad \frac{R_1^{8+4l} R_2^8}{A^8}\, m_{\rm IR}\, m^{8+4l} + \frac{R_1^{8+4l} R_2^8}{L^{12}}\, m_{\rm IR}\, m^{4+4l}\,. \end{aligned} \tag{6.13}$$

The applicability of this decay rate to more general throat geometries and embedding manifolds will be discussed in Chapter 7.

Let us now consider the case $m^{-1} \ll L$. We will also assume $A \ll L$ for simplicity. Recalling that $m_{\vec{n}} = 2\pi|\vec{n}|/L$ and $\vec{a} = 2\pi\vec{A}/L$, we can approximate the sum in Eq. (6.11) by an integral,

$$\frac{1}{L^6} \sum_{\vec{n}\in\mathbb{Z}^6} \frac{e^{2\pi i \vec{A}\,\vec{n}/L}}{m^2 - (2\pi)^2\vec{n}^2/L^2 + i\epsilon} \quad \longrightarrow \quad \int \frac{d^6\rho}{(2\pi)^6} \frac{e^{i\vec{A}\,\vec{\rho}}}{m^2 - \vec{\rho}^2 + i\epsilon}\,, \tag{6.14}$$

where $\vec{\rho} \equiv 2\pi\,\vec{n}/L$. The resulting expression is just the propagator of a massless particle in a mixed, energy-configuration-space representation, with the 'energy' m characterizing the invariant 4-momentum. This is of course expected in the large L limit, where the torus goes over to flat space and the infinite KK tower is replaced by the underlying higher-dimensional dilaton field. The integral is evaluated in Appendix C, the outcome being

$$\int \frac{d^6\rho}{(2\pi)^6}\,\frac{e^{i\vec{A}\vec{\rho}}}{m^2-\vec{\rho}^2+i\epsilon} \sim \frac{m^2}{A^2}\,H_2^+(mA)\,, \tag{6.15}$$

where $H_2^+(x) = J_2(x) + i\,Y_2(x)$ is a Hankel function and we have neglected prefactors of order one. Using the asymptotic forms of the Bessel functions for large and small arguments, Eq. (6.15) can be simplified as follows:

$$\frac{m^2}{A^2}\,H_2^+(mA) \sim \begin{cases} \frac{m^{3/2}}{A^{5/2}}\,e^{i\,mA} & \text{for } m^{-1} \ll A \\ \frac{1}{A^4} & \text{for } m^{-1} \gg A\,. \end{cases} \tag{6.16}$$

Inserting these results in Eq. (6.11), we get the matrix elements $\mathcal{M}$ for these two cases. The corresponding partial decay rates follow from Eq. (6.12). Summing over all final state species, we find

$$\Gamma \sim \begin{cases} \frac{R_1^{8+4l}R_2^8}{A^5}\,m_{\rm IR}\,m^{11+4l} & \text{for } m^{-1} \ll A \\ \frac{R_1^{8+4l}R_2^8}{A^8}\,m_{\rm IR}\,m^{8+4l} & \text{for } m^{-1} \gg A \end{cases}. \tag{6.17}$$

As a consistency check, we should examine, whether the appropriate limiting cases of Eqs. (6.13) and (6.17) coincide. The regions of validity of the two calculations have a common border for $A \ll m^{-1} \sim L$. Indeed, for this choice of parameters the first term in Eq. (6.13) dominates and the result agrees with the second line of Eq. (6.17).

6.3 Some calculations in the gravity picture and relation to earlier work

As in the sections before, we consider two $\mathrm{AdS}_5\times\mathrm{S}^5$ throats embedded in a 6-dimensional torus of uniform size L. The geometry is that of a multi-centered black 3-brane, the metric being (cf. Section 3.1)

$$ds^2 = H^{-1/2}\,\eta_{\mu\nu}dx_{\shortparallel}^{\mu}dx_{\shortparallel}^{\nu} + H^{1/2}\,dx_{\perp}^{i}dx_{\perp\,i} \tag{6.18}$$

with

$$H(\vec{x}_\perp) = 1 + \sum_{\vec{n}\in\mathbb{Z}^6}\left(\frac{R_1^4}{|\vec{x}_\perp - \vec{A}_1 + \vec{n}L|^4} + \frac{R_2^4}{|\vec{x}_\perp - \vec{A}_2 + \vec{n}L|^4}\right). \tag{6.19}$$

The positions of the two throats are denoted by $\vec{A}_1$ and $\vec{A}_2$, their AdS scales by R_1 and R_2. The $x_{\shortparallel}$ are coordinates along the 4 uncompactified dimensions and the $x_\perp$ refer to coordinates in the torus. The sum in the warp factor $H(\vec{x}_\perp)$ is due to mirror effects in the

torus. Again, this is not a consistent compactification. Including O-planes, for example, would give extra contributions to the warp factor (see [44]). We try to calculate the transition of a dilaton between different throat regions, which is the gravity counterpart to the gauge theory calculation in Sections 6.1 and 6.2. The equation of motion for the dilaton is given in Eq. (2.21). Inserting Eq. (6.18) in Eq. (2.21) and using $\sqrt{g} = H^{1/2}$, one gets

$$\partial_n \, \partial^n \, \phi + H(\vec{x}_\perp) \, \partial_\mu \, \partial^\mu \, \phi = 0 \, . \tag{6.20}$$

The indices μ and n run from 0 to 3 and from 4 to 9, respectively. Using the 4d Klein-Gordon equation, one arrives at

$$\partial_n \, \partial^n \, \phi + H(\vec{x}_\perp) \; m^2 \, \phi = 0 \, , \tag{6.21}$$

where m is the kinetic energy perpendicular to the branes. Like Eq. (2.23), this has the form of a Schrödinger equation. Contrary to Eq. (2.23), however, there is no potential barrier separating the throat region and asymptotically flat space, since the potential $V = -m^2 H(\vec{x}_\perp)$ is strictly negative. The difference comes from using cartesian coordinates perpendicular to the branes in Eq. (6.18) rather than spherical coordinates in Eq. (2.17). Still, a wave in the throat region, moving away from the horizon, is reflected to a large part before entering asymptotically flat space. In cartesian coordinates, however, this is due to the steepness of the potential well.

To determine the transition probability $\mathcal{P}$ of a dilaton between two throat regions, one has to solve Eq. (6.21) with appropriate boundary conditions. Then $\mathcal{P}$ is the ratio of incoming flux in one throat and outgoing flux in the other throat. In general, the corresponding calculation is difficult. However, if the torus is very large ($L \to \infty$) and the throats are sufficiently far apart ($A \gg m^{-1}$), the problem effectively splits into two simpler calculations. Namely, the latter condition means that the de Broglie wavelength of the particle is small compared to the distance of the throats. A transition between two throats can then be described as a two-step process. For simplicity, we take the initial state in the first throat to be an s-wave. Only a small fraction of the outgoing flux reaches the asymptotically flat region, the probability being given in Eq. (2.30) (with $l = 0$ and $\omega = m$)

$$\mathcal{P}_1 \sim (m R_1)^8 \, . \tag{6.22}$$

In between the two throats, one has a free spherical wave, approximating a plane wave near the second throat. The absorption cross section (per brane world-volume) for such a plane wave is given in Eq. (2.31):

$$\sigma_2 \sim m^3 R_2^8 \, . \tag{6.23}$$

Near the second throat, the incoming flux will be diluted by a factor of A^{-5}, since the free spherical wave is expanding in 6-dimensional flat space. The absorption probability by the second throat thus is

$$\mathcal{P}_2 \sim \frac{\sigma_2}{A^5} \sim \frac{m^3 R_2^8}{A^5} \, . \tag{6.24}$$

The transition probability between the two throats is just the product $\mathcal{P}_1 \mathcal{P}_2$. If we denote by m_{IR} the mass gap in the first throat, using Eqs. (4.10) and (4.14) the decay

rate from the gravity calculation follows as

$$\Gamma \sim \frac{R_1^8 R_2^8}{A^5}\, m^{11} m_{\text{IR}}\,. \tag{6.25}$$

This is precisely what we found in Eq. (6.17) for $A \gg m^{-1}$ and $l = 0$. The crucial ingredient is the A^{-5} dependence. That it agrees in both calculations is, however, not too surprising. In the gauge theory calculation, it came from the propagator in a mixed energy-configuration-space representation (cf. Eq. (6.14)). The same is of course true in the above gravity calculation, although we have not stated it explicitly.

As we have discussed in Section 4.3, there is yet another situation in which the decay rate of KK modes between two throats is comparatively easy to obtain. To this end, we assume that the AdS scale R_1 of the first throat is of the same order as the size L of the embedding space, i.e. $L \sim R_1$. We then have $R_1 \gtrsim R_2$, where R_2 is the AdS scale of the second throat. In this situation, we can approximate the first throat by a RS model, whereas the second throat corresponds to some degrees of freedom which live on the UV brane of this RS model. Furthermore, we restrict ourselves to s-waves in the throats, i.e. $l = 0$. The resulting decay rate Eq. (4.19) can be compared with Eq. (6.13) from the gauge theory calculation. The distance A between the two throats cannot be smaller than their AdS scales R_1 and R_2. Since we also have $L \sim R_1$ and $m \ll R_1^{-1}$, the second term in Eq. (6.13) is dominant. For $L \sim R_1$ and $l = 0$, this term gives the same result as Eq. (4.19)!

Tunneling in a compact 10d setup with throats was also considered in [62, 65]. For the case $m^{-1} > L$, a decay rate of $\Gamma \sim (mR)^{16}\, m_{\text{IR}}$ was derived, assuming that the particle has to tunnel through two barriers described by the potential in Eq. (2.23). We see a conceptual problem with this approach since we do not know how to justify a 1-dimensional quantum-mechanical picture (this 1 dimension being the radial coordinate) in the two-throat case. But even if we accept this description for the moment, there are further issues related to the two-barriers assumption: The barriers extend to values of $r \sim m^{-1}$ as can be seen from Fig. 2.1. Since $m^{-1} \gg R$ and r measures the physical distance for $r \gg R$ (cf. Eq. (2.17)), the width of each barrier is given by m^{-1}. This just reflects the fact that a particle with mass m has a de Broglie wavelength of m^{-1}. Accordingly, the particle has to tunnel through two entire barriers only if the distance A between the two throats is $\sim 2m^{-1}$. Indeed, from Eq. (6.13) for $l = 0$ and since $L > A$, we get a decay rate of $\Gamma \sim (mR)^{16}\, m_{\text{IR}}$ in this case, in agreement with [62, 65]. However, if A is smaller than $\sim 2m^{-1}$, the particle has to tunnel through a smaller barrier. Correspondingly, the decay rate becomes larger, as can be seen from Eq. (6.13).

The case $m^{-1} \lesssim L$ (without assuming $m^{-1} \ll L$) was also considered in [62, 65]. It was found that the decay rate can be much larger than $\Gamma \sim (mR)^{16}\, m_{\text{IR}}$ if a certain resonance condition is fulfilled. We have not determined the decay rate for this case and therefore have no result to compare with.[2] It would be interesting, though, to evaluate Eq. (6.11) for $m^{-1} \lesssim L$ and to see whether one can reproduce the results from [62, 65] as well as their resonance condition.

[2]Note that we have assumed that $L \gg A, m^{-1}$ in deriving Eq. (6.17). This result is therefore not suitable to compare with the results from [62, 65] where the limit of extremely large L was not taken.

Chapter 7

Modifications in more realistic setups

In the last chapters, we have calculated the heat transfer rate and the decay rate of KK modes for a simple geometry – two $AdS_5 \times S^5$ throats embedded in a 6d torus. In this chapter, we will argue, that these rates are also applicable to more general throat geometries and embedding manifolds. A complication arises, though, for the decay rate of KK modes in a KS throat. The 3-form flux, which is present in these throats, mixes field fluctuations in a complicated way. The determination of the glueball vertex along the lines of Section 6.1 is therefore in general difficult. We will show, however, that the glueballs decay to a certain lightest glueball on very short timescales. It is therefore sufficient to determine the decay rate to other throats only for this lightest glueball which, as we will argue, decays again with the vertex derived in Section 6.1. We will also see that an extra suppression can arise for decay rates in flux compactifications because certain fields which mediate the decay get high masses. This suppression is roughly compensated, on the other hand, if the corresponding KK mode mixes with tachyonic fields in the throat. Finally, we will generalize our results to processes involving the standard model.

7.1 Applicability to other geometries

An apparent limitation of our analysis in Chapters 5 and 6 is the assumption of a simple toroidal geometry for the embedding space. This assumption was used to determine the spectrum and the couplings of higher KK modes (which determine the first term in Eqs. (5.11), (5.16) and (6.13)). By contrast, the coupling of the zero mode (which determines the second term in Eqs. (5.11), (5.16) and (6.13)), depends only on the size of the embedding manifold and not on its geometry. To see the relative importance of the terms more clearly, we focus on the heat transfer rate and rewrite Eq. (5.16) as

$$\dot{\rho} \sim \frac{R_1^8 R_2^8}{A^8}\, T^{13} \left(1 + \left(\frac{A}{L}\right)^8 (L\,T)^{-4}\right) . \tag{7.1}$$

If the throat-to-throat distance is large, $A \sim L$, the second term dominates (recall that $LT < 1$) and the precise geometry is irrelevant. By contrast, for small throat separation, $A \ll L(LT)^{1/2}$, the contribution of the KK modes is dominant. In this case, the precise geometry of the embedding manifold may in principle be relevant. However, it is then natural to assume that the curvature scale in the region between the throats is smaller than $1/A$. Furthermore, as we have already pointed out in Section 5.3, the sum in Eq. (5.11) is dominated by contributions with $|\vec{n}| \sim L/A$, corresponding to masses $m_{\vec{n}} \sim A^{-1}$. Such modes are only sensitive to the geometry at distance scales A in the vicinity of the two throats, which we just argued to be approximately flat. Thus, the order of magnitude of our heat transfer rate will remain correct in most relevant cases, even if the overall geometry is very different from that of a torus.

Similar conclusions follow for the applicability of the decay rate in Eq. (6.13) to other embedding geometries. In particular, we see that O-planes and further D-brane stacks will not change our results as long as they are not too close to the two throats. In Section 7.4, we will see, however, that a suppression of the decay rate can arise due to the stabilization of certain moduli in flux compactifications.

We can also apply our heat transfer rate to situations with one KS throat and one $\mathrm{AdS}_5 \times \mathrm{S}^5$ throat or with two KS throats as long as the curvature scale of the space in between the two throats is not much larger than $1/A$. In particular, one can easily see from the gravity picture that the finite length of the KS throats will not change the heat transfer rate qualitatively. This is obvious for the heated throat since the black hole horizon hides the IR region.[1] Energy transfer from the heated throat is due to Hawking radiation which is absorbed by the other throat. But only the geometry in the UV region of the latter throat is important for the absorption of the Hawking radiation. In particular, due to the latter fact, the relevant AdS scales in Eq. (5.16) are those at the UV ends of the throats.

For the derivation of the decay rate, we have assumed that the decaying field fulfills the equation of motion of a minimally coupled, massless scalar field in the throat. This is no longer obvious for the dilaton in a KS throat because 3-form flux mixes field fluctuations in a complicated way. We will discuss the corresponding decay rate in Section 7.4. There is a different field which fulfills the aforementioned equation of motion in the throat: the graviton [64, 65]. Let us outline how to determine the decay rate of graviton KK modes in a KS throat:

Away from the bottom of the throat at $r = r_s$, the metric of a KS throat is well approximated by Eq. (2.39) with the warp factor which is given in Eq. (2.41):

$$H(r) = 1 + \frac{R_{\mathrm{IR}}^4 \ln(r/r_s)}{r^4} \,. \tag{7.2}$$

For $R_{\mathrm{IR}} \gg r \gg r_s$, which defines the throat region, the warp factor is approximately $H \simeq R_{\mathrm{IR}}^4 \ln(r/r_s)/r^4$. For $r \gg R_{\mathrm{IR}}$, where the geometry is asymptotically a cone over $T^{1,1}$, we have $H \simeq 1$. Near $r = r_s$, the geometry differs considerably from Eqs. (2.39)

[1] Otherwise, if the temperature of the throat is lower than the IR scale, it contains a non-relativistic gas of KK modes whose decay rate to the other throat will be discussed in Section 7.4.

and (2.41) and the throat is cut off by the KS region. For an order of magnitude estimate, we can neglect the logarithmic r dependence of the warp factor away from $r = r_s$ and approximate the KS region by a sharp cut off [40]. Thus, the tunneling probability from the throat into the conical region can be (approximately) calculated from the effective Schrödinger equation, Eq. (2.23). Note, however, that we have to replace the eigenvalues $l(l+4)$ of the angular Laplacian on S^5 by the corresponding eigenvalues on $T^{1,1}$ for a KS throat. Furthermore, since tunneling is mainly determined by the geometry in the UV, we should use the AdS scale $R_{\rm UV}$ at the UV end of the throat in Eq. (2.23). For an AdS warp factor and a sharp cut off, the incoming flux is as before given by Eq. (4.14). From Eq. (4.10), we can then determine the decay rate to the conical region and match the glueball vertex such that this decay rate is reproduced.

Once we have the glueball vertex, we can redo the steps which led to Eq. (6.13). The decay rate of graviton KK modes which are s-waves with respect to the $T^{1,1}$ in a KS throat is thus again given by Eq. (6.13). For higher partial waves, the dependence on the angular quantum number is different from that displayed in Eq. (6.13).

7.2 Some remarks on the spectrum of the Klebanov-Strassler theory

A number of papers [65, 73–80] have calculated parts of the bosonic glueball spectrum of the KS gauge theory. In [78], masses of KK towers of 7 coupled scalar fields and the graviton polarized parallel to the uncompactified dimensions were determined. In particular, several scalar states lighter than the lowest spin-2 state were found. In [74], the mass of the lowest KK mode of the dilaton was calculated using some approximations in the geometry. Again, it was found to be lighter than a spin-1 and a spin-2 state [74,75]. In the light of these findings, we expect the lightest state in the bosonic sector to be a scalar glueball.

The KS gauge theory has $\mathcal{N} = 1$ supersymmetry and the lightest scalar glueball has a spin-$\frac{1}{2}$ superpartner. In a phenomenologically viable setup, supersymmetry is broken and the masses of the scalar and the spin-$\frac{1}{2}$ glueball are no longer degenerate. Let us estimate the resulting mass splitting:

To this end, note that we expect the throat to be sequestered from the rest of the compact space in the sense of [81]. To explain this in more detail, let us consider a chiral multiplet X from the throat sector and another chiral multiplet Y from somewhere in the rest of the compact space. The Lagrangian can be written in standard $\mathcal{N} = 1$ supergravity form

$$\mathcal{L} = \int d^4\theta\, \varphi\bar{\varphi}\, \Omega + \left(\int d^2\theta\, \varphi^3\, W + \text{ h.c.} \right), \tag{7.3}$$

where $\varphi = 1 + \theta^2 F_\varphi$ is the chiral compensator, Ω is the kinetic function and W is the

superpotential. The sectors X and Y are said to be sequestered if [81]

$$\begin{aligned} \Omega(X,\bar{X},Y,\bar{Y}) &= \Omega(X,\bar{X}) + \Omega(Y,\bar{Y}) \\ W(X,Y) &= W(X) + W(Y)\,. \end{aligned} \tag{7.4}$$

In this case, supersymmetry breaking is communicated to the X-sector only by the F-term of the chiral compensator φ and not by the Y-sector.

The sequestering assumption in our setup follows from the interpretation of a Calabi-Yau orientifold with a long throat as supersymmetric RS model [40]. In this 5d framework [81], this assumption has been widely accepted and has also been used in the context of type IIB models with strongly warped regions (see e.g. [82, 83] as well as the detailed discussion of [84] and references therein).

We thus assume that supersymmetry breaking is communicated to the lightest glueball multiplet X only by the F-term vev $\langle F_\varphi \rangle$ of the chiral compensator.[2] The relevant part of the effective Lagrangian Eq. (7.3) is

$$\mathcal{L} \supset \int d^4\theta\, \varphi\bar{\varphi}\, X\bar{X} + \left(\int d^2\theta\, m_{\text{IR}} X^2 \varphi^3 + \text{ h.c.} \right) . \tag{7.5}$$

We have to discuss two cases separately. For $\langle F_\varphi \rangle \ll m_{\text{IR}}$, one can expand X in components and split the lowest component of X into real and imaginary parts. Inserting this expression in Eq. (7.5) and diagonalizing the resulting mass matrix for the real and imaginary part, one finds two scalar eigenstates with masses

$$m_{1,2}^2 = 4\, m_{\text{IR}}^2 \pm 2\, m_{\text{IR}}\, |\langle F_\varphi \rangle| \,. \tag{7.6}$$

Moreover, the mass of the fermion is $2m_{\text{IR}}$ and receives no contribution from $\langle F_\varphi \rangle$. Therefore, one scalar glueball is lighter than its former spin-$\frac{1}{2}$ superpartner and the mass splitting is $|\langle F_\varphi \rangle|/2$.

For $\langle F_\varphi \rangle \gg m_{\text{IR}}$, Eq. (7.6) is obviously not applicable. In this case, one can analyse the situation from the perspective of a chiral superfield with vanishing mass, i.e. one considers the limit $m \to 0$. The theory then possesses a chiral symmetry which ensures the masslessness of the fermion even in the presence of supersymmetry breaking. Thus, in analogy to the matter superfields of the minimal supersymmetric standard model, we expect that the scalar glueballs will be heavier than the fermions if supersymmetry breaking in the throat is a large effect relative to the supersymmetric mass term.

Finally, we note that we can expect the F-term vev $\langle F_\varphi \rangle$ of the chiral compensator to be of the same order of magnitude as the gravitino mass $m_{3/2}$. In the following, we will therefore refer to the two aforementioned cases as $m_{3/2} \ll m_{\text{IR}}$ and $m_{3/2} \gg m_{\text{IR}}$, respectively.

[2] Actually, the situation might be more complicated since the lightest glueball multiplet couples strongly to heavier glueballs, which are themselves affected by supersymmetry breaking and which might therefore influence the mass splitting of the lightest multiplet in a non-negligible way. We therefore view the present calculation only as a reasonable first guess.

7.3 Processes in the throat sector

In Section 7.4, we will discuss modifications in the decay rates of glueballs (respectively KK modes) to other sectors which are due to flux-induced masses. We can restrict the analysis in that section to the decay rates of the lightest glueball and its superpartner (a scalar and a fermion according to the last section):[3] As we will now discuss, all heavier glueballs decay to these states on timescales which are short compared to the timescales for decays to other sectors.

Below the confinement scale, the glueballs are described by an effective field theory. Generically, tree-level couplings and loop effects induce various cubic interactions. For example, for a scalar glueball $\mathcal{G}$, a spin-1 glueball $\mathcal{A}_\mu$ and a spin-2 glueball $\mathcal{H}_{\mu\nu}$, we expect interactions of the type

$$\partial_\mu \mathcal{G}\, \mathcal{A}_\nu\, \mathcal{H}^{\mu\nu} + m_{\rm IR}\, \mathcal{A}_\mu \mathcal{A}^\mu\, \mathcal{G} + m_{\rm IR}^{-1} \partial_\mu \mathcal{G}\, \partial_\nu \mathcal{G}\, \mathcal{H}^{\mu\nu} + \dots \tag{7.7}$$

The coupling strengths follow on dimensional grounds up to possible factors of $N_{\rm IR}$ (which do not follow from dimensional analysis). Also, there may be more partial derivatives involved or they may act differently. Interactions of this type allow for the decay of heavy glueballs to a few light states which cannot decay further for kinematic reasons.

Note, however, that the KS gauge theory has a global SU(2)×SU(2) symmetry which forbids certain couplings of the type of Eq. (7.7). From the dual gravity point of view, this symmetry is due to isometries of the $T^{1,1}$ inside a KS throat. In a compactified setup, the KS throat is attached to a Calabi-Yau manifold which breaks this isometry in the UV. This symmetry breaking is mediated to the IR as discussed in [60, 85–87]. We therefore expect that couplings of the type of Eq. (7.7) which violate the global symmetry are nevertheless present, albeit with a possibly smaller coupling strength. In the following, we ignore the effects of glueballs charged under the SU(2)×SU(2) symmetry. In particular, from the gauge theory point of view, we expect that the lightest glueball and its superpartner are singlets with respect to this symmetry.

There are more induced interactions: Recall that Eq. (6.10) is the vertex between a dilaton KK mode in the embedding manifold and a scalar glueball. As we have discussed in Section 7.1, the steps leading to this result are also valid for the mixing of graviton KK modes with spin-2 glueballs. In particular, the mixing between the 4d graviton (i.e. the zero mode in the graviton KK tower, $\vec{n} = 0$ and $l = 0$) and a spin-2 glueball is

$$N_{\rm UV} \frac{m_{\rm IR}^{1/2} m^{5/2}}{M_4}\,. \tag{7.8}$$

We have used Eqs. (2.20) and (3.3). This mixing is similar to the mixing between the photon and the ρ meson known from QCD and was also observed in [88] for the gauge theory dual of a 5d RS model.

[3] It may happen that the lightest fermionic glueball is not the superpartner of the lightest bosonic glueball. Moreover, it may happen that the mass of the lightest bosonic glueball is larger than twice the mass of the lightest fermionic glueball. The former could then decay to the latter via couplings discussed below. We will not consider these possibilities in the following.

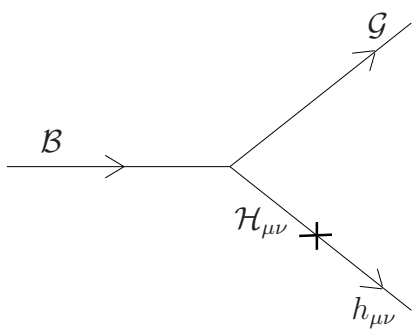

Figure 7.1: *Decay of a bosonic glueball $\mathcal{B}$ into a bosonic glueball $\mathcal{G}$ and a graviton $h_{\mu\nu}$ via a spin-2 glueball $\mathcal{H}_{\mu\nu}$.*

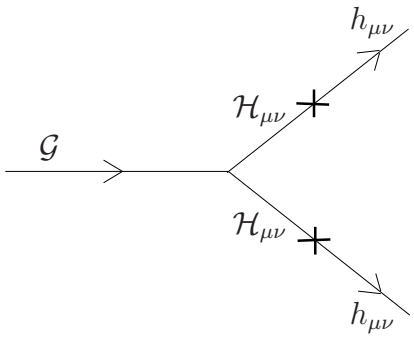

Figure 7.2: *Decay of a scalar glueball $\mathcal{G}$ into two gravitons $h_{\mu\nu}$ via spin-2 glueballs $\mathcal{H}_{\mu\nu}$.*

The mixing in Eq. (7.8) combined with interactions of the type of Eq. (7.7) allow for processes such as that shown in Fig. 7.1: A bosonic glueball $\mathcal{B}$ decays to the lightest bosonic glueball $\mathcal{G}$ and, via a virtual spin-2 glueball $\mathcal{H}_{\mu\nu}$, to a 4d graviton $h_{\mu\nu}$. Using Eq. (7.8), the decay rate is (for $m \sim m_{\text{IR}}$ and up to an unknown factor of N_{IR} which may result from the three-glueball vertex)

$$\Gamma \sim N_{\text{UV}}^2 \frac{m_{\text{IR}}^3}{M_4^2} . \tag{7.9}$$

Similarly, fermionic glueballs decay to the lightest fermionic glueball and a 4d graviton with the same rate.

The couplings in Eqs. (7.7) and (7.8) allow for another process, shown in Fig. 7.2: The decay of the lightest scalar glueball into two 4d gravitons. The decay rate is (again up to an unknown factor of N_{IR})

$$\Gamma \sim N_{\text{UV}}^4 \frac{m_{\text{IR}}^5}{M_4^4} . \tag{7.10}$$

By supersymmetry, there are processes in which one graviton in Figs. 7.1 and 7.2 is replaced by a gravitino and one bosonic glueball is replaced by a fermion. For $m_{3/2} \gg m_{\text{IR}}$, the corresponding decays are kinematically not allowed. The case $m_{3/2} \ll m_{\text{IR}}$ is more involved: As we have discussed in Section 7.2, we expect the lightest scalar glueball to be lighter than its fermionic superpartner in this case. A process of the type shown in Fig. 7.1 may thus lead to the decay of the lightest fermionic glueball to the lighter scalar superpartner. The mass splitting between the superpartners, though, is just of the order of magnitude of the gravitino mass (cf. Eq. (7.6)). It thus depends on the precise relation between the gravitino mass and the mass splitting whether this decay is kinematically allowed or not. The process of the type in Fig. 7.2, on the other hand, allows for the decay of fermionic glueballs to a graviton and a gravitino if $m_{3/2} \ll m_{\text{IR}}$.

Finally, let us summarize the decay channels discussed in this section. Due to the interactions in Eq. (7.7) and processes of the type in Fig. 7.1, all glueballs (neglecting

the glueballs charged under the R-symmetry) decay to the lightest glueball and its superpartner. This typically happens on cosmologically short timescales. For example, for a sector with $m_{\rm IR} \sim 10^7$ GeV and $N_{\rm UV} \sim 10$, this process takes 10^{-10} s. For the case $m_{3/2} \gg m_{\rm IR}$, the only other possible decay (of the channels discussed in this section) is the decay of scalar glueballs to 4d gravitons. Due to the suppression by four powers of the 4d Planck scale in the corresponding rate, this decay happens on timescales much longer than those of the decays discussed before (e.g. 10^{10} s for $m_{\rm IR} \sim 10^7$ GeV, $N_{\rm UV} \sim 10$). In particular, the lightest spin-$\frac{1}{2}$ glueballs are stable if $m_{3/2} \gg m_{\rm IR}$.

7.4 Decay of scalar and fermionic KK modes to other throats

Of the processes described in the last section, only the decay to two gravitons (or to graviton and gravitino, if the gravitino is light enough) can be sufficiently slow to be relevant for late cosmology. The other processes have a time scale much shorter than the age of the universe for all relevant choices of parameters. Thus, in late cosmology, the energy density in the throat sector is completely in the form of the lightest glueball and its superpartner. It is therefore sufficient to discuss the decay to other throats only for these lightest states which we expect to be a scalar and a spin-$\frac{1}{2}$ fermion (cf. Section 7.2).

The vertex in Eq. (6.9) was derived for a field which fulfills the equation of motion of a minimally coupled scalar in the effective 5d description of the throat. An example of such a field is the dilaton in an $\mathrm{AdS}_5 \times \mathrm{S}^5$ throat. In a KS throat, the situation is more complicated because 3-form flux mixes the field fluctuations in a complicated way. Nevertheless, Eq. (6.9) for an s-wave (i.e. $l = 0$) applies to the coupling of scalar glueballs from a KS sector to fields in the embedding manifold. To see this, we again consider the dilaton ϕ, whose equation of motion is

$$\nabla^2 \phi \;=\; \frac{1}{12}\, e^{\phi}\, \tilde{F}_{MNP} \tilde{F}^{MNP} - \frac{1}{12}\, e^{-\phi} H_{MNP} H^{MNP} \,. \tag{7.11}$$

Here, $\tilde{F}_3 = F_3 - C H_3$ and $F_3 = dC_2$ and $H_3 = dB_2$ are the field strengths of the RR 2-form C_2 and the NS 2-form B_2, respectively. We have taken the RR scalar C to be constant in Eq. (7.11). In a background with imaginary self-dual 3-form flux [3], the flux fulfills

$$H_{MNP} H^{MNP} = e^{2\phi}\, \tilde{F}_{MNP} \tilde{F}^{MNP} \tag{7.12}$$

for the background value of ϕ and the right-hand side of Eq. (7.11) vanishes. This is no longer the case if one shifts the background value of ϕ while keeping B_2 and C_2 fixed. If one simultaneously shifts B_2 in such a way that Eq. (7.12) remains fulfilled, however, the right-hand side of Eq. (7.11) still vanishes. In other words, there exists a flat direction in the 5d effective theory which one can parameterize, e.g., by the value of the dilaton. The corresponding field fulfills the equation of motion of a minimally coupled, massless scalar in 5d. Such a field couples with the s-wave vertex from Eq. (6.9).[4] A light scalar

[4]The angular momentum with respect to the S^5 in an $\mathrm{AdS}_5 \times \mathrm{S}^5$ throat acts as a mass term in the

KK mode localized at the bottom of the throat, i.e. a scalar glueball, will generically mix with this flat direction in the upper part of the throat [89,90]. Thus, scalar glueballs couple to fields in the embedding manifold with the previously derived s-wave vertex given in Eq. (6.9). Note, though, that stronger couplings arise for KK modes mixing with fields of the 5d effective theory which have tachyonic mass. We will analyse this effect in the next section.

In a phenomenologically viable setup, the scalar fields in the embedding manifold, which mediate the decay of scalar glueballs to other throats, all have to be massive. This fact can lead to a suppression of decay rates. Note that the heat transfer between different sectors can proceed via the massless graviton. The heat transfer rate in Eq. (5.16) is therefore not suppressed by flux-induced mass terms. We now discuss three classes of mediating fields separately:

Dilaton and complex structure moduli In flux compactifications à la GKP, the lowest KK mode of the dilaton and the complex structure moduli get a mass

$$m_\tau \sim \frac{M_{10}^2}{M_4}\,, \tag{7.13}$$

where we have assumed that $g_s \sim 1$. Redoing the calculation leading to Eq. (6.13) with a massive instead of a massless propagator for the mediating field, we get an extra factor of

$$\left(\frac{m^2}{m^2 - m_\tau^2}\right)^2 \sim \left(\frac{m}{m_\tau}\right)^4 \tag{7.14}$$

in the second term. In the last step, we have assumed that the dilaton, respectively the complex structure modulus, is much heavier than the decaying glueball. In this case, Eq. (7.14) suppresses the decay rate of scalar glueballs. Note that the second term in Eq. (6.13) always dominates if $m < m_\tau$ (since $A^{-1} < M_{10}$). We then have

$$\Gamma \sim \frac{N_1^2 N_2^2}{M_{10}^8}\, m_{\rm IR}\, m^8\,. \tag{7.15}$$

This is the decay rate of scalar glueballs (which are s-waves, i.e. singlets, with respect to the R-symmetry of the theory) to other sectors. By supersymmetry, it also applies to their spin-$\frac{1}{2}$ superpartners.[5]

Kähler moduli The Kähler moduli do not become massive by 3-form flux, and perturbative or non-perturbative corrections have to be taken into account in order to achieve their stabilization (cf. Section 3.2). In particular, the Kähler moduli can be much lighter than the flux-stabilized complex structure moduli and the dilaton. This is the case e.g. in the KKLT scenario. One may therefore expect that decays mediated by the Kähler moduli have a higher rate than Eq. (7.15).

5d effective theory. A massless 5d scalar is the s-wave part of a 10d scalar in such a geometry.

[5]This is certainly true for unbroken supersymmetry in which case the total decay rates of two superpartners are related by a supersymmetry transformation. For broken supersymmetry, one has to check that the relevant vertices agree (up to $\mathcal{O}(1)$ prefactors) and that the suppression by the mediating-field propagator is the same for both superpartners. We expect this to be the case.

We believe that this is not the case. To explain this in more detail, we restrict ourselves to the universal Kähler modulus. The crucial point is that in the 5d effective theory of a KS throat, the universal Kähler modulus is localized on the UV brane and is thus sequestered from the bottom of the throat [40,82,83]. This is the situation discussed in Section 7.2: If we denote the universal Kähler modulus by X and the glueball by Y (more precisely, the corresponding superfields), the kinetic function $\Omega(X, \bar{X}, Y, \bar{Y})$ and the superpotential $W(X, Y)$ fulfill Eq. (7.4). Terms mixing the two superfields appear neither in the kinetic part nor in the superpotential. Thus, since the universal Kähler modulus does not mix with the glueballs, it cannot mediate their decays to other sectors. Even if the sequestered form of Eq. (7.4) turns out to be violated, we expect that the cross-couplings are much more suppressed than the mixing vertex of Eqs. (6.9) and (6.10) between glueball and dilaton or complex structure modulus. The effect of the Kähler moduli in mediating glueball decays is then still negligible.

Gravitino Also the gravitino can be considerably lighter than the dilaton and the complex-structure moduli and may therefore play an important role in mediating decays. Unfortunately, we have not completely settled this issue. There are two relevant processes: The gravitino may mix with the fermionic glueballs and may thus mediate their decays to other sectors. In addition, the heavier superpartner may decay to the lightest glueball by the emission of a gravitino. This process follows from the process shown in Fig. 7.1 by replacing the virtual spin-2 glueball by a virtual spin-$\frac{3}{2}$ glueball, the outgoing graviton by a gravitino and one of the bosonic glueballs by a fermionic glueball. If the gravitino mass is large, $m_{3/2} > m_{\text{IR}}$, the gravitino is off-shell and must in turn decay to another sector. It is not immediately clear how strongly the gravitino propagator suppresses the decay rate for these two processes, i.e. with which power the gravitino mass enters. In the following, we will assume that there is a limit of large gravitino mass $m_{3/2} \gg m_{\text{IR}}$ for which decays mediated by the gravitino are subdominant.

7.5 Decay of KK modes via tachyonic fields in the throat

As we have mentioned in the last section, scalar KK modes which mix with tachyons in the effective 5d description of the throat couple to supergravity in the embedding space with a stronger vertex than that in Eq. (6.9). The reason is that the profile of a tachyon, i.e. a scalar with a negative mass squared, is less suppressed than the profile of the dilaton if one moves from the IR to the UV end of the approximate AdS_5 geometry.

To see this in more detail, we determine the decay rate of KK modes of such a tachyon between two throats. For simplicity, we assume that both throats have the same AdS scale R and that one throat can well be approximated by the RSI model, whereas the other throat can be accounted for by fields which live on the UV brane of this RSI model. As we have discussed in Section 4.3, this approximation is valid if the size of the embedding space is of the same order as the AdS scales of the throats. A

tachyonic scalar ϕ in the RSI model is described by the action

$$S_{5\mathrm{d}} \;=\; \int d^4x \int_{-\ell}^{\ell} dy\, \sqrt{g}\, \frac{1}{2}\left(g^{MN}\partial_M\Phi\partial_N\Phi + m_{5\mathrm{d}}^2\Phi^2\right)\,, \tag{7.16}$$

where $m_{5\mathrm{d}}^2 < 0$ is the negative mass squared of the scalar. As in Section 2.1, we view the RSI model as an $S^1/\mathbb{Z}_2$ orbifold and use the same parametrization of AdS_5 as in Eqs. (2.3) and (2.6).

In the full AdS_5-space (i.e. without branes), tachyonic scalars do not lead to instabilities if the masses fulfill the Breitenlohner-Freedman bound $m_{5\mathrm{d}}^2 \geq -4k^2$ [6], where k is the AdS scale. Let us consider a scalar Φ in the RSI model which just satisfies this bound, i.e. $m_{5\mathrm{d}}^2 = -4k^2$. The KK expansion of the scalar is

$$\Phi(x,y) \;=\; \sum_n \chi_n(x)\phi_n(y)\,, \tag{7.17}$$

where the $\chi_n(x)$ are eigenmodes of the 4d d'Alembertian with eigenvalues m_n^2.

We define a new coordinate $\hat{z} \equiv \mathrm{sgn}(y)\, k^{-1}(e^{k|y|}-1)$.[6] In the orbifold, positive and negative $\hat{z}$ corresponding to positive and negative y are identified. For a rescaled field $\psi_n \equiv (1+|\hat{z}|k)^{-3/2}\phi_n$, the equation of motion that follows from Eq. (7.16) can be written as

$$-\frac{d^2}{d\hat{z}^2}\psi_n \;+\; \left(3k\, e^{-k\ell}\delta(|\hat{z}|-\hat{z}_{\mathrm{IR}}) - 3k\,\delta(\hat{z}) - \frac{1}{4\,(k^{-1}+|\hat{z}|)^2}\right)\psi_n \;=\; m_n^2\psi_n\,, \tag{7.18}$$

where $\hat{z}_{\mathrm{IR}} = k^{-1}(e^{k\ell}-1)$ denotes the position of the IR brane. The position of the UV brane is $\hat{z}_{\mathrm{UV}} = 0$. This equation has the form of a Schrödinger equation with 'energy' $E = m_n^2$ and a potential V which is given by the term in brackets. We have plotted this potential for positive $\hat{z}$ in Fig. 7.3. From the equivalent quantum-mechanical problem with that potential, we expect a mode with negative 'energy' $E = m_n^2$ and accordingly a mode with tachyonic mass in the 4d KK spectrum. Such a mode is indeed contained in the KK spectrum and the Breitenlohner-Freedman bound is no longer sufficient to ensure stability in a RS model [91].

The absence of tachyonic directions in the 4d theory can be achieved by switching on a localized mass term on the UV brane for the scalar Φ. To see this in more detail, we consider the corresponding term in the action,

$$S_{\mathrm{UV}} \;\supset\; \int d^4x \int_{-\ell}^{\ell} dy\, \sqrt{g}\, \lambda k\, \delta(y)\,, \Phi^2 \tag{7.19}$$

where the dimensionless parameter λ measures the mass in units of the AdS scale k. If we redo the steps leading to Eq. (7.18) taking Eq. (7.19) into account, we find an additional term in the potential:

$$V \;=\; 3k\, e^{-k\ell}\delta(|\hat{z}|-\hat{z}_{\mathrm{IR}}) + \Big(2\,\lambda - 3\Big)\, k\,\delta(\hat{z}) - \frac{1}{4\,(k^{-1}+|\hat{z}|)^2}\,. \tag{7.20}$$

[6] This coordinate is related to the coordinate z, which appeared in earlier sections, by a shift: $|\hat{z}| = |z| - k^{-1}$.

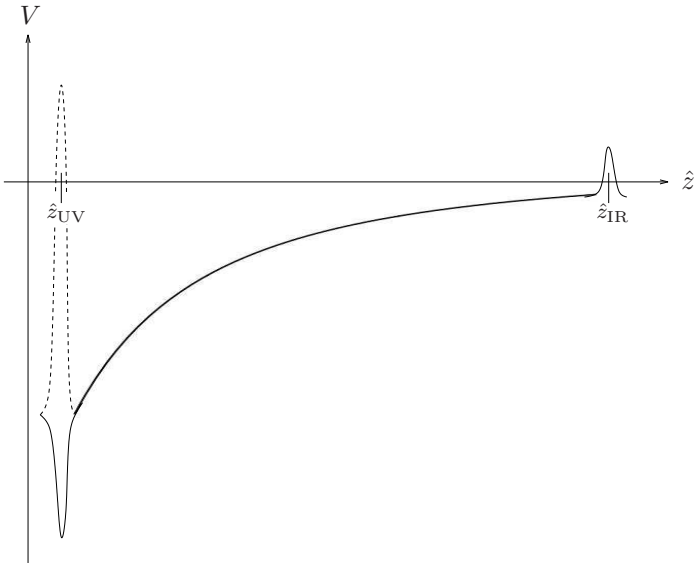

Figure 7.3: *Schematic plot of the potential in the effective Schrödinger equation for a tachyon in a RSI model. The dotted δ-peak appears when a large mass term on the UV brane is switched on.*

We have plotted the resulting δ-peak at the UV brane for λ much larger than 3/2 schematically as a dotted curve in Fig. 7.3. As one can see, this δ-peak has changed the sign as compared to the setup without a mass term at the UV brane and now leads to a repulsive instead of an attractive contribution to the potential. Due to this fact, as we will discuss in more detail in Appendix B, there are no longer modes with negative 'energy' $E = m_n^2$ in the KK spectrum for sufficiently large λ. Instead, all the modes have a positive mass squared.

Thus, a scalar with a tachyonic bulk mass in a RS model must have an appropriate mass on the UV brane in order to avoid tachyonic KK modes. Furthermore, the Breitenlohner-Freedman bound has no particular meaning in a RS model. Even tachyonic scalars with bulk masses $m_{\rm 5d}^2 < -4k^2$ do not lead to instabilities if they are stabilized by sufficiently masses on the UV brane. Nevertheless, we still consider a tachyon which just satisfies the Breitenlohner-Freedman bound, i.e. with $m_{\rm 5d}^2 = -4k^2$, in the following. The reason is that such scalars appear in the 5d effective theory of the KS throat: The geometry of the KS throat in the UV is approximately $\mathrm{AdS}_5 \times \mathrm{T}^{1,1}$ and scalars with negative mass squared down to the Breitenlohner-Freedman bound are contained in the spectrum of type IIB supergravity on $\mathrm{AdS}_5 \times \mathrm{T}^{1,1}$ [92].

For each tachyonic bulk mass, there exists a value of the mass on the UV brane which lifts the tachyonic mode in 4d to a massless mode. As we will derive in Appendix B, for a scalar with $m_{\rm 5d}^2 = -4k^2$, this happens for $\lambda \simeq 2$. The resulting massless scalar KK mode, however, would be in conflict with observations, as we have discussed in Section 1.1. In the following, we therefore assume that λ is somewhat larger than 2, say $\lambda \approx 3$. This lifts the tachyonic mode in 4d to a very massive mode.

We now want to determine the decay rate of KK modes of such a tachyon between

two throats. We replace first throat by the RSI model and the second throat by a gauge theory with $\sim N^2$ degrees of freedom which lives on the UV brane of the RSI model. Here, N is related to the AdS scale R of the throat by Eq. (2.20). We assume that the 10d scalar leading to the tachyon in 5d effective theory couples to the operator $F_{\mu\nu}^2$ of the gauge theory in the same way as the dilaton couples to that operator in the DBI action. This gives the effective 5d coupling

$$S_{\rm UV} \supset \frac{1}{M_{10}^4 R^{5/2}} \int d^4x \int_{-\ell}^{\ell} dy \sqrt{g} F_{\mu\nu} F^{\mu\nu} \Phi \delta(y) . \tag{7.21}$$

The prefactor can be understood as follows: We consider a setup in which the AdS scales R of the throats are of the same order as the size L of the embedding space. A reduction from 10d to 5d then gives a factor of $L^5 \sim R^5$ in the kinetic term of the scalar. This factor can be absorbed into a field redefinition and leads to the factor $R^{-5/2}$ in Eq. (7.21) in addition to the factor M_{10}^{-4} from the DBI action.

We consider a field which is even under the orbifold $\mathbb{Z}_2$-action, i.e. $\psi_n(\hat{z}) = \psi_n(-\hat{z})$. The δ-function peaks in the potential can be rewritten as boundary conditions on the branes. Furthermore, it is sufficient to consider the field only for positive $\hat{z}$. It is then more convenient to use a shifted and rescaled variable $\bar{z} \equiv m_n(\hat{z} + k^{-1})$.[7] For an even field, a Schrödinger-equation with the potential Eq. (7.20) is equivalent to the equation

$$\left(\frac{d^2}{d\bar{z}^2} + \frac{1}{4\,\bar{z}^2} + 1 \right) \psi_n = 0 \tag{7.22}$$

with the boundary conditions

$$\bar{z}_{\rm UV} \frac{d}{d\bar{z}} \psi_n(\bar{z}_{\rm UV}) = \left(\lambda - \frac{3}{2} \right) \psi_n(\bar{z}_{\rm UV}) \qquad \text{and} \qquad \bar{z}_{\rm IR} \frac{d}{d\bar{z}} \psi_n(\bar{z}_{\rm IR}) = -\frac{3}{2} \psi_n(\bar{z}_{\rm IR}) . \tag{7.23}$$

Here, $\bar{z}_{\rm UV} = m_n k^{-1}$ and $\bar{z}_{\rm IR} = m_n k^{-1} e^{k\ell}$ are the positions of the UV brane and the IR brane, respectively. The wave functions and the spectrum, which follow from Eqs. (7.22) and (7.23), are determined in Appendix B. Here, a simplified analysis will be sufficient:

Since Eqs. (7.22) and (7.23) correspond to a quantum-mechanical problem in a box of size $\bar{z}_{\rm IR} - \bar{z}_{\rm UV}$, it is clear that the masses are quantized approximately in units of $(\bar{z}_{\rm IR} - \bar{z}_{\rm UV})^{-1} \simeq k e^{-k\ell}$, such that $m_n \sim n\, k\, e^{-k\ell}$ with $n \in \{1, 2, 3, \dots\}$. In the following, we consider a KK mode with a mass somewhat larger than the minimal mass and correspondingly n somewhat larger than 1. For such a KK mode, we can solve Eq. (7.22) approximately in two regions: For $\frac{1}{2} \ll \bar{z} \leq \bar{z}_{\rm IR} \sim n$, we can neglect the z-dependent term in the potential in Eq. (7.22). Similarly, for $\frac{1}{2} \gg \bar{z} \geq \bar{z}_{\rm UV} \sim n\, e^{-k\ell}$, we can neglect the constant term. Approximate solutions to Eq. (7.22) in these regions are

$$\psi_n(\bar{z}) \simeq \begin{cases} \frac{1}{N_n} \left(\bar{z}^{\frac{1}{2}} + A_n\, \bar{z}^{\frac{1}{2}} \ln \bar{z} \right) & \text{for} \quad \bar{z}_{\rm UV} \leq \bar{z} \ll \frac{1}{2} \\ \frac{1}{N_n} \left(\cos \bar{z} + B_n \sin \bar{z} \right) & \text{for} \quad \frac{1}{2} \ll \bar{z} \leq \bar{z}_{\rm IR} . \end{cases} \tag{7.24}$$

[7] This coordinate is related to the coordinate z, which appeared in earlier sections, by a rescaling: $\bar{z} = m_n\, z$.

The constant A_n can be determined from the boundary condition on the UV brane in Eq. (7.23). We find

$$A_n \;=\; \frac{\lambda-2}{1-(\lambda-2)\,\ln \bar{z}_{\rm UV}}\,. \tag{7.25}$$

We choose the constant N_n such that the kinetic term of the 4d field χ_n is canonically normalized. With the relations $\bar{z} = \frac{m_n}{k} e^{k\ell}$ and $\phi_n = (\frac{\bar{z}k}{m_n})^{3/2}\psi_n$ as well as with Eqs. (7.16) and (7.17), one can check that this is fulfilled if

$$m_n^{-1} \int_{\bar{z}_{\rm UV}}^{\bar{z}_{\rm IR}} d\bar{z}\, \psi_n^2 \;\sim\; 1\,, \tag{7.26}$$

up to $\mathcal{O}(1)$ prefactors. We can split this integral and use the approximate solutions in Eq. (7.24) in the regions $\bar{z}_{\rm UV} \leq \bar{z} \lesssim \frac{1}{2}$ and $\frac{1}{2} \lesssim \bar{z} \leq \bar{z}_{\rm IR}$, respectively. Since $A_n < 1$ and we have assumed that $\bar{z}_{\rm IR} \sim n \gg 1$, the integral is dominated by the latter region. In Appendix B, we find that the constant B_n, which is determined by the boundary condition at the IR brane in Eq. (7.23) and the precise relation for the masses m_n, is also small, i.e. $B_n < 1$. We then find

$$N_n \;\sim\; \sqrt{\frac{\bar{z}_{\rm IR}}{m_n}}\,. \tag{7.27}$$

Inserting the KK expansion Eq. (7.17) into the coupling Eq. (7.21) and using the approximate solution near the UV brane in Eq. (7.24) together with Eqs. (7.25) and (7.27), the coupling of the n-th KK mode χ_n to the operator $F_{\mu\nu}^2$ follows as:

$$S_{\rm 4d} \;\supset\; \frac{g_n}{M_{10}^4\, R^3} \int d^4x\, F_{\mu\nu}F^{\mu\nu}\,\chi_n\,, \qquad \text{where} \quad g_n \;\sim\; \sqrt{m_n\, m_{\rm IR}}\,\frac{R^2}{\ell}\,. \tag{7.28}$$

We have used $\lambda \approx 3$ and the fact that $\log \bar{z}_{\rm UV} = \log(m_n/k) \sim -k\,\ell = -\ell/R$. This factor is approximately the logarithm of the generated hierarchy of the throat and therefore typically at most of the order 10. Up to $\mathcal{O}(1)$ prefactors, our simplified analysis reproduces the coupling in Eqs. (B.16) and (B.17) from the rather lengthy KK decomposition in Appendix B.

The resulting decay rate of a KK mode into $\sim N^2$ degrees of freedom on the UV brane, and thus into another throat, is

$$\Gamma \;\sim\; (m_n R)^4\, m_{\rm IR} \left(\frac{R}{\ell}\right)^2, \tag{7.29}$$

where we have used Eq. (2.20). Since typically $\ell/R = \mathcal{O}(10)$, this decay rate is only slightly smaller than the corresponding decay rate of graviton KK modes Eq. (4.15).

We want to compare this decay rate with the flux-suppressed decay rate Eq. (7.15) that we have derived in Section 7.4. Using Eq. (2.20) and assuming that both throats have the same number of degrees of freedom, i.e. $N_1 = N_2$, Eq. (7.15) can be written as

$$\Gamma \;\sim\; N^2 (m_n R)^8\, m_{\rm IR}\,. \tag{7.30}$$

Since the mass m_n is exponentially smaller than the AdS scale R^{-1}, whereas typically $\ell/R = \mathcal{O}(10)$ and $n \lesssim 10^4$ (cf. Section 9.1), the relative factor $(m_n R)^4 N^2 (\ell/R)^2$ between Eqs. (7.29) and (7.30) is usually very small. Decays of KK modes which are mediated by a tachyon in the KS throat therefore have a much higher rate than decays which are mediated by the flat direction in the KS throat that we have discussed in Section 7.4.

7.6 Processes involving the standard model sector

The results from Chapters 5 and 6 were derived for stacks with a large number of D-branes because these stacks are dual to throats. These results, however, are also applicable to small stacks of D-branes. In particular, we can consider a realization of the standard model on some D3- and/or D7-branes which live in the unwarped part of the compact space.[8] The heat transfer rate between the standard model and a throat is then given by Eq. (5.15) if we set $N_1^2 = g$ to account for the standard model with $g \sim 100$ degrees of freedom. According to the discussion in Section 7.1, N_2 is the number N_{UV} of 5-form flux at the UV end of the throat.

Similarly, Eq. (7.15) with $N_1^2 = g$ and $N_2 = N_{\text{UV}}$ is the decay rate of scalar glueballs to the standard model. Note, however, that this decay rate is not applicable to the inverse process (a decay from the standard model to a throat sector) since our derivation of the vertex in Eq. (6.9) assumed a weakly curved gravity description. This is not fulfilled for a small stack of D-branes.

There is a subtlety concerning the decay rate of spin-$\frac{1}{2}$ glueballs to the standard model which arises for large gravitino masses, $m_{3/2} \gg m_{\text{IR}}$. Namely, we expect the mass splitting between superpartners in the standard model sector to be of the order of the gravitino mass. This means that the superpartners of standard model particles are heavier than the decaying spin-$\frac{1}{2}$ glueballs. If R-parity is conserved, most decay channels involve such a superpartner as a final state and the corresponding decays are therefore kinematically forbidden. A coupling that does not involve a superpartner is

$$\lambda \, \bar{l} \, \psi \, H \,, \tag{7.31}$$

where l is a lepton doublet, H is the Higgs doublet and ψ is a dilatino or any other modulino.[9] The coupling strength λ may be $\mathcal{O}(1)$ or it may be suppressed as $\lambda = m/M_4$ where m is some low mass scale.

Note, however, that the coupling in Eq. (7.31) probably requires R-parity violation. Namely, the corresponding coupling containing the modulus instead of the modulino generates a bilinear R-parity violating term for nonzero modulus vev. For high-scale supersymmetry breaking, a large coupling λ may nevertheless be allowed. Moreover,

[8] In the literature, it is often assumed that the standard model is realized in a throat. In this case, the standard model couples to supergravity modes in that throat which in turn couple to other throats according to Eqs. (5.16) and (6.13).

[9] This coupling was already considered in [93] since it also leads to a mixing between the modulino and the neutrino.

even for maximally broken R-parity, all other decay channels involve standard model superpartners which further decay into standard model particles. The corresponding decay rates are therefore suppressed by the propagators of the heavy superpartners and are smaller than the decay rate resulting from Eq. (7.31). Therefore, we focus on this coupling. Redoing the steps leading to Eq. (7.15) with the vertex of Eq. (7.31), we find

$$\Gamma \sim \lambda^2 N_{\rm UV}^2 \frac{m^6 m_{\rm IR}}{M_{10}^8/M_4^2} \tag{7.32}$$

for the decay rate of spin-$\frac{1}{2}$ glueballs to the standard model if $m_{3/2} \gg m_{\rm IR}$.

Finally, we note that, in absence of the coupling in Eq. (7.31) and of R-parity violation, the spin-$\frac{1}{2}$ glueballs can not decay at all to the standard model sector. If, in addition, there is no throat with lower IR scale (otherwise decays to this sector with the rate in Eq. (7.15) are possible), the spin-$\frac{1}{2}$ glueballs are absolutely stable.

Chapter 8

Sequestered Dark Matter: Thermal production

8.1 Preliminaries

Dark matter is frequently assumed to consist of massive weakly interacting particles which are stable (or have a very long lifetime) because their decay is forbidden by some (approximate) symmetry. The observed dark matter abundance is obtained if these particles were in thermal equilibrium in the early universe and later fell out of equilibrium with an appropriate freeze-out abundance.

But it is also well-known that dark matter may originate in a hidden sector which is coupled to the standard model only via higher-dimension operators, ensuring that dark matter has a sufficiently long lifetime (see e.g. [62, 63, 94]). Since the annihilation cross section of these particles is suppressed by a high mass scale (proceeding via a higher-dimension operator), they may overclose the universe today if they had been in thermal equilibrium in the early universe. Instead, one often assumes that the hidden sector particles were not in thermal equilibrium after reheating and that they were produced by thermal reactions in the hot standard model plasma. The resulting abundance is typically much lower than the equilibrium abundance since the relevant rates are again suppressed by a high mass scale. Depending on the reheating temperature, the abundance can have the right magnitude to account for the observed dark matter. A well-known particle which falls into this class of dark matter candidates is (to a certain extent[1]) the gravitino.

In the following sections, we present a new dark matter candidate with the aforementioned properties (we discuss earlier related work in Section 9.4): KK modes in a throat or, equivalently, glueballs of the dual gauge theory. Due to the warping, these particles have highly suppressed couplings to other sectors and can therefore be very

[1]The gravitino would decay too quickly were it not (at least partially, see [95, 96]) protected by R-symmetry. Moreover, another well-known production mechanism of gravitino LSPs is by the decay of NLSPs which had an appropriate freeze-out abundance.

stable. By the same token, they have redshifted and thus relatively low masses which allows them to be produced thermally, even if the reheating temperature is not very high.

The throats respectively the dual gauge theories would lead to too much dark radiation during big bang nucleosynthesis and/or would overclose the universe if they were in thermal equilibrium after reheating. We therefore assume that only the standard model is reheated initially and that the throats receive no energy from the reheating process.[2] Glueballs are then produced by thermal reactions in the hot standard model plasma. Nevertheless, it is of course possible that the inflaton interacts only very weakly with the throats respectively the dual gauge theories, thereby producing an abundance of glueballs during reheating which is not too high. Since this abundance depends on the coupling of the inflaton and on the model at hand, we can view our result for the produced amount of dark matter, that we derive, as a model-independent lower bound.

There is an important aspect of the production mechanism of our dark matter candidate that can best be seen from the gauge theory point of view: Annihilating particles in the hot standard model plasma inject energy into the gauge theory. The gauge theory states which are produced in that way hadronize shortly afterwards (if the energy density in the gauge theory sector is not above the confinement scale). As we will discuss in the next section, there are no jets in the large-N, large-λ gauge theories which are dual to throats. Instead, after hadronization, all the energy is in the form of slow glueballs with masses and kinetic energies of the order of $m_{\rm IR}$. These glueballs immediately scale like matter with the expansion of the universe and thereby give an important contribution to the total energy density at our epoch already for reheating temperatures which are only moderately high.

For definiteness, we focus on scenarios in which the standard model is realized on some D3- and/or D7-branes in the unwarped part of the compact space (as discussed in Section 7.6). The fact that the glueball couplings to the standard model are highly suppressed ensures a long lifetime of the dark matter particles. Nevertheless, it turns out that in many cases decays mediated by the gravitino must be negligible because otherwise the decay rate of glueballs would be too high. We therefore focus on scenarios with high-scale supersymmetry breaking in which the gravitino is much heavier than the glueballs, $m_{3/2} \gg m_{\rm IR}$. We comment on models with low-scale supersymmetry breaking in Section 9.3.

[2]This is, for example, not fulfilled for reheating after brane-antibrane inflation. In this scenario (cf. Section 4.1), the throat in which inflation takes place is heated by the annihilation of the brane with the antibrane. This energy is subsequently transferred to other throats and the standard model as discussed in earlier sections. Aspects of KK dark matter in such a scenario were discussed in [62] (cf. Section 9.4).

8.2 Energy transfer

As outlined in the last section, we assume that the throats have received no energy from the reheating process, whereas the standard model is heated to a temperature $T_{\rm RH}$ initially. Subsequently, energy will be transferred from the standard model to the throats. Note that this process is similar to the energy transfer from the hot brane to the bulk in RSII models [68] (see also [27]). The AdS_5 bulk plays the role of the throat, which we however assume to be of finite length, with the KS region corresponding to the IR brane.

We assume that the temperature of the standard model is smaller than the compactification scale, i.e. $T < L^{-1}$. Furthermore, we consider the generic situation that the distance between the two throats is of the same order of magnitude as the size of the embedding manifold, i.e. $A \sim L$. The heat transfer rate is then given by Eq. (5.15) and the second term in that rate dominates. We set $N_1^2 = g$ to account for the standard model sector with $g \sim 100$ degrees of freedom and $N_2 = N_{\rm UV}$ for the throat at hand. Using Eq. (3.3), the heat transfer rate can be written as

$$\dot{\rho} \;\sim\; g\, N_{\rm UV}^2 \frac{T^9}{M_4^4}\,. \tag{8.1}$$

This rate is easily understood as being due to a gravitational strength coupling between a sector with g degrees of freedom (the standard model) and a sector with $N_{\rm UV}^2$ degrees of freedom (the throat). Note that, due to the existence of a confinement scale $m_{\rm IR}$, glueballs can only be created if $T_{\rm RH} > m_{\rm IR}$. We expect these initial gauge theory states to have masses up to $m \sim T_{\rm RH}$.

The glueballs may decay back to the standard model. As we have discussed in Section 7.1, spin-2 glueballs have the highest decay rate. From Eq. (6.13), we get

$$\Gamma(m) \;\sim\; g\, N_{\rm UV}^2 \frac{m^4 m_{\rm IR}}{M_4^4}\,. \tag{8.2}$$

On the other hand, glueballs can also decay to lighter glueballs within the same throat. We will have to discuss this process in some detail below. At the moment, it is sufficient to establish that the decay to lighter glueballs wins over the possible decay back to the standard model. For this purpose, we recall that we are dealing with a strongly coupled system with a dense spectrum. Thus, the initially created gauge theory state of mass m will have a lifetime $\sim 1/m$. In the most conservative scenario, it will decay to 2 states of mass $m/2$. These states will in turn decay to states of mass $m/2^2$ after a time-interval $\sim 2/m$, and so on. Summing up the probabilities for the decay back to the standard model at each step of this cascade, we arrive at a total probability

$$w \sim \sum_{n=0} \Gamma(m/2^n) \cdot \frac{2^n}{m}\,. \tag{8.3}$$

This sum is of the same order of magnitude as the first term and hence very small in all cases of interest. Clearly, we could equally well have assumed that each glueball

decays to k_1 lighter states with mass m/k_2, arriving at the same conclusion for any $\mathcal{O}(1)$ numbers k_1 and k_2. Thus, the relaxation to lighter states within the same throat always wins over the decay back to the standard model or to other throats.

The heat transfer rate Eq. (8.1) is strongly temperature dependent, $\dot{\rho} \propto T^9$. Therefore, heat transfer is effectively finished soon after reheating and the corresponding time scale is $|T/\dot{T}|$ at $T = T_{\rm RH}$. The total energy density after reheating is dominated by the relativistic gas in the standard model sector with $\rho = g\frac{\pi^2}{30}T^4$. We find

$$|T/\dot{T}| \;=\; H^{-1} \;\sim\; \frac{M_4}{g^{1/2}T^2}\,, \tag{8.4}$$

where H is the Hubble rate. Using Eqs. (8.1) and (8.4) at $T \sim T_{\rm RH}$, the energy density deposited in a throat directly after reheating is

$$\rho \;\sim\; \dot{\rho}\,|T/\dot{T}| \;\sim\; g^{1/2}N_{\rm UV}^2\frac{T_{\rm RH}^7}{M_4^3}\,. \tag{8.5}$$

Before closing this section, we note that the heat transfer processes we consider compete with the unavoidable energy deposition in the throat sectors occurring during inflation. This can be understood by noting that de Sitter space has a temperature $T_{\rm dS} \sim 1/R_{\rm dS} \sim M_{\rm inf}^2/M_4$. We assume that inflation lasts long enough for the throats to be thermalized with this temperature. Furthermore, parameterizing the efficiency of reheating by an efficiency factor $\epsilon \leq 1$, we have $gT_{\rm RH}^4 \sim \epsilon M_{\rm inf}^4$. Thus, all throats have a temperature $T_{\rm dS} \sim \sqrt{g/\epsilon}\,T_{\rm RH}^2/M_4$ at the time of reheating. Jumping ahead, we note that for typical long throats (where this effect is most relevant), we find initial throat temperatures $\sim 10^6$ GeV for a reheating temperature $\sim 10^{11}$ GeV. For such throats, 'de-Sitter heating' in fact wins over the heating process analysed in this section if $\epsilon < 1$, allowing in principle for even more throat dark matter than we find in our conservative analysis.

8.3 Time evolution of the energy density

The result in Eq. (8.5) is the energy density in the gauge theory sector directly after reheating. During cosmological evolution, this energy density is diluted by the expansion of the universe. To determine the contribution of glueballs to the total energy density at our epoch, it is important to know how their energy density scales with the scale factor a of the universe.

Let us first consider the case that the energy density is above the critical value for a deconfinement phase transition directly after reheating. The gauge theory thermalizes in this situation. To see this in more detail, we view each initially created gauge theory state as a localized excitation of a strongly coupled system with energy $\sim T_{\rm RH}$. The localization assumption can be justified by recalling that, from the D-brane perspective, the mediating bulk supergravity fields couple to local gauge theory operators like

$F_{\mu\nu}F^{\mu\nu}$. We model the further evolution of this state as a ball of gauge theory plasma expanding with the velocity of light.[3] The number density of these balls is

$$n \sim \frac{\rho}{T_{\rm RH}} \sim g^{1/2} N_{\rm UV}^2 \frac{T_{\rm RH}^6}{M_4^3}\,, \tag{8.6}$$

where we have used Eq. (8.5). It follows that the balls fill out the whole space after a time

$$t \sim n^{-1/3} \sim \frac{M_4}{g^{1/6} N_{\rm UV}^{2/3} T_{\rm RH}^2}\,. \tag{8.7}$$

Comparing this with the Hubble time Eq. (8.4) at $T = T_{\rm RH}$, we see that the gauge theory plasma fills out the whole space before the Hubble expansion becomes relevant if $N_{\rm UV}^2 \gtrsim g$, which holds for all relevant throats.

The gauge theory dual to a KS throat has a logarithmically varying number of degrees of freedom, corresponding to the logarithmic deviation of the KS geometry from AdS_5. In the deconfined phase, the effective number of colours $N_{\rm eff}$ of the gauge theory depends on the temperature $\tilde{T}$ of the plasma as

$$N_{\rm eff} \sim N_{\rm IR} \ln\left(\frac{\tilde{T}}{m_{\rm IR}}\right)\,. \tag{8.8}$$

The deconfined phase of the gauge theory is dual to a throat with a black hole horizon which replaces the IR end. The highest meaningful value in Eq. (8.8) is $N_{\rm eff} \sim N_{\rm UV}$. This corresponds to a temperature where the black hole horizon reaches the UV end of the throat. The energy density as a function of the plasma temperature $\tilde{T}$ is

$$\rho \sim N_{\rm eff}^2 \tilde{T}^4\,. \tag{8.9}$$

Since the logarithmic variation of $N_{\rm eff}$ with $\tilde{T}$ is small compared to the variation of the $\tilde{T}^4$-term, we will neglect it in the following. The deconfined phase can then be described by an approximate conformal field theory and the energy density correspondingly scales like radiation with a^{-4}.

When the energy density drops to $\rho \sim N_{\rm IR}^2 m_{\rm IR}^4$, a confinement phase transition begins which lasts until the energy density has reached $\rho \sim \lambda\, m_{\rm IR}^4$, where $\lambda = g_s N_{\rm IR}$ is the 't Hooft coupling.[4] In the transition region for ρ, space is divided into separate regions in either the confined phase with $\rho < \lambda\, m_{\rm IR}^4$ or the still deconfined phase with $\rho > N_{\rm IR}^2 m_{\rm IR}^4$. At even lower energy densities $\rho < m_{\rm IR}^4$ (assuming $\lambda > 1$), a description in terms of a nonrelativistic glueball gas is applicable and the energy density correspondingly scales with a^{-3}. We do not know the scaling of ρ with a in the transition region $N_{\rm IR}^2 m_{\rm IR}^4 > \rho > m_{\rm IR}^4$ though, since the equation of state during the phase transition is unknown. Since we expect the scaling to be in between the two extremes $\rho \propto a^{-3}$ and

[3] Note that this physical picture is equivalent to the picture of a cascade decay used in the derivation of Eq. (8.3) if we assume that a glueball with mass $m/2^n$ fills out a volume $(2^n/m)^3$.

[4] The thermodynamics of large-N gauge theories is reviewed e.g. in Appendix A in [97].

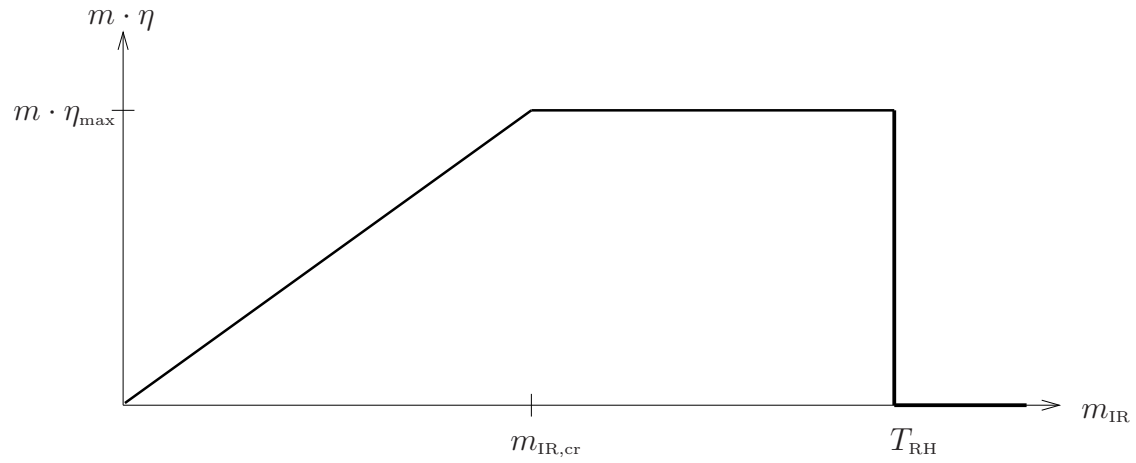

Figure 8.1: *Schematic plot of $m \cdot \eta$ as a function of the IR scale m_{IR} of the throat. Here, $m_{IR,cr}$ is the IR scale for which $T_{pt} \sim T_{RH}$, i.e., for which the throat is heated precisely to its phase transition temperature. See text for more details.*

$\rho \propto a^{-4}$ in this region, we will take $\rho \propto a^{-4}$ for $\rho > N_{\rm IR} m_{\rm IR}^4$ and $\rho \propto a^{-3}$ for $\rho < N_{\rm IR} m_{\rm IR}^4$ for simplicity.[5]

Thus, the energy density in the gauge theory sector, Eq. (8.5), initially scales like radiation if it is larger than $\rho \sim N_{\rm IR} m_{\rm IR}^4$. As a function of the standard model temperature T, we have

$$\rho \sim g^{1/2} N_{\rm UV}^2 \left(\frac{T_{\rm RH}}{M_4}\right)^3 T^4 \,. \tag{8.10}$$

We assume the scaling behaviour to change when the energy density has dropped to $\rho \sim N_{\rm IR} m_{\rm IR}^4$. This happens when the standard model has a temperature

$$T_{\rm pt} \sim m_{\rm IR} \frac{N_{\rm IR}^{1/4}}{N_{\rm UV}^{1/2}} \left(\frac{M_4}{T_{\rm RH}}\right)^{3/4} , \tag{8.11}$$

where we have neglected a factor of $g^{1/8}$ which is close to 1. The energy density scales like matter afterwards and the ratio of energy density and entropy density, $\rho/s = m \cdot \eta$, stays constant. Here $\eta = n/s$ is the glueball number density normalized by the entropy density. Using Eq. (8.10) and $s = g\frac{2\pi^2}{45} T^3$ (dominated by the standard model sector) at $T = T_{\rm pt}$, we find the glueball mass density per entropy density

$$m \cdot \eta \sim \frac{N_{\rm UV}^2}{g^{1/2}} \left(\frac{T_{\rm RH}}{M_4}\right)^3 T_{\rm pt} \,. \tag{8.12}$$

[5]Using the intermediate value $\rho \sim N_{\rm IR} m_{\rm IR}^4$ for the distinction between the two behaviours, the error in ρ is a factor of $(N_{\rm IR} m_{\rm IR}^4 / N_{\rm IR}^2 m_{\rm IR}^4)^{1/4} = N_{\rm IR}^{-1/4}$ if $\rho \propto a^{-3}$ in the entire transition region or a factor of $(N_{\rm IR} m_{\rm IR}^4 / m_{\rm IR}^4)^{1/3} = N_{\rm IR}^{1/3}$ if $\rho \propto a^{-4}$ in the entire transition region. In both cases, this factor is typically $\mathcal{O}(1)$.

The factor of $T_{\rm pt}$ is smaller than or equal to $T_{\rm RH}$ and reflects the fact that the energy density undergoes a phase of a^{-4} dilution. The quantity $m \cdot \eta$ is useful because it determines the contribution of the glueballs to the total energy density in the late universe. We have plotted $m \cdot \eta$ as a function of $m_{\rm IR}$ schematically in Fig. 8.1. The part corresponding to Eq. (8.12) is the line which grows linearly[6] with the IR scale from $m_{\rm IR} = 0$ up to an $m_{\rm IR}$ such that $T_{\rm pt}$ in Eq. (8.11) is of the same order of magnitude as $T_{\rm RH}$. This is the maximal IR scale for which Eq. (8.12) is valid because at this point the initial energy density in the gauge theory sector, Eq. (8.5), is of the same order of magnitude as the critical energy density $\rho \sim N_{\rm IR} m_{\rm IR}^4$.

Dividing Eq. (8.12) by $\rho_c/s_0 \simeq 2 \cdot 10^{-9}\,\text{GeV}$, where ρ_c is the current critical energy density for a flat universe and s_0 is the current entropy density, and using $g \sim 100$ as well as $M_4 \simeq 2 \cdot 10^{18}\,\text{GeV}$, we have

$$\Omega \,=\, \frac{\rho}{\rho_c} \,\sim\, \left(\frac{T_{\rm RH}\, N_{\rm UV}^{1/2}}{6 \cdot 10^{11}\,\text{GeV}}\right)^4 \left(\frac{T_{\rm pt}}{T_{\rm RH}}\right) . \tag{8.13}$$

This is the contribution of the gauge theory sector to the density parameter. The second factor is smaller than or equal to 1 and again reflects the fact that the corresponding energy density undergoes a phase of a^{-4} dilution.

Let us now consider the case that the initial energy density in the gauge theory sector, Eq. (8.5), is smaller than $\rho \sim N_{\rm IR} m_{\rm IR}^4$. Recall that the energy density is due to standard model particles which annihilate via a KK mode of supergravity fields in the embedding space into gauge theory states (cf. Fig. 5.2). This is similar to electron-positron annihilation via a photon into a quark and an antiquark. In QCD, these partons subsequently radiate other partons in a narrow cone along their trajectories, leading to two jets. The hadrons which are formed in this process are ultrarelativistic and would initially scale like radiation with a^{-4} with the expansion of the universe. In contrast, in the large-N, large-λ gauge theories which are dual to throats, no jets are formed [98–100] (see also [8, 101]). Instead, if the energy density is below the critical energy density, the initial gauge theory states hadronize to slow and light glueballs, i.e. with masses and kinetic energies $\sim m_{\rm IR}$. This is not surprising since the gauge theory is strongly coupled on all scales.[7] Highly energetic partons which result from the annihilation of standard model particles will therefore split into more and more partons until the individual energy of the partons reaches the confinement scale [99]. This leads to the aforementioned distribution of light and slow glueballs. These glueballs immediately become nonrelativistic and then scale like matter with a^{-3} with the expansion of the universe.

Note that Refs. [98–100], in which the hadronization in large-N, large-λ gauge theories was analysed in great detail, appeared after Ref. [8], on which this chapter is based. Ref. [8] additionally analyzed the evolution of the energy density for the case that jets are formed in gauge theories which are dual to throats. This analysis is now obsolete.

[6] Note that this plot has to be read either at fixed $N_{\rm UV}$, in which case $N_{\rm IR}$ must be interpreted as function of $N_{\rm UV}$ and $m_{\rm IR}$, or at fixed $N_{\rm IR}$, in which case $N_{\rm UV}$ must be interpreted as function of $N_{\rm IR}$ and $m_{\rm IR}$. In both cases an extra logarithmic dependence of $m \cdot \eta$ on $m_{\rm IR}$ is introduced, which we however neglect.

[7] The calculations in [98–100] were mainly performed on the gravity side of the duality.

Taking this scaling into account, the mass density over entropy density $m \cdot \eta$ and the density parameter Ω are given by

$$m \cdot \eta_{\max} \sim \frac{N_{\rm UV}^2}{g^{1/2}} \frac{T_{\rm RH}^4}{M_4^3}, \qquad \Omega_{\max} = \left(\frac{T_{\rm RH} N_{\rm UV}^{1/2}}{6 \cdot 10^{11}\,{\rm GeV}} \right)^4 . \tag{8.14}$$

Note that these expressions are just those in Eqs. (8.12) and (8.13) with $T_{\rm pt}$ replaced by $T_{\rm RH}$. This reflects the fact that the energy density now scales like matter from the beginning on. As a function of $m_{\rm IR}$, $m \cdot \eta$ is thus constant in this case. Note, though, that throats with $m_{\rm IR} > T_{\rm RH}$ are not heated for kinematic reasons. The mass density over entropy density $m \cdot \eta$ is therefore zero in this region. Again, we have plotted the corresponding parts of $m \cdot \eta$ as a function of $m_{\rm IR}$ in Fig. 8.1.

Chapter 9

Sequestered Dark Matter: Cosmological scenarios

9.1 A single throat

Glueballs are an interesting dark matter candidate if they are stable until our epoch. In this section, we analyse the prospects of this new kind of dark matter for a compactification which has only a single throat region. Setups with a large number of throats are discussed in Section 9.2.

As one can see from Fig. 8.1, the glueball mass density over entropy density $m \cdot \eta$ or, equivalently, the contribution of glueballs to the density parameter Ω is maximized for throats with IR scales in the range $m_{\rm IR,cr} \lesssim m_{\rm IR} \lesssim T_{\rm RH}$. This is therefore an interesting region to look for glueball dark matter.

Let us first consider throats at the lower end of the 'optimal' interval, i.e. with IR scales of the order of $m_{\rm IR,cr}$. For this IR scale, the initial energy density in the throat, Eq. (8.5), is just the critical energy density $\rho \sim N_{\rm IR} m_{\rm IR}^4$ of that throat. Solving for $m_{\rm IR}$, we find

$$m_{\rm IR,cr} \sim \left(\frac{N_{\rm UV}^2 \, T_{\rm RH}^7}{N_{\rm IR} \, M_4^3} \right)^{1/4} , \tag{9.1}$$

where we have neglected a factor of $g^{1/8}$ which is $\mathcal{O}(1)$.

In order to evaluate Eq. (9.1) as well as other relevant equations, we have to fix $N_{\rm IR}$ and $N_{\rm UV}$. These numbers determine the warp factor which in turn is related to the IR scale of the throat:[1]

$$h \sim e^{2\pi N_{\rm UV}/3N_{\rm IR}} \qquad\qquad m_{\rm IR} \sim h^{-1} N_{\rm IR}^{-1/4} M_{10} \, . \tag{9.2}$$

[1]For the warp factor, we have used Eq. (3.9) and the fact that $N_{\rm UV} \sim KM$ and $N_{\rm IR} \sim g_s M^2$, where K and M are the relevant numbers of H_3-flux and F_3-flux, respectively. The mass quantization follows from Eqs. (2.10) and (2.20) and the fact that the masses of light KK modes are determined by the geometry near the IR end of the throat.

To simplify the discussion and to avoid uncertainties associated with unknown factors of $N_{\rm IR}$ in the various glueball decay rates, we focus on throats where $N_{\rm IR} = \mathcal{O}(1)$. In this case, $N_{\rm UV}$ is a function of $m_{\rm IR}$ and M_{10}. For our purposes it will be sufficient to use the typical values $N_{\rm UV} \approx 10$ for long throats (e.g. for $m_{\rm IR} \sim 10^6$ GeV and $M_{10} \sim 10^{15}$ GeV) and $N_{\rm UV} \approx 4$ for shorter throats (e.g. for $m_{\rm IR} \sim 10^{11}$ GeV).

Inserting $N_{\rm UV} \approx 10$ and $N_{\rm IR} \approx 1$ in Eq. (8.14), we can determine the reheating temperature which leads to the right amount of dark matter, i.e. $\Omega \sim 1$. The mass of the dark matter candidate subsequently follows from Eq. (9.1). We find

$$T_{\rm RH} \sim 10^{11}\,\text{GeV} \qquad \text{and} \qquad m_{\rm IR} \sim 10^6\,\text{GeV}\,. \tag{9.3}$$

Thus, for a reheating temperature $\sim 10^{11}$ GeV and a throat with IR scale $\sim 10^6$ GeV, we get the right amount of glueballs to explain the observed dark matter.

In the late universe, this kind of dark matter consists solely of the lightest scalar glueball and its spin-$\frac{1}{2}$ superpartner, due to the processes discussed in Section 7.3. Let us consider the fermionic glueballs for the moment. For reason that we have discussed in Section 8.1, here and below, we focus on setups in which the gravitino is much heavier than the glueballs, $m_{3/2} \gg m_{\rm IR}$. The decay of spin-$\frac{1}{2}$ glueballs to a graviton and a gravitino is then kinematically forbidden. If the coupling in Eq. (7.31) is present, the spin-$\frac{1}{2}$ glueballs decay to the standard model with the rate given in Eq. (7.32). The resulting lifetime depends on the coupling strength λ:

$$\tau \sim 10^{26} \left(\frac{M_{10} \cdot \lambda^{-1/4}}{2 \cdot 10^{16}\,\text{GeV}} \right)^8 \text{s}\,. \tag{9.4}$$

It is not sufficient to make this lifetime just longer than the present age of the universe (which is $\sim 10^{17}$ s): The glueball decays produce photons (e.g. via hadronic showers) which contribute with a continuous spectrum to the diffuse γ-radiation. The γ-ray flux measured e.g. by the EGRET experiment gives constraints on the lifetime of unstable particles in dependence of their mass density (see e.g. [95,96,102–104]). In particular, an unstable particle with the mass density of dark matter has to live longer than $\sim 10^{26}$ s to comply with observations [102].[2] Thus, it depends on the two unknown parameters M_{10} and λ whether the spin-$\frac{1}{2}$ glueballs are a good dark matter candidate or not.

An interesting scenario is to have $\lambda = \mathcal{O}(1)$.[3] To get a viable dark matter candidate, the 10d Planck scale has a rather limited range in this case according to Eq. (9.4). This makes it more probable that the lifetime of the glueballs is in a range that can be probed by new γ-ray telescopes like GLAST. If this scenario with $\lambda = \mathcal{O}(1)$ is realized in nature, one may be able to see a signal in the near future.

[2] Here we have used that the hadronic branching ratio for decays via the coupling in Eq. (7.31) is $\mathcal{O}(1)$. For decays exclusively to photons or leptons, the constraints are less severe.

[3] The coupling in Eq. (7.31) leads to a mixing between the modulino ψ and a left-handed neutrino ν after electroweak symmetry breaking. Since the modulino has a large mass m_τ, the seesaw mechanism results in a light mass eigenstate. For $M_{10} \sim 10^{16}$ GeV (the minimal value allowed for $\lambda \sim 1$ according to Eq. (9.4)), Eq. (7.13) gives $m_\tau \sim 10^{14}$ GeV. Using this value and the mixing mass term for $\lambda \sim 1$ in the seesaw formula, the resulting neutrino mass is ~ 0.1 eV. Interestingly, this is precisely the mass range indicated by various experiments.

The scalar glueballs from a throat with IR scale 10^6 GeV decay to gravitons after approximately 10^{15} s according to Eq. (7.10). Note, however, that this lifetime is proportional to $m_{\rm IR}^{-5}$. The lifetime will thus be somewhat larger or smaller for IR scales slightly different from 10^6 GeV. If the lifetime is in the range of 10^{17} s (the present age of the universe) to 10^{12} s (the time of matter-radiation equality), the resulting decrease in the dark matter density may have interesting observable consequences. Note that, if the initial energy density was slightly above the critical energy density, a gauge theory with confinement scale of the order of $m_{\rm IR,cr}$ was thermalized in the early universe. In this case, part of the scalar glueballs (which we expect to be heavier than their superpartners for $m_{3/2} \gg m_{\rm IR}$, cf. Section 7.2) annihilate into their superpartners after the phase transition. The remaining abundance of scalar glueballs is the freeze-out abundance for this process which we determine in Appendix D. Inserting the above values for $N_{\rm UV}$, $m_{\rm IR}$ and $T_{\rm RH}$ into the relation for the depletion factor, Eq. (D.5), we see that the scalar glueballs make up for only 10^{-2} of the total dark matter abundance in this case. The loss of mass density due to their decay is correspondingly small. If the gauge theory was never thermalized, on the other hand, the initial abundance of scalar glueballs and fermionic glueballs is equal and the dark matter mass density is halved due to the decay of the scalar glueballs. It would be interesting to see whether such a large decrease of the dark matter abundance may still be allowed by observations and which observable consequences (e.g. on structure formation) it might have.

If the lifetime of scalar glueballs is large enough, a non-negligible amount still exists at our epoch. Decays of the glueballs to the standard model again produce γ-rays. The corresponding decay rate is given by Eq. (7.15) for $N_1^2 = g$ and $N_2 = N_{\rm UV}$ (cf. Section 7.6). For $m_{\rm IR} \sim 10^6$ GeV, the partial lifetime of scalar glueballs with respect to decays to the standard model is

$$\tau \sim 10^{26} \left(\frac{M_{10}}{3 \cdot 10^{13}\,\text{GeV}}\right)^8 \text{s}\,. \tag{9.5}$$

If the scalar glueballs still make up an $\mathcal{O}(1)$ fraction of the dark matter at our epoch, this partial lifetime has to be larger than $\sim 10^{26}$ s to comply with the EGRET measurements. If the current abundance of scalar glueballs is reduced (by decays to gravitons or by annihilation in a thermalized situation), the lower bound on the lifetime becomes correspondingly weaker.

In contrast to fermionic glueballs, scalar glueballs can decay directly to two photons. Decays via this channel in the halo of our galaxy lead to a sharp line in the γ-ray spectrum. The γ-rays at energies around 10^6 GeV cannot be measured by satellite-based experiments like EGRET or GLAST. Ground-based γ-ray telescopes like HESS have the necessary energy range, but a limited sensitivity due to the cosmic ray background. At 10^6 GeV, the measured flux in the cosmic ray spectrum is (see e.g. [105])

$$F \sim 10^{-12}\,(\text{m}^2\ \text{sr}\ \text{s}\ \text{GeV})^{-1}\,. \tag{9.6}$$

To be detectable against this background, the flux from the decaying glueballs in the halo has to have the same order of magnitude. This flux is emitted as a sharp line at

energy $m_{\rm IR}$ but smeared out by the detector due to a finite energy resolution ΔE. We model this effect by replacing the δ-function peak of the flux by a box of width ΔE. The flux is also inversely proportional to the mass $m_{\rm IR}$ and the lifetime τ of the glueballs. Assuming that the scalar glueballs make up an $\mathcal{O}(1)$ fraction of the dark matter at our epoch, we find (see e.g. [95])

$$F \sim 10^{-12} \left(\frac{10^5 \text{ GeV}}{\Delta E}\right) \left(\frac{10^6 \text{ GeV}}{m_{\rm IR}}\right) \left(\frac{10^{26} \text{ s}}{\tau}\right) (\text{m}^2 \text{ sr s GeV})^{-1} . \tag{9.7}$$

For $m_{\rm IR} \sim 10^6$ GeV and $\Delta E \sim 10^{-1} \cdot E \sim 10^5$ GeV as quoted by the HESS collaboration, the partial lifetime of scalar glueballs (for decays to the standard model) has to be less than $\sim 10^{26}$ s to be detectable against the cosmic ray background. If the partial lifetime is somewhat larger, the γ-line may nevertheless become detectable in the near future with an improved rejection of cosmic ray events and a better sensitivity and energy resolution.

In summary, if an $\mathcal{O}(1)$ fraction of the dark matter at our epoch are scalar glueballs and if their partial lifetime is not much larger than 10^{26} s, two experiments may see a signal: The contribution of glueball decays to the γ-ray spectrum below 10^2 GeV may be detected by GLAST. Moreover, the γ-line near 10^6 GeV may be seen by HESS. A lifetime of the order of 10^{26} s follows if $M_{10} \sim 10^{13}$ GeV according to Eq. (9.5). Such a low 10d Planck scale may be realized in a large-volume compactification along the lines of [106]. Note that this scenario is incompatible with the aforementioned scenario in which $\lambda = \mathcal{O}(1)$: According to Eq. (9.4), λ has to be very small (or zero) for such a low 10d Planck scale.

Throats with IR scales smaller than 10^6 GeV also lead to an interesting dark matter candidate. According to Eqs. (8.11) and (8.13), Ω is proportional to $T_{\rm RH}^{9/4} m_{\rm IR}$. In order still to have the abundance of dark matter with $\Omega \sim 1$, we have to increase the reheating temperature as $T_{\rm RH} \propto m_{\rm IR}^{-4/9}$ if we lower the IR scale. For example, for a throat with IR scale 10^4 GeV, a reheating temperature of $10^{12 \text{ GeV}}$ would give the right abundance (again assuming that $N_{\rm UV} \approx 10$). Since the various glueball decay rates are proportional to $m_{\rm IR}$ to some positive power, the glueballs become more stable for lower IR scales.

Let us now analyse throats with IR scales still in the 'optimal' interval between $m_{\rm IR,cr}$ and $T_{\rm RH}$ but much larger than the critical value $m_{\rm IR,cr}$. For definiteness, we consider a throat with IR scale $\sim T_{\rm RH}$ and take $N_{\rm UV} \approx 4$ in order to have $N_{\rm IR} = \mathcal{O}(1)$. According to Eq. (8.14), such a throat again gives the right amount of dark matter for a reheating temperature $\sim 10^{11}$ GeV. The mass of this dark matter candidate correspondingly is $\sim 10^{11}$ GeV.[4] The scalar glueballs decay to gravitons already after 10^{-8} s, according to Eq. (7.10). If the coupling in Eq. (7.31) is present, the spin-$\frac{1}{2}$ glueballs decay to the standard model after

$$\tau \sim 10^{27} \left(\frac{M_{10} \cdot \lambda^{-1/4}}{5 \cdot 10^{20} \text{ GeV}}\right)^8 \text{ s} . \tag{9.8}$$

[4]Note that the glueballs are never in thermal equilibrium for such short throats. Therefore, the heavier superpartners do not annihilate into the lightest glueball states and the initial abundance of scalar and spin-$\frac{1}{2}$ glueballs is equal.

Hadronic decays of particles in this mass range have been considered in [107] to explain events in the cosmic ray spectrum beyond the GZK cutoff. Taking the measured flux in this energy range, claimed by several collaborations, as an upper limit, a lifetime of at least 10^{27} s is required for a particle with mass 10^{11} GeV. If $\lambda = \mathcal{O}(1)$, the spin-$\frac{1}{2}$ glueballs decay too quickly since M_{10} cannot be larger than $M_4 \simeq 2 \cdot 10^{18}$ GeV. The coupling λ can be much smaller, though, and the spin-$\frac{1}{2}$ glueballs may be sufficiently stable for large enough M_{10}.

Finally, let us comment on throats with higher 5-form flux numbers $N_{\rm IR}$ and $N_{\rm UV}$. Since $N_{\rm IR}$ is no longer of the order 1, we have only rough estimates of the glueball decay rates in these cases. In the following, we ignore this issue and assume that the glueballs are sufficiently stable. The number $N_{\rm UV}$ is constrained by the requirement that the Calabi-Yau orientifold has enough negative charge to compensate for the flux. If one considers the orientifold limit of an F-theory compactification, then this amount of negative charge is given by $\chi_4/24$, where χ_4 is the Euler number of the underlying Calabi-Yau fourfold. Examples with $\chi_4/24$ up to 10^4 are known (see e.g. [108]) and we therefore assume that $N_{\rm UV} \lesssim 10^4$.

It follows from Eq. (8.14) that throats with maximal $N_{\rm UV} \sim 10^4$ and with IR scales in the range $m_{\rm IR,cr} \lesssim m_{\rm IR} \lesssim T_{\rm RH}$ can account for the observed dark matter if the reheating temperature was $\sim 10^{10}$ GeV. The mass of these dark matter candidates is between $\sim 10^5$ GeV (using Eq. (9.1)) and $\sim 10^{10}$ GeV. Together with the results from the first part of this section (where we have chosen the other extreme with $N_{\rm IR} = \mathcal{O}(1)$) this gives the possible range of parameters in our scenario if the 5-form flux number is varied from its minimal to its maximal value: For a throat in the 'optimal' range $m_{\rm IR,cr} \lesssim m_{\rm IR} \lesssim T_{\rm RH}$ to account for the observed dark matter, the required reheating temperature is between 10^{10} GeV and 10^{11} GeV. The IR scale and thus the mass of the corresponding dark matter particles can vary between 10^5 GeV and 10^{11} GeV.

9.2 Many throats

As we have discussed in Section 3.3, typical vacua in the type IIB string theory landscape can have a large number of throats. An estimate of the expected number of throats with a hierarchy h larger than some h_* for a Calabi-Yau orientifold with K 3-cycles was given in Eq. (3.11). Using this estimate and Eq. (9.2) and neglecting a factor $N_{\rm IR}^{-1/4}$ for simplicity, the expected number of throats with IR scale in the range $m_{\rm min} < m_{\rm IR} < m_{\rm max}$ follows as

$$\bar{n}(m_{\rm min} < m_{\rm IR} < m_{\rm max}) = \frac{K/3}{\log(M_{10}/m_{\rm max})} - \frac{K/3}{\log(M_{10}/m_{\rm min})}\,. \tag{9.9}$$

Here, we have assumed that $c = 1$.

The function $m \cdot \eta$ (and correspondingly Ω) is maximal for throats with IR scales between $m_{\rm IR,cr}$ and $T_{\rm RH}$ (cf. Fig. 8.1). If many throats are present, we can expect that the observed dark matter (or at least the dominant throat contribution to dark matter) will

come from throats with an IR scale in this region. As before, we simplify the analysis by using $N_{\rm UV} \approx 10$ for long throats ($m_{\rm IR} \sim 10^6$ GeV) and $N_{\rm UV} \approx 4$ for short throats ($m_{\rm IR} \sim 10^{11}$ GeV). As we have discussed in the last section, a reheating temperature of the order of 10^{11} GeV then leads to the observed amount of dark matter for all throats with IR scales between $m_{\rm IR,cr} \sim 10^6$ GeV and $T_{\rm RH} \sim 10^{11}$ GeV. Note that, in general, the situation might be more complicated: For example, a throat with an IR scale smaller than the critical value $m_{\rm IR,cr}$ but with very large $N_{\rm UV}$ (recall that $N_{\rm UV}$ is fairly arbitrary if we do not insist on $N_{\rm IR} = \mathcal{O}(1)$) may provide the dominant contribution to dark matter (cf. Eqs. (8.13) and (8.14)).

It is clear from Eq. (9.9) that the expected number of throats with IR scales in the aforementioned region grows with the number of 3-cycles K. Moreover, one can easily check that this number of throats also becomes larger for smaller 10d Planck scales M_{10}. We begin the evaluation of Eq. (9.9) with an optimistic scenario in which $K = 200$ and $M_{10} \sim 10^{14}$ GeV. The number of 3-cycles is a moderately high but not untypical value within the set of known Calabi-Yau spaces [109]. The value of the 10d Planck scale, on the other hand, is roughly the minimal value for which our analysis is valid: In deriving the heat transfer rates in Eqs. (5.16) and (8.1), we have assumed that the reheating temperature is smaller than the compactification scale, i.e. $T_{\rm RH} < L^{-1}$. Using Eq. (3.3), we find that the compactification scale $L^{-1} \sim 10^{12}$ GeV corresponds to the 10d Planck scale $M_{10} \sim 10^{14}$ GeV. Thus, since we consider a reheating temperature of the order of 10^{11} GeV, the assumption would no longer be fulfilled for a much lower 10d Planck scale.

For the aforementioned values of K and M_{10}, the expected number of throats with IR scales in the range $10^6 \text{ GeV} \lesssim m_{\rm IR} \lesssim 10^{11}$ GeV follows as[5]

$$\bar{n}\left(10^6 \text{ GeV} \lesssim m_{\rm IR} \lesssim 10^{11} \text{ GeV}\right) \simeq 9.1\,. \tag{9.10}$$

For definiteness, we restrict ourselves to setups which have a throat with IR scale of the order of 10^6 GeV. This is the case in a large fraction of models, since the mean number of throats with this IR scale is[6]

$$\bar{n}\left(m_{\rm IR} \sim 10^6 \text{ GeV}\right) \simeq 0.5\,. \tag{9.11}$$

Certain partial lifetimes of glueballs with mass $\sim 10^6$ GeV have been determined in the last section. In particular, we see from Eq. (9.5) (with $M_{10} \sim 10^{14}$ GeV) that the scalar glueballs may lead to interesting observable signatures if they do not decay too quickly to two gravitons. The fermionic glueballs cannot decay to a graviton and a gravitino for kinematic reasons since we still assume that $m_{3/2} \gg m_{\rm IR}$. They can therefore account for the observed dark matter even if the scalar glueballs decay to gravitons already at an early epoch. According to Eq. (9.4) (with $M_{10} \sim 10^{14}$ GeV), the fermionic glueballs must not couple too strongly to the standard model sector, i.e. λ must not be too large.

[5] More precisely, we have evaluated Eq. (9.9) for the range $5 \cdot 10^5 \text{ GeV} < m_{\rm IR} < 5 \cdot 10^{11}$ GeV. The mean number of throats in other ranges of IR scales have been calculated in a similar way.

[6] We have used the interval $5 \cdot 10^5 \text{ GeV} < m_{\rm IR} < 5 \cdot 10^6$ GeV to estimate the number of throats with IR scale $\sim 10^6$ GeV from Eq. (9.9).

In addition, we now expect

$$\bar{n}\left(m_{\rm IR} \lesssim 10^5 \text{ GeV}\right) \simeq 3.5 \tag{9.12}$$

throats with IR scales smaller than 10^6 GeV which provide another decay channel for the glueballs. These throats can have a large number $\tilde{g}$ of degrees of freedom. We want the glueballs from the throat at $\sim 10^6$ GeV to account for the observed dark matter and we therefore have to check whether their lifetime is still larger than the current age of the universe. If we denote the 5-form flux number at the UV end of the ith throat by N_i, we have

$$\tilde{g} = \sum_i N_i^2 \,, \tag{9.13}$$

where the sum runs over all throats with IR scales smaller than 10^6 GeV. Using Eq. (7.15) with $N^2 = \tilde{g}$, the partial lifetime of the dark matter glueballs for decays to these throats is

$$\tau \sim \tilde{g}^{-1}\, 10^{32} \text{ s} \,. \tag{9.14}$$

According to the discussion at the end of the last section, we expect $\tilde{g}$ to be somewhere in the range of 10^2 to 10^8. Even for maximal $\tilde{g}$ this partial lifetime is thus much larger than the current age of the universe and the glueballs are still a good dark matter candidate.

There are also throats with IR scales larger than the IR scale of the dark matter throat (cf. Eq. (9.10)). Glueballs from these throats have shorter lifetimes than the dark matter glueballs. The abundance of particles which decay to the standard model with a lifetime in the range of 10^{-2} s and 10^{12} s is severely constrained by nucleosynthesis [103, 110, 111]. For lifetimes larger than 10^{12} s, bounds from the diffuse γ-radiation are again important [102]. Therefore, we have to check whether the decaying glueballs fulfill these observational constraints.

We analyse only decays of scalar glueballs. The discussion can be easily extended to include the fermionic glueballs. Since fermionic glueballs decay to the standard model via the operator in Eq. (7.31), nucleosynthesis or the diffuse γ-radiation may give a bound on the coupling strength λ. Furthermore, we assume that the aforementioned throats have IR scales of at least 10^7 GeV. One can check that the corresponding glueballs decay already after 10^{10} s or earlier. These lifetimes are too short (i.e. shorter than 10^{12} s) to give relevant constraints from the diffuse γ-radiation. We will therefore restrict our analysis to bounds from nucleosynthesis. Scalar glueballs have three important decay channels: They decay to gravitons, to throats with lower IR scales and to the standard model. The total decay rate is the sum of the three corresponding decay rates:[7]

$$\Gamma_{\rm total} \sim \tilde{g}\, N_{\rm UV}^2 \frac{m_{\rm IR}^9}{M_{10}^8} + g\, N_{\rm UV}^2 \frac{m_{\rm IR}^9}{M_{10}^8} + N_{\rm UV}^4 \frac{m_{\rm IR}^5}{M_4^4} \,. \tag{9.15}$$

[7] In deriving the decay rate in Eq. (7.15), we have assumed that the mass m_τ of the modulus which mediates the decay is larger than the mass $m_{\rm IR}$ of the decaying glueball. According to Eq. (7.13), we have $m_\tau \sim 10^{10}$ GeV for $M_{10} \sim 10^{14}$ GeV. For a throat with IR scale larger than 10^{10} GeV we would therefore have to use the unsuppressed decay rate in Eq. (6.13) instead of Eq. (7.15). We will not have to consider such heavy glueballs in the following.

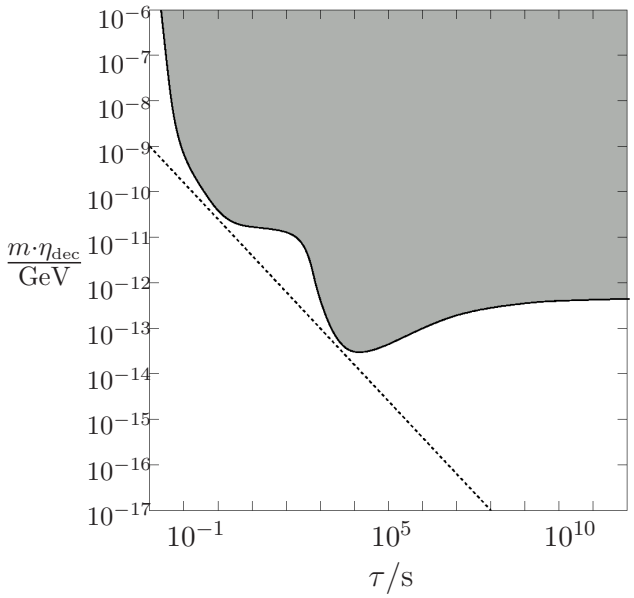

Figure 9.1: *Nucleosynthesis constraints on the mass density $m \cdot \eta_{\rm dec}$ of the fraction of particles that have decayed to the standard model in dependence of their lifetime τ (the shaded region is excluded, schematic plot based on results from [111]). The corresponding function for the glueballs is also shown (the dotted curve). See text for more details.*

Here, $\tilde{g}$ is the combined number of degrees of freedom of all the throats with IR scales smaller than the IR scale $m_{\rm IR}$ of a given throat.

Since $\tilde{g} \gtrsim g$, we can neglect the decay rate to the standard model (the g-dependent term) in Eq. (9.15). Furthermore, we can see from Eq. (9.15) that for sufficiently large glueball lifetimes (i.e. small $m_{\rm IR}$), the total decay rate is dominated by decays to gravitons (the last term in Eq. (9.15)). To be conservative, we take $\tilde{g} \sim 10^2$ in the following. Higher values of $\tilde{g}$ would give a smaller branching ratio for decays to the standard model and would thus make the constraints from nucleosynthesis easier to fulfill. One can then check that, for $M_{10} \sim 10^{14}$ GeV and $N_{\rm UV} \approx 4$ to 10, the decay rate to gravitons dominates for glueballs which live longer than 10^{-2} s. Since nucleosynthesis gives no constraints for particles which decay earlier than 10^{-2} s, we can restrict our analysis to these glueballs. We thus have

$$\Gamma_{\rm total} \;\sim\; N_{\rm UV}^4 \frac{m_{\rm IR}^5}{M_4^4} \,. \tag{9.16}$$

We denote the mass density over entropy density of the fraction of glueballs that have decayed to the standard model by $m \cdot \eta_{\rm dec}$ and the branching ratio for decays to the standard model by br:

$$m \cdot \eta_{\rm dec} \;=\; br \cdot m \cdot \eta \,. \tag{9.17}$$

Dividing the decay rate to the standard model by the total decay rate in Eq. (9.16), we

find

$$br \;=\; \frac{\Gamma_{\rm SM}}{\Gamma_{\rm total}} \;\sim\; \frac{g\, M_4^4\, m_{\rm IR}^4}{N_{\rm UV}^2\, M_{10}^8}\,. \tag{9.18}$$

Using again Eq. (9.16), this branching ratio and correspondingly $m \cdot \eta_{\rm dec}$ can be expressed as a function of the lifetime $\tau = \Gamma_{\rm total}^{-1}$. Furthermore, we know from Fig. 8.1 that the decaying glueballs initially have the same mass density as dark matter, i.e. $m \cdot \eta \approx 10^{-9}\,\text{GeV}$.

In Fig. 9.1, we have plotted $m \cdot \eta_{\rm dec}$ as a function of τ as a dotted curve. The shaded region in this plot is the parameter space that is excluded by the requirement of successful nucleosynthesis. Note, however, that these constraints were calculated in [111] for a decaying particle of mass $10^4\,\text{GeV}$ (and with an $\mathcal{O}(1)$ hadronic branching ratio). Using Eq. (9.16), the glueball masses which correspond to the range of lifetimes in Fig. 9.1 are between $10^7\,\text{GeV}$ and $10^9\,\text{GeV}$. This is much heavier than the particle mass $10^4\,\text{GeV}$ for which the constraints were actually determined. On the other hand, in [111], constraints were also calculated for lighter particles with masses 10^2 GeV and 10^3 GeV. The results differ only slightly from the constraints for particle mass 10^4 GeV. We therefore believe that it is a reasonable approximation to extrapolate the bounds to particles with masses in the range of $10^7\,\text{GeV}$ to $10^9\,\text{GeV}$. Assuming that this is the case, we see from Fig. 9.1 that glueball decays from throats with IR scales larger than $10^6\,\text{GeV}$ do not destroy nucleosynthesis.

Up to now, we have considered a scenario in which $K = 200$ and $M_{10} \sim 10^{14}\,\text{GeV}$. This choice of parameters led to a relatively large number of throats in the interesting region of IR scales between $10^6\,\text{GeV}$ and $10^{11}\,\text{GeV}$. Let us finally analyse a more conservative scenario in which we choose $K = 60$ and $M_{10} \sim 10^{18}\,\text{GeV}$. The number of 3-cycles is, for example, roughly the minimal value consistent with fine-tuning of the cosmological constant in the KKLT construction [9]. According to Eq. (9.9), the expected number of throats with IR scales between $10^6\,\text{GeV}$ and $10^{11}\,\text{GeV}$ then is

$$\bar{n}\left(10^6\,\text{GeV} \lesssim m_{\rm IR} \lesssim 10^{11}\,\text{GeV}\right) \;\simeq\; 0.7\,. \tag{9.19}$$

Thus, a significant fraction of vacua has a throat in this range of IR scales and a reheating temperature of the order of $10^{11}\,\text{GeV}$ would give the right amount of dark matter for such a throat.

For definiteness, we assume that there is a single throat with IR scale $\sim 10^{11}\,\text{GeV}$ in the aforementioned range. This choice of IR scale reflects our knowledge of the distribution of throats: As we have discussed above, the expected number of throats in a given interval, Eq. (9.9), becomes smaller if the 10d Planck scale becomes larger. By the same token, the mean number of throats in the interval also becomes smaller if the interval is shifted to smaller IR scales. This means that it is more probable to find a throat at large IR scales.

Certain partial lifetimes of the glueballs from a throat with IR scale $\sim 10^{11}\,\text{GeV}$ have been discussed in the last section. In addition, there may be throats with lower IR scales which provide new decay channels for the glueballs. Their mean number is

$$\bar{n}\left(m_{\rm IR} < 10^6\,\text{GeV}\right) \;\simeq\; 0.7\,. \tag{9.20}$$

We denote the number of degrees of freedom of this sector by $\tilde{g}$. As before, we have to check that the dark matter glueballs do not decay too quickly to this sector. Using Eq. (7.15), the partial lifetime for this decay channel is

$$\tau \sim \tilde{g}^{-1}\, 10^{20}\ \mathrm{s}\,. \tag{9.21}$$

Thus, $\tilde{g}$ must not be larger than $\sim 10^3$ for the dark matter glueballs still to live longer than the current age of the universe. If $\tilde{g}$ is larger than that, on the other hand, a throat with a lower IR scale would be required (cf. Eq. (7.15)).

Obviously, many other cases, including more extreme choices of parameters, are conceivable. However, an exhaustive study of the parameter space is beyond the scope of this thesis.

9.3 Scenarios with low-scale supersymmetry breaking

In this section, we consider the limit of light gravitinos or, equivalently, low-scale supersymmetry breaking. As we have discussed in Section 7.3, the fermionic glueballs can decay to a graviton and a gravitino if the gravitino is lighter than the glueballs. The scalar glueballs decay to two gravitons with the same rate. As we have seen in Section 9.1, scalar glueballs with mass 10^6 GeV have a lifetime of

$$\tau \sim 10^{15}\ \mathrm{s}\,. \tag{9.22}$$

This is shorter than the current age of the universe. This lifetime now also applies to the fermionic glueballs which accordingly decay too quickly to be a good dark matter candidate. On the other hand, the partial lifetime for this decay channel is proportional to m_{IR}^{-5} according to Eq. (7.10). Thus, we obtain a longer lifetime if the IR scale is somewhat lower than 10^6 GeV. In this case, throat dark matter is still possible even if the supersymmetry breaking scale is low.

There are additional decay channels which are relevant in the limit of light gravitinos: Recall that, in Section 7.2, we have found that a scalar glueball is lighter than its fermionic superpartner in the limit of low-scale supersymmetry breaking. Depending on the precise relation between the F-term vev of the chiral compensator and the gravitino mass, the fermionic glueball can or can not decay to this lighter scalar glueball with the emission of a gravitino (cf. Fig. 7.1). If this decay is kinematically not allowed, the fermionic glueball can still decay via a gravitino to standard model particles and the lighter scalar glueball. The gravitino propagator gives no suppression of the decay rate in this case and the decay rate is given by Eq. (6.13). For a throat with $m_{\mathrm{IR}} \sim 10^6$ GeV and $N_{\mathrm{IR}} \sim \mathcal{O}(1)$, the partial lifetime of the fermionic glueballs for this decay channel is again

$$\tau \sim 10^{15}\ \mathrm{s}\,. \tag{9.23}$$

Since decays of this kind are constrained by diffuse γ-ray measurements, a partial lifetime larger than $\sim 10^{26}$ s is actually required. Since the partial lifetime is again proportional to m_{IR}^{-5} (cf. Eq. (6.13)), the glueballs can as before be made sufficiently stable if the IR scale is somewhat smaller than 10^6 GeV. As we have explained in Section 9.1, in order to obtain the observed amount of dark matter, a higher reheating temperature is then required.

9.4 Relation to earlier work

The fact that dark matter can come from a hidden (or more precisely conformally sequestered) sector realized by a KS throat has already been emphasized in [62]. This paper focuses on scenarios where a KS throat is heated by the annihilation of a brane with an antibrane at the end of inflation. Subsequently, energy is transferred from this throat to other throats which may be present in the compact space. Throat-localized KK modes, which are produced in this way, can be the observed dark matter if they are sufficiently long-lived and if certain parameters which determine their relic density are tuned. More precisely, three types of dark matter candidates are discussed in [62]: KK modes which are localized in the throat where inflation took place and those localized in the throat where the standard model lives have to carry an (approximately) conserved angular momentum in the throat in order to be sufficiently stable. KK modes which are localized in other throats can, by contrast, be long-lived also without such an angular momentum.[8]

We have approached the possibility of throat dark matter from a different and, to a certain extent, more general perspective: We have not assumed that reheating is due to brane-antibrane annihilation in a warped region. Instead, we have only relied on the fact that the standard model has a certain reheating temperature after inflation ends. In our approach, throats are not a 'model building feature' introduced to realize inflation, uplifting, etc. Instead, we view the presence of (a potentially large number of) throats as a prediction of the type IIB string theory landscape. Accordingly, we have considered scenarios in which various throats are present. The amount of dark matter in these throats that we have derived can be viewed as a generic prediction of the type IIB landscape.

We have focused in particular on the phenomenological importance of fermionic KK modes in the throat. To the best of our knowledge, this point has so far not received sufficient attention in the literature. As we have seen, fermionic KK modes play a central role in the phenomenology of sequestered dark matter. Furthermore, we have used our values for the heat transfer rate and the decay rates between throats from Chapters 5 to 7. For temperatures and Kaluza-Klein masses smaller than the compactification scale, our rates differ from the values used in [62]. We have restricted our analysis to this case, for the following reasons: On the one hand, a large compactification scale is required to make the KK modes sufficiently stable against decay to the standard model or other

[8] In addition, [62] also discusses particles on D-branes in these throats as a dark matter candidate.

throats.[9] On the other hand, temperatures above the compactification scale would imply that also the unwarped part of the manifold is heated up. The resulting gas of KK modes in the compact space may then destabilize the volume modulus, making the analysis of the early cosmological evolution much more difficult. Furthermore, the suppression of the decay rates due to the flux-stabilization of certain moduli was not taken into account in [62] and our decay rates differ also in this respect.

[9] An exception is the decay rate of fermionic KK modes to the standard model sector which can be made small even for small compactification scales (cf. Section 7.6).

Chapter 10

Conclusions

10.1 General review

In this thesis, we have studied throats in the early, hot universe. We have reviewed various aspects of throats and of their dual gauge theories in Chapters 2 and 3. A throat is a region in higher-dimensional space with a strong gravitational potential along a certain direction. Energy scales of physical processes, that are localized at different positions along this direction, are exponentially redshifted or blueshifted relative to a fixed observer. In that way, large hierarchies of scales can be generated.

The Randall-Sundrum (RS) I model [1] realizes this generation of hierarchies in a simple geometry: A slice of 5-dimensional anti-de-Sitter space (AdS_5) which is cut off by two branes. As Randall and Sundrum have shown, the 4-dimensional graviton is localized towards one of the branes, called the UV brane, in this geometry. Energy scales of physical process that are localized near the other brane, called the IR brane, are exponentially redshifted relative to the 4-dimensional Planck scale. In particular, the RSI model allows for a solution to the hierarchy problem of the standard model.

In string theory, a throat is, for instance, realized near a black 3-brane. This background solution of type IIB supergravity can be viewed as an $AdS_5 \times S^5$ throat which is embedded into flat 10d space. As Verlinde has shown [44], a string realization of the RSII model [2] (without IR brane) can be obtained from such a black 3-brane if one compactifies the 6 dimensions perpendicular to the brane on a torus.

Black 3-branes are equivalent to stacks of D3-branes of type IIB string theory. This equivalence can e.g. be tested by comparing the absorption cross sections of particles for both objects. We have reviewed the corresponding calculation for incident dilatons in Section 2.3. The fact that the absorption cross sections agree exactly is evidence that black 3-branes and D3-brane stacks are just two descriptions of the same object.

A string realization of the RSI model can be obtained if one places D3-branes and fractional D3-branes on a conifold singularity of a Calabi-Yau orientifold [3]. The back-reaction of these branes on the geometry creates a Klebanov-Strassler (KS) throat [4]

which is embedded into the compact space. Alternatively, the KS throat in this setup can be viewed as the result of the backreaction of 3-form flux on the geometry. In the landscape of type IIB flux compactifications, 3-form flux is distributed in various ways over the 3-cycles of the compact space and it turns out that throats are commonly created from the backreaction of this 3-form flux. In Section 3.3, we have reviewed how the expected number of throats in a given Calabi-Yau orientifold can be determined.

10.2 Throats in the early universe

Since throats are a common feature of type IIB string compactifications, it is interesting to think about observable signals which can result from their presence in the early universe. In particular, as high temperatures have been involved at this stage of the cosmological evolution, the throats can have been heated to a certain temperature. If the energy density in a throat is above its IR scale (which is related to the length of the throat), the backreaction of the thermal plasma on the geometry creates a black hole horizon which replaces the IR end of the throat. This black hole horizon emits Hawking radiation which in turn can heat up other throats and the standard model. The rate of this process is an important quantity for the further cosmological evolution.

In Chapter 5, we have calculated this heat transfer rate a simple setup – a heated $AdS_5 \times S^5$ throat and another $AdS_5 \times S^5$ throat embedded into a 6d torus. Due to the warping, the Hawking radiation from the black hole horizon in the heated throat has to tunnel through an effective energy barrier before it can reach the other throat. The corresponding tunneling probability determines the rate of heat transfer. The calculation of this probability, however, is a multi-dimensional tunneling problem which is difficult to solve. Therefore, we have chosen a different approach and replaced the $AdS_5 \times S^5$ throats by equivalent stacks of D3-branes. These D3-brane stacks carry gauge theories on their world-volume. Correspondingly, we have referred to the description in terms of D-branes as the gauge theory picture as opposed to the gravity picture in terms of throats.

In particular, the heated throat is equivalent to a D3-brane stack with a heated world-volume gauge theory. After a KK expansion of supergravity fields in the embedding torus, our 10d setup can be described by a 4d theory: A heated gauge theory which is coupled by a tower of KK modes to another gauge theory. Heat transfer is in this description due to the annihilation of fields in the thermal plasma of the heated gauge theory into KK modes which in turn decay to the other gauge theory. The calculation of the heat transfer rate is then a straightforward exercise in quantum field theory. In particular, it is much simpler than the calculation involving the tunneling problem.

If the temperature drops below the IR scale of a throat, a phase transition takes place. During this phase transition, the black hole horizon is replaced by the IR end of the throat and a nonrelativistic gas of throat-localized KK modes is formed. These KK modes decay to other throats and the standard model with a certain rate. Again, we have calculated this rate, which is another important quantity for the cosmology of

throats, in the gauge theory picture.

A KK mode which is localized in a throat corresponds to a glueball of the dual gauge theory. The coupling of such a glueball to supergravity fields in the embedding space, however, can not be read off from any Lagrangian. Therefore, in Chapter 6, we have first calculated the decay rate in a simpler setup using the gravity picture: The decay rate of a dilaton KK mode from the $AdS_5 \times S^5$ part of a black 3-brane to the asymptotically flat part. Using this result, we have determined the coupling between the glueball and supergravity fields in the embedding space from the requirement that the decay rates from the gravity picture and the gauge theory picture agree. Redoing the calculation from Chapter 5 using this coupling, we have found the decay rate of glueballs between the two gauge sectors or, equivalently, of KK modes between the two throats.

The heat transfer rate and the decay rate that we have found depend on the distance between the throats and on the size of the embedding compact space. The rates become smaller for larger distances and larger embedding spaces. In addition, the decay rate depends on the angular quantum number of the decaying mode with respect to the S^5 in the $AdS_5 \times S^5$ throat containing the initial state. Modes with angular momentum have a much lower decay rate than modes which are s-waves with respect to the S^5.

If the size of the embedding space is of the same order as the AdS scales of the throats, a compact space with two throats can be approximated by two RS models which are glued together at a common UV brane. As we have reviewed in Chapter 4, the decay rate of graviton KK modes in this situation follows from a straightforward calculation of the tunneling probability between the two RS models. The decay rate that we have found in our setup with two $AdS_5 \times S^5$ throats in a torus should reproduce this result in the aforementioned limit of small embedding space. In Section 6.3, we have shown that this is indeed the case. Furthermore, in Chapter 4, we have also presented an alternative derivation of the decay rate of KK modes between two RS models. To this end, we have replaced one RS model by its dual gauge theory. From the point of view of the remaining RS model, this gauge theory lives on the UV brane. The decay rate of graviton KK modes in the remaining RS model into gauge fields on the UV brane reproduces the decay rate of graviton KK modes between two RS models.

As we have discussed in Chapter 7, our results for the heat transfer rate and the decay rate of KK modes can be applied to other geometries of the throats and the embedding space. In particular, the heat transfer rate is applicable to two KS throats if the curvature of the space connecting them is not larger than the inverse distance. Furthermore, the decay rate can be applied to the decay of graviton KK modes between such throats. For KK modes of other supergravity fields, on the other hand, the decay rate is in general difficult to determine since the 3-form flux in a KS throat mixes field fluctuations in a complicated way. In order to determine the vertex between glueballs and supergravity fields in the embedding space as discussed above, we would have to solve the resulting complicated equations of motion of the field fluctuations. We have shown, however, that the glueballs in a given sector decay to a lightest scalar glueball and its fermionic superpartner on cosmologically short timescales. For the purpose of cosmology,

it is then sufficient to determine only the decay rate of these glueballs. Furthermore, we have found a flat direction for the supergravity fields in a KS throat. The scalar which parameterizes this flat direction fulfills the same equation of motion as the dilaton in an $AdS_5 \times S^5$ throat. Accordingly, it couples to supergravity in the embedding space with the previously derived vertex. A scalar KK mode in general mixes with this flat direction in a KS throat and therefore also decays via the previously derived vertex.

A suppression of the decay rate can arise, on the other hand, since certain fields which mediate decays get high masses in flux compactifications. As we have discussed in Section 7.5, this suppression is roughly compensated by a stronger decay vertex if the decaying KK mode mixes with tachyons in the 5d effective description of the throat. The reason is that tachyons, i.e. scalars with a negative mass squared, are less suppressed in the UV direction than scalars with a vanishing or positive mass. To analyse this effect in more detail, we have calculated the decay rate of KK modes of a tachyon between two RS models. For the calculation, we have replaced one RS model by its dual gauge theory which then lives on the UV brane of the remaining RS model. In the full AdS_5-space (without branes), scalars with negative mass squared down to the Breitenlohner-Freedman bound [6] do not lead to instabilities. In a RS model, however, the tachyon must have a large mass term on the UV brane in order to avoid tachyonic KK modes. Similar to the mass of mediating fields in flux compactifications, this UV-localized mass leads to a suppression of the decay rate. The stronger decay vertex of KK modes of a tachyon, however, compensates this suppression. These KK modes and KK modes which mix with a tachyon therefore decay roughly with the previously derived rate of graviton KK modes.

10.3 Dark matter in throats

We have presented an application of the heat transfer rate and the decay rate in Chapters 8 and 9: KK modes whose wavefunctions are localized in a throat are an interesting dark matter candidate. These KK modes have redshifted masses, allowing for their production after reheating in the standard model, even if the reheating temperature is not very high. In addition, their decay rates are highly suppressed, potentially resulting in a very long lifetime.

We have considered scenarios in which the standard model lives in the unwarped part of a compact space, which in addition has a certain number of throats. To be conservative, we have assumed that the throats receive no energy from the reheating mechanism and that the reheating mechanism only heats up the standard model. Even under this minimal assumption, the throats are heated up by energy transfer from the hot standard model plasma.

From the dual gauge theory point of view, the resulting energy density in a throat is initially in the form of gauge theory states with energy of the order of the reheating temperature. As we have shown, if the total energy density is above the critical energy density for a deconfinement phase transition, the gauge theory thermalizes. Accordingly,

the energy density initially scales like radiation with the expansion of the universe until a confinement phase transition takes place. Afterwards, the energy density is in the form of nonrelativistic glueballs whose energy density correspondingly scales like matter. In Section 8.3, we have determined the resulting contribution of glueballs to the total energy density at our epoch.

If the energy density is always below the critical energy density, on the other hand, the initial gauge theory states hadronize to a large number of nonrelativistic glueballs. As we have explained in Section 8.3, this is due to the fact that the gauge theory (which is dual to a throat) is strongly coupled on all scales. In an asymptotically free theory such as QCD, jets with ultrarelativistic particles would instead be formed during hadronization. The energy density in the throat sector thus scales like matter immediately after reheating and the resulting contribution to the total energy density at our epoch is relatively large already for reheating temperatures which are only moderately high.

We have plotted the contribution of a throat to the total energy density for fixed reheating temperature T_{RH} and as a function of the IR scale m_{IR} in Fig. 8.1. As one can see, this function has a maximum between IR scales $m_{\mathrm{IR,cr}}$ and T_{RH}. Here, $m_{\mathrm{IR,cr}}$ is the IR scale for which the dual gauge theory thermalizes precisely to the phase transition temperature. Since throats are a common feature in the landscape of type IIB string theory and a given compact space typically has several throats, it is probable to have throats with IR scales in the 'optimal' range between $m_{\mathrm{IR,cr}}$ and T_{RH}. We can therefore expect that dark matter is due to these throats.

As we have discussed in Section 7.3, scalar glueballs decay to two gravitons with a certain rate. Similarly, fermionic glueballs can in principle decay to a graviton and a gravitino. In order to obtain a stable dark matter candidate, we have focused on scenarios in which such decays are kinematically forbidden due to a heavy gravitino. This requires that the supersymmetry breaking scale is larger than the mass of the glueball. It may also mean that the superpartners of standard model particles are heavier than the glueballs. If R-parity is conserved, most decay channels of fermionic glueballs to the standard model involve such a superpartner and are therefore kinematically forbidden. In Section 7.6, we have identified an operator which does not involve a superpartner and which would allow the decay of fermionic glueballs to a Higgs and a lepton. If present, this operator would give the dominant decay channel even for maximally broken R-parity.

In Section 9.1, we have first discussed scenarios with a single throat in the 'optimal' range of IR scales between $m_{\mathrm{IR,cr}}$ and T_{RH}. We have found that, in many cases, KK modes in throats with IR scale T_{RH} have a decay rate which is too high for them to be a good dark matter candidate. However, if the gravitino is very heavy (high-scale supersymmetry breaking) and the aforementioned operator is suppressed, the lightest fermionic glueballs may nevertheless survive and play the role of dark matter. The more promising case is that of throats with lower IR scales. For definiteness, we have analysed a throat with IR scale $m_{\mathrm{IR,cr}}$, which is the lower end of the 'optimal' range of IR scales. We have found that a reheating temperature of 10^{10} GeV to 10^{11} GeV leads to the right

amount of glueballs to account for the observed dark matter. The critical IR scale $m_{\mathrm{IR,cr}}$ is a function of T_{RH}. After having fixed T_{RH}, we find a mass for the dark matter candidate in this scenario which is between 10^5 GeV and 10^6 GeV.

Our dark matter scenario may lead to some interesting observable signatures. The dark matter glueballs decay to the standard model with a very low, but non-negligible rate. The decays produce photons to which experiments like GLAST or HESS may be sensitive. It turns out that the decay rates depend on two parameters: The 10d Planck mass enters via the flux stabilized mass of fields which mediate the decay. Moreover, the decay rate of fermionic glueballs depends on the dimensionless coupling strength λ of the aforementioned operator which allows their decay to a lepton and a Higgs. In Section 9.1, we have identified two interesting scenarios:

If λ is of the order 1, the 10d Planck scale has to be very large in order to get a sufficiently stable dark matter candidate. Namely, for a lower 10d Planck scale, the fermionic glueballs decay to the standard model with a rate which is in conflict with measurements of the diffuse γ-radiation. On the other hand, the 10d Planck scale cannot be larger than the 4d Planck scale. This makes it more probable that the lifetime of fermionic glueballs is in a range that can be probed with new experiments like GLAST. If the scenario with $\lambda = \mathcal{O}(1)$ is realized in nature, one can hope to detect a signal from the decaying glueballs in the near future.

If λ is much smaller than 1, a lower 10d Planck scale still leads to sufficiently stable fermionic glueballs. For a low 10d Planck scale, also the decay of scalar glueballs can become relevant for detection. In contrast to fermionic glueballs, scalar glueballs can decay directly to two photons. This decay channel leads to a sharp γ-line at an energy of 10^5 GeV to 10^6 GeV which could be detected with experiments like HESS. In addition, the scalar glueball decays also produce a continuous γ-ray spectrum to which e.g. GLAST may again be sensitive. If the scalar glueballs make up an $\mathcal{O}(1)$ fraction of the dark matter at our epoch, a 10d Planck scale of the order of 10^{13} GeV would allow for a detection of both signals in the near future. Such a 10d Planck scale corresponds to a compactification radius of the order of just 50 times the string length, which is not extremely large.

Finally, in Section 9.2, we have considered scenarios with a large number of throats, using the result for the expected number of throats in a given Calabi-Yau orientifold that we have reviewed in Section 3.3. We have found that there are setups in which the probability of having a throat with IR scale in the aforementioned 'optimal' range is large. The only free parameter which has then to be fixed in order to obtain the observed amount of dark matter is the reheating temperature. The lifetime of the glueballs strongly depends on their mass and therefore on the IR scale of the corresponding throat. In a scenario with several throats with various IR scales, it is therefore possible to have glueballs which decay already at early epochs while other glueballs are sufficiently stable to account for the observed dark matter. Decays to the standard model at early epochs are severely constrainted by nucleosynthesis. We have checked in a specific example that these constraints can be fulfilled.

10.4 Outlook

Our results for the heat transfer rate and the decay rate depend on the distance between the throats and the size of the embedding compact space. They generalize the aforementioned decay rate of graviton KK modes between two RS models. This dependence on distance and size is, for instance, relevant for the analysis of reheating after brane-antibrane inflation. At the end of inflation in this scenario, the brane annihilates with the antibrane and the energy which is released in this process subsequently thermalizes. If the standard model is realized in another throat, at least part of this energy has to be channeled to this throat in order to allow for the reheating of the standard model.

We find that, as long as the embedding manifold is not of minimal size, our decay rate is considerably lower than the decay rate of graviton KK modes between two RS models which was used in previous analyses [58–61] of this reheating mechanism. Given our results, it will be interesting to reconsider reheating after brane-antibrane inflation.

Apart from reheating after brane-antibrane inflation and our dark matter scenario, one can apply our results to several cosmological scenarios where reheating takes place either in the standard model or in a throat and the standard model resides either at the bottom of a throat or somewhere in the rest of the Calabi-Yau orientifold. The heat transfer rate and the decay rates that we have calculated can then be used in a set of Boltzmann equations to determine the evolution of energy densities of the standard model and the throats.

For our dark matter scenario in Chapters 8 and 9, we have assumed that the dark matter glueballs decay via the vertex from Chapter 6 for a dilaton in an $AdS_5 \times S^5$ throat. The decay rate of these glueballs is suppressed relative to the decay rate from Chapter 6, however, since certain fields which mediate the decay get high masses in flux compactifications.

On the other hand, we have found in Section 7.5 that KK modes mixing with tachyons in the throat decay with a considerably stronger vertex than that from Chapter 6. Such tachyons also appear in the 5d effective description of the KS throat. We expect that the KK modes dual to the dark matter glueballs mix with these tachyons in the KS throat. The resulting stronger decay vertex of these particles would then roughly compensate the suppression of the decay rate due to flux-induced masses of mediating fields. In particular, the dark matter glueballs would decay with a higher rate than that used in Chapters 8 and 9. It will be interesting to work out the consequences of such a higher decay rate for our dark matter scenario. The resulting shorter lifetimes of the dark matter may eliminate a large portion of the phenomenologically viable region in parameter space. On the other hand, the remaining region in parameter space may be so small that our dark matter scenario could either be excluded or verified by experiments in the near future.

In Chapter 8, we have mentioned an alternative production mechanism of the dark matter. This mechanism is operative during inflation and is due to the fact that de Sitter space has a temperature. It would be interesting to investigate this mechanism

and its influence on our dark matter scenario in more detail. Furthermore, we have mainly neglected KK modes which are charged under global (approximate) symmetries in the throat. As we have seen in Chapter 6, in an $AdS_5 \times S^5$ throat these charged KK modes decay with a considerably lower rate than KK modes which are s-waves. It would be interesting to determine whether such a suppression also arises in a KS throat or whether the KK modes again mix with a tachyon in such a throat. Part of the global symmetries in some throats are only present in the high-temperature phase and are broken at the phase transition during which the black hole horizon is replaced by the IR end of the throat. As we have seen in Chapter 6, long throats are heated to the black-hole phase for a sufficiently large reheating temperature. They subsequently cool with the cosmological expansion until the aforementioned phase transition takes place. The breaking of global symmetries during the phase transition can then lead to the formation of topological defects. It would be interesting to investigate this possibility in more detail.

Appendix A

Kaluza-Klein expansion of the graviton in a Randall-Sundrum model

In the following, we perform the KK expansion of the 5d graviton h_{MN} in the RS background discussed in Section 2.1 and determine the couplings of the KK modes to field theories on the UV brane and the IR brane. The results in this section are taken from [2, 112, 113].

Due to the orbifold symmetry $y \to -y$, there is no zero mode of the graviphoton $h_{\mu N}$. The massless spectrum thus consists of the 4d graviton $h^{(0)}_{\mu\nu}$ and the radion. In addition, there is a tower of massive spin-2 fields $h^{(n)}_{\mu\nu}$. By counting the number of degrees of freedom, it becomes clear that there are no massive vectors or scalars in the spectrum. In a phenomenologically viable theory, the radion has to be stabilized, e.g. with the Goldberger-Wise mechanism [15]. In the following, we assume that this has been achieved and we do not consider the radion any more. A convenient parametrization for the spin-2 fluctuations is

$$ds^2 \;=\; e^{-2k|y|}\,\left(\eta_{\mu\nu} + h_{\mu\nu}(x,y)\right)\,dx^\mu dx^\nu + dy^2\,, \tag{A.1}$$

where $h_{\mu\nu}$ is chosen to be transverse and traceless. With this parametrization, the equation of motion for $h_{\mu\nu}$ is just a Laplace equation in the background geometry [64,65]:

$$\partial_M\left(\sqrt{g}g^{MN}\partial_N h_{\mu\nu}\right) = 0\,. \tag{A.2}$$

Next, we perform the KK expansion of the 5d field $h_{\mu\nu}$:

$$h_{\mu\nu}(x,y) \;=\; \sum_{n=0}^{\infty} h^{(n)}_{\mu\nu}(x)\,\chi^{(n)}(y)\,. \tag{A.3}$$

Using this expansion and denoting the mass of the n-th KK mode by m_n, the equation of motion for the profile $\chi^{(n)}$ of the n-th KK mode along the 5th dimension reads

$$\frac{d}{dy}\left(e^{-4k|y|}\frac{d\chi^{(n)}}{dy}\right) \;+\; m_n^2\,e^{-2k|y|}\,\chi^{(n)} \;=\; 0\,. \tag{A.4}$$

For a field which is even under the orbifold $\mathbb{Z}_2$-action $y \to -y$, the boundary conditions at the two branes follow from Eq. (A.4) as

$$\frac{d}{dy}\chi^{(n)}(0) \,=\, 0 \quad \text{and} \quad \frac{d}{dy}\chi^{(n)}(\ell) \,=\, 0\,. \tag{A.5}$$

For $m_n = 0$, the solution to Eqs. (A.4) and (A.5) is $\chi^0 = \text{const}$. The corresponding KK mode is the 4d graviton. The wave functions $\chi^{(n)}$ have to be normalized according to

$$\int_{-\ell}^{\ell} dy\, e^{-2k|y|} \left(\chi^{(n)}(y)\right)^2 \stackrel{!}{=} 1 \tag{A.6}$$

in order to obtain a canonically normalized kinetic term for the corresponding KK mode. The norm of the wavefunction χ^0 is dominated by the region near the UV brane. This means that 4d gravity is localized near the UV brane and is the reason for the appearance of the unrescaled metric $g^{(4)}$ in Eq. (2.8).

Solutions to Eqs. (A.4) and (A.5) for $m_n \neq 0$ are

$$\chi^{(n)} \,=\, \frac{1}{N_n} e^{2k|y|} \left[J_2\left(\frac{m_n}{k} e^{k|y|}\right) + B_n Y_2\left(\frac{m_n}{k} e^{k|y|}\right)\right], \tag{A.7}$$

where J_2 and Y_2 are Bessel functions. The constant B_n is determined by the boundary conditions. Using the boundary condition at the UV brane in Eq. (A.5), we find

$$B_n \,=\, -\frac{J_1\left(\frac{m_n}{k}\right)}{Y_1\left(\frac{m_n}{k}\right)}\,. \tag{A.8}$$

Alternatively, we can determine B_n from the boundary condition at the IR brane in Eq. (A.5). Since both results for B_n have to agree, we get a condition on the masses m_n:

$$\frac{J_1\left(\frac{m_n}{k}\right)}{Y_1\left(\frac{m_n}{k}\right)} \,=\, \frac{J_1\left(\frac{m_n}{k} e^{k\ell}\right)}{Y_1\left(\frac{m_n}{k} e^{k\ell}\right)}\,. \tag{A.9}$$

We consider only light modes with masses $m_n \ll k$. Furthermore, we assume that $m_n \gg k\, e^{-k\ell}$. This assumption will be justified in a moment. Using the asymptotic forms of the Bessel functions for large and small arguments, we find that the mass spectrum is determined by

$$J_1\left(\frac{m_n}{k} e^{k\ell}\right) \simeq 0 \quad \Rightarrow \quad m_n \simeq \left(n + \frac{1}{4}\right)\pi\, e^{-k\ell}\, k \quad \text{for} \quad n \in \mathbb{N}\,. \tag{A.10}$$

We see that the aforementioned assumption can be justified. The last approximation becomes better for larger n but works already well for the lowest mass eigenvalue (which to a higher precision is $m_1 \simeq 1.22\,\pi\, e^{-k\ell}\, k$).

The normalization constants N_n follow from Eq. (A.6) and are given by

$$N_n \,=\, \frac{1}{\sqrt{k}} \left[e^{2k\ell} Z_2^2\left(\frac{m_n}{k} e^{k\ell}\right) - Z_2^2\left(\frac{m_n}{k}\right)\right]^{1/2}, \tag{A.11}$$

where $Z_2(x) \equiv J_2(x) - B_n\, Y_2(x)$. The norm of the wavefunctions Eq. (A.7) is dominated by the region near the IR brane. Intuitively, this is the reason why the masses, Eq. (A.10), are quantized in units of the warped curvature scale, i.e. $e^{-k\ell}k$.

Using the results for the wavefunctions $\chi^{(n)}$, we can determine the couplings of the KK modes to theories on the UV brane and the IR brane. The 4d action for the tower of KK modes reads [2, 112, 113]:

$$\begin{aligned} S = \int d^4x\, \frac{1}{2} \sum_{n=0}^{\infty} \big(\partial_\alpha h^{(n)}_{\mu\nu}\, \partial^\alpha h^{\mu\nu(n)} + m_n^2\, h^{(n)}_{\mu\nu}\, h^{\mu\nu(n)} \big) \\ + \frac{1}{\sqrt{2}} \left(\frac{1}{M_4} T^{\mu\nu}_{\rm UV} + \frac{1}{M_4} T^{\mu\nu}_{\rm IR} \right) h^{(0)}_{\mu\nu} + \frac{1}{\sqrt{2}} \sum_{n=1}^{\infty} \left(\frac{g_n}{M_4}\, T^{\mu\nu}_{\rm UV} + \frac{1}{e^{-k\ell} M_4} T^{\mu\nu}_{\rm IR} \right) h^{(n)}_{\mu\nu} \,. \end{aligned} \tag{A.12}$$

Here, $T^{\mu\nu}_{\rm UV}$ and $T^{\mu\nu}_{\rm IR}$ are the energy-momentum tensors on the UV and IR brane, respectively. In particular, note that the coupling of the massive KK modes to the IR brane is only suppressed by the warped Planck scale. The other coupling constants are

$$g_n = \left(\left(\frac{Y_1\left(\frac{m_n}{k}\right)}{Y_1\left(\frac{m_n}{k} e^{k\ell}\right)} \right)^2 - 1 \right)^{-1/2} \simeq \sqrt{\frac{n}{2}}\, \pi\, e^{-k\ell} \,. \tag{A.13}$$

In the last step we have used the asymptotic forms of the Bessel function Y_1. The approximation is valid for $n \ll e^{k\ell}$. As one can see, the coupling of massive KK modes to the UV brane has an extra exponential suppression factor.

Appendix B

Kaluza-Klein expansion of a tachyon in a Randall-Sundrum model

In Section 7.5, we have considered a scalar with a tachyonic mass in the RSI model. We have seen that, in order to avoid a tachyonic KK mode, a sufficiently large mass term on the UV brane has to be switched on. The action of such a scalar then reads

$$S \,=\, \int d^4x \int_{-\ell}^{\ell} dy\, \sqrt{g}\, \left(\frac{1}{2}\, g^{MN} \partial_M \Phi \partial_N \Phi \,+\, \frac{1}{2}\, m_{5\mathrm{d}}^2 \Phi^2 \,+\, \lambda k\, \delta(y)\, \Phi^2 \right) , \tag{B.1}$$

where $m_{5\mathrm{d}}^2 < 0$ is the tachyonic mass squared in the bulk and λ measures the mass on the UV brane in units of the AdS scale k. We use the same parametrization of AdS_5 as in Eqs. (2.3) and (2.6). In the following, we perform the KK decomposition of such a scalar and determine the couplings of the corresponding KK modes to a theory on the UV brane. For more details, see [7].

The equation of motion, which follows from the action Eq. (B.1), is

$$\frac{1}{\sqrt{g}} \partial_M \left(\sqrt{g} g^{MN} \partial_N \Phi \right) \,-\, m_{5\mathrm{d}}^2\, \Phi \,-\, 2\lambda k\, \delta(y)\, \Phi = 0\,. \tag{B.2}$$

The δ-function can be absorbed into the boundary condition at the UV brane. The KK expansion of the scalar is

$$\Phi(x,y) \,=\, \sum_n \chi_n(x) \phi_n(y)\,, \tag{B.3}$$

where the $\chi_n(x)$ are eigenmodes of the 4d d'Alembertian with eigenvalues m_n^2. The equation of motion for the ϕ_n then reads

$$\frac{d}{dy} \left(e^{-4k|y|} \frac{d\phi_n}{dy} \right) \,-\, e^{-4k|y|}\, m_{5\mathrm{d}}^2\, \phi_n \,+\, m_n^2\, e^{-2k|y|}\, \phi_n \,=\, 0\,. \tag{B.4}$$

We consider a field which is even under the orbifold $\mathbb{Z}_2$-action, i.e. $\phi_n(y) = \phi_n(-y)$. The boundary conditions for the ϕ_n then read

$$\frac{d}{dy}\phi_n(0) \,=\, \lambda\, k\, \phi_n(0) \quad \text{and} \quad \frac{d}{dy}\phi_n(\ell) \,=\, 0\,. \tag{B.5}$$

Let us consider a scalar which just satisfies the Breitenlohner-Freedman bound, i.e. $m_{5\mathrm{d}}^2 = -4k^2$. As we have discussed in Section 7.5, for a vanishing mass on the UV brane, i.e. for $\lambda = 0$, the 4d spectrum contains a tachyonic KK mode. If the mass on the UV brane is switched on, this KK mode becomes 'less tachyonic' for growing λ and for a certain value of λ, the mass of the KK mode vanishes. Let us determine this value of λ. The solution to Eq. (B.4) for $m_n = 0$ is

$$\phi_0 \;=\; A_0\, e^{2k|y|} \,+ B_0\, e^{2k|y|}\, k\,|y|\,. \tag{B.6}$$

The overall prefactor of this solution is fixed by the normalization of the wave function. The remaining constant is determined by the boundary conditions on the UV brane and the IR brane in Eq. (B.5). This fixes λ. We then find that a massless KK mode exists only if

$$\lambda \;=\; \frac{4\,\ell k}{1+2\,\ell k} \;\simeq\; 2\,. \tag{B.7}$$

The last step is valid since $k\ell \gg 1$. For this value of λ, the tachyonic mode is lifted to a massless mode. However, in a phenomenologically viable setup, no massless scalars should appear. We therefore choose λ somewhat larger than this value, say $\lambda \approx 3$, which lifts the tachyonic mode to a very massive mode.

Solutions to Eqs. (A.4) and (A.5) for $m_n \neq 0$ are

$$\phi_n \;=\; \frac{e^{2k|y|}}{N_n}\left[J_0\left(\frac{m_n}{k}e^{k|y|}\right) + B_n Y_0\left(\frac{m_n}{k}e^{k|y|}\right)\right]\,, \tag{B.8}$$

where J_0 and Y_0 are Bessel functions. Using the boundary condition at the UV brane in Eq. (B.5), we can determine the constant B_n:

$$B_n \;=\; -\frac{(2-\lambda)\,J_0\left(\frac{m_n}{k}\right) - \frac{m_n}{k}\,J_1\left(\frac{m_n}{k}\right)}{(2-\lambda)\,Y_0\left(\frac{m_n}{k}\right) - \frac{m_n}{k}\,Y_1\left(\frac{m_n}{k}\right)}\,. \tag{B.9}$$

We consider only light modes with masses $m_n \ll k$. Using the asymptotic forms of the Bessel functions for small arguments, we find that $B_n \sim \log(m_n/k)^{-1} \ll 1$ for $m_n \ll k$ and $\lambda \approx 3$. We have used this fact in Section 7.5. Alternatively, we can determine the constant B_n from the boundary condition at the IR brane in Eq. (B.5). Both results for B_n have to agree and we therefore get a condition on the masses m_n:

$$\frac{(2-\lambda)\,J_0\left(\frac{m_n}{k}\right) - \frac{m_n}{k}\,J_1\left(\frac{m_n}{k}\right)}{(2-\lambda)\,Y_0\left(\frac{m_n}{k}\right) - \frac{m_n}{k}\,Y_1\left(\frac{m_n}{k}\right)} \;=\; \frac{2\,J_0\left(\frac{m_n}{k}e^{k\ell}\right) - \frac{m_n}{k}\,e^{k\ell} J_1\left(\frac{m_n}{k}e^{k\ell}\right)}{2\,Y_0\left(\frac{m_n}{k}e^{k\ell}\right) - \frac{m_n}{k}\,e^{k\ell}\,Y_1\left(\frac{m_n}{k}e^{k\ell}\right)}\,. \tag{B.10}$$

For $m_n \ll k$ and $\lambda \approx 3$, this condition simplifies to

$$\begin{aligned}\mathcal{O}(1)\left[2\,Y_0\left(\frac{m_n}{k}e^{k\ell}\right) - \frac{m_n}{k}\,e^{k\ell}\,Y_1\left(\frac{m_n}{k}e^{k\ell}\right)\right]& \\ \sim\; \log\!\left(\frac{m_n}{k}\right)\left[2\,J_0\left(\frac{m_n}{k}e^{k\ell}\right) - \frac{m_n}{k}\,e^{k\ell} J_1\left(\frac{m_n}{k}e^{k\ell}\right)\right]\,.&\end{aligned} \tag{B.11}$$

If we assume that the masses fulfill $m_n k^{-1} e^{k\ell} \gg 1$, we can use the asymptotic forms of the Bessel functions for large arguments in Eq. (B.11). Since $\log(m_n/k) \gg 1$, Eq. (B.11) is then approximately solved for

$$J_1\left(\frac{m_n}{k}e^{k\ell}\right) \ll 1 \quad \Rightarrow \quad m_n \approx \left(n+\frac{1}{4}\right)\pi\, e^{-k\ell}\, k \quad \text{for} \quad n \in \mathbb{N}\,. \tag{B.12}$$

For n somewhat larger than 1, the assumption that $m_n k^{-1} e^{k\ell} \gg 1$ is indeed fulfilled. For smaller n, the masses differ from the result in Eq. (B.12) but are still quantized in units of the warped AdS scale, i.e. $ke^{-k\ell}$, as we have discussed in Section 7.5.

In order to obtain a canonically normalized kinetic term for the KK modes, the wave functions ϕ_n have to be normalized according to

$$\int_{-\ell}^{\ell} dy\, e^{-2k|y|}\,(\phi_n(y))^2 \stackrel{!}{=} 1\,. \tag{B.13}$$

This fixes the constant N_n in Eq. (B.8) and we find

$$N_n = \frac{1}{\sqrt{k}}\left[Z_0^2\left(\frac{m_n}{k}e^{k\ell}\right)\left(e^{2k\ell}+\frac{4\,k^2}{m_n^2}\right) - Z_0^2\left(\frac{m_n}{k}\right)\left(1+\frac{k^2}{m_n^2}(\lambda-2)^2\right)\right]^{1/2}, \tag{B.14}$$

where $Z_0 \equiv J_0 + B_n Y_0$.

The coupling of the tachyonic scalar to a gauge theory on the UV brane is given in Eq. (7.21) and reads

$$S_{\text{UV}} \supset\sim \frac{1}{M_{10}^4\, R^{5/2}} \int d^4x \int_{-\ell}^{\ell} dy\, \sqrt{g}\, F_{\mu\nu}F^{\mu\nu}\, \Phi\, \delta(y)\,, \tag{B.15}$$

where $F_{\mu\nu}$ is the gauge field strength. As we have discussed in Section 7.5, the prefactor is motivated by the DBI action and a dimensional reduction from 10d to 5d. Inserting the KK expansion Eq. (B.3) in Eq. (B.15), the coupling of the n-th KK mode to the gauge theory follows as

$$S_{\text{4d}} \supset\sim \frac{g_n}{M_{10}^4\, R^3} \int d^4x\, F_{\mu\nu}F^{\mu\nu}\, \chi_n\,. \tag{B.16}$$

The coupling strengths g_n are determined by the value $\phi_n(0)$ of the wave functions at the UV brane and read

$$g_n = \left[\left(\frac{(2-\lambda)J_0\left(\frac{m_n}{k}\right) - \frac{m_n}{k}J_1\left(\frac{m_n}{k}\right)}{2J_0\left(\frac{m_n}{k}e^{k\ell}\right) - \frac{m_n}{k}e^{k\ell}J_1\left(\frac{m_n}{k}e^{k\ell}\right)}\right)^2\left[e^{2k\ell}+\frac{4k^2}{m_n^2}\right] - \left[1+\frac{k^2}{m_n^2}(\lambda-2)^2\right]\right]^{-1/2}. \tag{B.17}$$

This rather complicated expression can be evaluated by using the asymptotic forms of the Bessel functions and the mass quantization in Eq. (B.12). For $\lambda \approx 3$, we find

$$g_n \sim \frac{1}{k\,\ell}\sqrt{\frac{m_n e^{-k\ell}}{k}}\,. \tag{B.18}$$

Appendix C

Evaluation of a propagator

In Eq. (6.14), we had to evaluate the following propagator in a mixed, energy-configuration-space representation:

$$\int \frac{d^6\rho}{(2\pi)^6} \, \frac{e^{i\vec{A}\,\vec{\rho}}}{m^2 - \vec{\rho}^2 + i\epsilon} \, . \tag{C.1}$$

We perform the integral for imaginary values $m \to e^{i\pi/2} m$ and use analytic continuation. The integral changes into

$$-\int \frac{d^6\rho}{(2\pi)^6} \, \frac{e^{i\vec{A}\,\vec{\rho}}}{m^2 + \vec{\rho}^2} \, . \tag{C.2}$$

We can then employ the identity $c^{-1} = \int_0^\infty d\tau e^{-c\tau}$ for $\mathrm{Re}\, c > 0$ and get

$$\begin{aligned} &\frac{-1}{(2\pi)^6} \int_0^\infty d\tau \int d^6\rho \;\; e^{i\vec{A}\,\vec{\rho}}\, e^{-(m^2+\vec{\rho}^2)\tau} \\ =&\frac{-1}{(2\pi)^6} \int_0^\infty d\tau \;\left(\left[\int d\rho_1 \; e^{iA_1\,\rho_1} \, e^{-\rho_1^2 \tau} \right] \cdots \left[\int d\rho_6 \; e^{iA_6\,\rho_6} \, e^{-\rho_6^2 \tau} \right] e^{-m^2\tau} \right) \\ =&\frac{-1}{(4\pi)^3} \int_0^\infty d\tau \; \frac{1}{\tau^3} \, e^{-A^2/4\tau} \, e^{-m^2\tau} \, . \end{aligned} \tag{C.3}$$

We have used that $A^2 = A_1^2 + \cdots + A_6^2$. According to Eq. 3.471.9 in [114], this integral can be evaluated in terms of the modified Bessel function $K_{-2} \equiv K_2$, which yields

$$\frac{-1}{(2\pi)^3} \frac{m^2}{A^2} \, K_2(mA) \, . \tag{C.4}$$

Following from Eq. 9.6.4 in [115], K_2 is related to the Hankel function $H_2^+ = J_2 + iY_2$. The above expression can be written as

$$\frac{i}{(4\pi)^2} \frac{m^2}{A^2} \, H_2^+(e^{i\pi/2} mA) \, . \tag{C.5}$$

The Hankel function has a branch cut along the negative real axis. Therefore, one can analytically continue back to real values $m \to e^{-i\pi/2} m$, which gives

$$\frac{-i}{(4\pi)^2} \frac{m^2}{A^2} \, H_2^+(mA) \, . \tag{C.6}$$

Appendix D

Additional processes in a thermalized situation

In Section 7.3, we have discussed several decay processes of glueballs to lighter glueballs in the gauge theory sectors which are dual to throats. There is another process in these sectors which can take place if the gauge theory was initially in the deconfined phase. The glueballs which are formed at the confinement phase transition then interact with each other for a certain period of time. This leads to a significant reduction of the abundances of all the states heavier than the lightest glueball, including its superpartner if the mass splitting from supersymmetry breaking is not too small. In this Appendix, we analyse this process in some detail:

For simplicity, we focus on only two glueball species. Generically, the glueball effective action includes couplings of the type

$$\mathcal{H}\mathcal{H}\,\mathcal{G}\mathcal{G}\,, \tag{D.1}$$

where $\mathcal{H}$ and $\mathcal{G}$ are the heavy and light glueball respectively, and all Lorentz- and/or spinor-indices are appropriately contracted. By assumption, the masses of the two glueball species satisfy $m_{\mathcal{G}} < m_{\mathcal{H}}$. As long as the two glueball species are in equilibrium, the density $n_{\mathcal{H}}$ of the heavy glueballs is suppressed relative to the light glueball density $n_{\mathcal{G}}$ by an exponential factor

$$e^{-(m_{\mathcal{H}}-m_{\mathcal{G}})/\tilde{T}} \tag{D.2}$$

after the temperature $\tilde{T}$ of the glueball gas falls below $m_{\rm IR}$. This exponential decrease of the number density of $\mathcal{H}$ glueballs continues until they are so dilute that they decouple. This happens, when

$$n_{\mathcal{H}} \cdot \langle \sigma v \rangle \;\sim\; H\,. \tag{D.3}$$

Here $\langle \sigma v \rangle$ is the thermally averaged product of cross section and relative velocity for the $2 \cdot \mathcal{H} \leftrightarrow 2 \cdot \mathcal{G}$ process, which evaluates to [72][1]

$$\langle \sigma v \rangle \;\sim\; m_{\rm IR}^{-2}\,. \tag{D.4}$$

[1] If the mass difference $m_{\mathcal{H}} - m_{\mathcal{G}}$ is very small, this cross section is kinematically suppressed. This may happen, for example, for the superpartner of the lightest glueball. These glueballs are then diluted to a lesser extent.

Since $n_{\mathcal{H}}$ drops exponentially after the temperature $\tilde{T}$ falls below $m_{\rm IR}$, the heavy glueballs decouple when the temperature of the glueball gas is still of the order of $m_{\rm IR}$. We can therefore derive the freezeout density of the heavy glueballs from Eq. (D.3) by using the phase-transition Hubble rate $H(T_{\rm pt})$. Furthermore, we can approximate the light glueball density by $m_{\rm IR}^3$. The ratio of heavy and light glueball densities directly after freezeout, i.e. the dilution factor, is then given by

$$\frac{n_{\mathcal{H}}}{n_{\mathcal{G}}} \sim \frac{H(T_{\rm pt})}{m_{\rm IR}} \sim \frac{g^{1/2} m_{\rm IR} M_4^{1/2}}{N_{\rm UV} T_{\rm RH}^{3/2}} \,. \tag{D.5}$$

Here we have calculated the Hubble rate according to Eqs. (8.4) and (8.11) and disregarded a small power of $N_{\rm IR}$. Our formula is valid if the right-hand side is smaller than 1. If, however, the right-hand side is formally larger than 1, the $\mathcal{H}$ glueballs are decoupled from the beginning and not diluted at all.

Acknowledgements

First and foremost, I would like to express my gratitude to Arthur Hebecker for his supervision of this thesis. He helped me in many ways and always had an open ear when I had questions. For instance, I remember discussing with him on a sunday evening, the day before Christmas Eve! There are certainly not many supervisors who care so much for their students. Even more, I have also considerably benefited from his knowledge and intuition in physics and from his pedagogical talent. For all this, many thanks!

I am also indebted to Michael G. Schmidt for kindly agreeing to co-referee this thesis, for teaching me a lot and for his support during the last years.

Part of the research for this thesis was done together with Sebastian Halter and Tatsuya Noguchi (in addition to Arthur Hebecker). I would like to thank them for an enjoyable collaboration. Furthermore, this thesis and myself have benefited from interesting and helpful discussions with Andreas Braun, Jens Braun, Wilfried Buchmüller, Xingang Chen, Jim Cline, Thomas Dent, Dennis Dietrich, Hassan Firouzjahi, Andrew Frey, Christoph Lüdeling, Stefan Groot Nibbelink, Kris Sigurdson, Hagen Triendl, Roberto Valandro and Michele Trapletti. Special thanks go to Andreas Braun and Christoph Lüdeling for their comments on a draft of this thesis. In addition, I would like to thank my other colleagues in Heidelberg for creating a very pleasant and stimulating atmosphere, especially Rainer Ebert, Sebastian Gerigk, Christian Gross, Tae-Won Ha, Johannes Held, Patrick Plötz, Christian Viereck and Robert Ziegler.

My thesis was financially backed by a position at the Institute for Theoretical Physics in Heidelberg, for which I am grateful. In this respect, I would also like to thank the "Ritterschaft des Fürstentums Lüneburg" for additional financial support.

I am grateful to my parents for so much help and support. Et enfin, mais sûrement pas en dernier lieu, j'aimerais dire merci mille fois à Emilie Omnès pour son soutien and sa compréhension pendant les derniers années.

Bibliography

[1] L. Randall and R. Sundrum, "A large mass hierarchy from a small extra dimension," Phys. Rev. Lett. **83** (1999) 3370 [arXiv:hep-ph/9905221].

[2] L. Randall and R. Sundrum, "An alternative to compactification," Phys. Rev. Lett. **83** (1999) 4690 [arXiv:hep-th/9906064].

[3] S. B. Giddings, S. Kachru and J. Polchinski, "Hierarchies from fluxes in string compactifications," Phys. Rev. D **66** (2002) 106006 [arXiv:hep-th/0105097].

[4] I. R. Klebanov and M. J. Strassler, "Supergravity and a confining gauge theory: Duality cascades and chiSB-resolution of naked singularities," JHEP **0008** (2000) 052 [arXiv:hep-th/0007191].

[5] B. v. Harling, A. Hebecker and T. Noguchi, "Energy Transfer between Throats from a 10d Perspective," JHEP **0711** (2007) 042 [arXiv:0705.3648 [hep-th]].

[6] P. Breitenlohner and D. Z. Freedman, "Positive Energy In Anti-De Sitter Backgrounds And Gauged Extended Supergravity," Phys. Lett. B **115** (1982) 197 and "Stability In Gauged Extended Supergravity," Annals Phys. **144** (1982) 249.

[7] S. Halter, B. v. Harling and A. Hebecker, "Tachyons in Throat Cosmology", to appear.

[8] B. v. Harling and A. Hebecker, "Sequestered Dark Matter," JHEP **0805** (2008) 031 [arXiv:0801.4015 [hep-ph]].

[9] A. Hebecker and J. March-Russell, "The ubiquitous throat," Nucl. Phys. B **781** (2007) 99 [arXiv:hep-th/0607120].

[10] O. Aharony, S. S. Gubser, J. M. Maldacena, H. Ooguri and Y. Oz, "Large N field theories, string theory and gravity," Phys. Rept. **323** (2000) 183 [arXiv:hep-th/9905111].

[11] R. Rattazzi, "Cargese lectures on extra dimensions," arXiv:hep-ph/0607055.

[12] T. Gherghetta, "Warped models and holography," arXiv:hep-ph/0601213.

[13] J. Garriga and T. Tanaka, "Gravity in the brane-world," Phys. Rev. Lett. **84** (2000) 2778 [arXiv:hep-th/9911055].

[14] S. B. Giddings, E. Katz and L. Randall, "Linearized gravity in brane backgrounds," JHEP **0003** (2000) 023 [arXiv:hep-th/0002091].

[15] W. D. Goldberger and M. B. Wise, "Modulus stabilization with bulk fields," Phys. Rev. Lett. **83** (1999) 4922 [arXiv:hep-ph/9907447].

[16] J. Polchinski, "Dirichlet-Branes and Ramond-Ramond Charges," Phys. Rev. Lett. **75** (1995) 4724 [arXiv:hep-th/9510017].

[17] R. Sundrum, "Effective field theory for a three-brane universe," Phys. Rev. D **59** (1999) 085009 [arXiv:hep-ph/9805471].

[18] I. Low and A. V. Manohar, "Spontaneously broken spacetime symmetries and Goldstone's theorem," Phys. Rev. Lett. **88** (2002) 101602 [arXiv:hep-th/0110285].

[19] G. T. Horowitz and A. Strominger, "Black strings and P-branes," Nucl. Phys. B **360** (1991) 197.

[20] I. R. Klebanov, "World-volume approach to absorption by non-dilatonic branes," Nucl. Phys. B **496** (1997) 231 [arXiv:hep-th/9702076].

[21] S. S. Gubser, I. R. Klebanov and A. A. Tseytlin, "String theory and classical absorption by three-branes," Nucl. Phys. B **499** (1997) 217 [arXiv:hep-th/9703040].

[22] I. R. Klebanov, W. Taylor and M. Van Raamsdonk, "Absorption of dilaton partial waves by D3-branes," Nucl. Phys. B **560** (1999) 207 [arXiv:hep-th/9905174].

[23] S. S. Gubser, A. Hashimoto, I. R. Klebanov and M. Krasnitz, "Scalar absorption and the breaking of the world volume conformal invariance," Nucl. Phys. B **526** (1998) 393 [arXiv:hep-th/9803023].

[24] S. S. Gubser and A. Hashimoto, "Exact absorption probabilities for the D3-brane," Commun. Math. Phys. **203** (1999) 325 [arXiv:hep-th/9805140].

[25] S. S. Gubser and I. R. Klebanov, "Absorption by branes and Schwinger terms in the world volume theory," Phys. Lett. B **413** (1997) 41 [arXiv:hep-th/9708005].

[26] J. M. Maldacena, "The large N limit of superconformal field theories and supergravity," Adv. Theor. Math. Phys. **2** (1998) 231 [Int. J. Theor. Phys. **38** (1999) 1113] [arXiv:hep-th/9711200].

[27] S. S. Gubser, "AdS/CFT and gravity," Phys. Rev. D **63** (2001) 084017 [arXiv:hep-th/9912001] and references therein.

[28] N. Arkani-Hamed, M. Porrati and L. Randall, "Holography and phenomenology," JHEP **0108** (2001) 017 [arXiv:hep-th/0012148].

[29] P. Candelas and X. C. de la Ossa, "Comments on Conifolds," Nucl. Phys. B **342** (1990) 246.

[30] I. R. Klebanov and E. Witten, "Superconformal field theory on threebranes at a Calabi-Yau singularity," Nucl. Phys. B **536** (1998) 199 [arXiv:hep-th/9807080].

[31] I. R. Klebanov and N. A. Nekrasov, "Gravity duals of fractional branes and logarithmic RG flow," Nucl. Phys. B **574** (2000) 263 [arXiv:hep-th/9911096].

[32] I. R. Klebanov and A. A. Tseytlin, "Gravity duals of supersymmetric SU(N) x SU(N+M) gauge theories," Nucl. Phys. B **578** (2000) 123 [arXiv:hep-th/0002159].

[33] S. S. Gubser, I. R. Klebanov and A. W. Peet, "Entropy and Temperature of Black 3-Branes," Phys. Rev. D **54**, 3915 (1996) [arXiv:hep-th/9602135].

[34] Y. Satoh, "Propagation of scalars in non-extremal black hole and black p-brane geometries," Phys. Rev. D **58** (1998) 044004 [arXiv:hep-th/9801125];
S. Musiri and G. Siopsis, "Temperature of D3-branes off extremality," Phys. Lett. B **504** (2001) 314 [arXiv:hep-th/0003284];
J. F. Vazquez-Poritz, "Absorption by nonextremal D3-branes," arXiv:hep-th/0007202;
G. Policastro and A. Starinets, "On the absorption by near-extremal black branes," Nucl. Phys. B **610** (2001) 117 [arXiv:hep-th/0104065];
J. A. Garcia and A. Guijosa, "Threebrane absorption and emission from a brane-antibrane system," JHEP **0409** (2004) 027 [arXiv:hep-th/0407075].

[35] E. Witten, "Anti-de Sitter space, thermal phase transition, and confinement in gauge theories," Adv. Theor. Math. Phys. **2** (1998) 505 [arXiv:hep-th/9803131].

[36] P. Creminelli, A. Nicolis and R. Rattazzi, "Holography and the electroweak phase transition," JHEP **0203** (2002) 051 [arXiv:hep-th/0107141].

[37] A. Buchel, C. P. Herzog, I. R. Klebanov, L. A. Pando Zayas and A. A. Tseytlin, "Non-extremal gravity duals for fractional D3-branes on the conifold," JHEP **0104** (2001) 033 [arXiv:hep-th/0102105];
S. S. Gubser, C. P. Herzog, I. R. Klebanov and A. A. Tseytlin, "Restoration of chiral symmetry: A supergravity perspective," JHEP **0105** (2001) 028 [arXiv:hep-th/0102172].

[38] O. Aharony, A. Buchel and P. Kerner, "The black hole in the throat - thermodynamics of strongly coupled cascading gauge theories," Phys. Rev. D **76** (2007) 086005 [arXiv:0706.1768 [hep-th]];
M. Mahato, L. A. P. Zayas and C. A. Terrero-Escalante, "Black Holes in Cascading Theories: Confinement/Deconfinement Transition and other Thermal Properties," JHEP **0709** (2007) 083 [arXiv:0707.2737 [hep-th]].

[39] B. Hassanain, J. March-Russell and M. Schvellinger, "Warped Deformed Throats have Faster (Electroweak) Phase Transitions,"
JHEP **0710** (2007) 089 [arXiv:0708.2060 [hep-th]].

[40] F. Brümmer, A. Hebecker and E. Trincherini, "The throat as a Randall-Sundrum model with Goldberger-Wise stabilization," Nucl. Phys. B **738** (2006) 283 [arXiv:hep-th/0510113].

[41] A. R. Frey, "Warped strings: Self-dual flux and contemporary compactifications," arXiv:hep-th/0308156.

[42] M. Grana, "Flux compactifications in string theory: A comprehensive review," Phys. Rept. **423** (2006) 91 [arXiv:hep-th/0509003].

[43] M. R. Douglas and S. Kachru, "Flux compactification," Rev. Mod. Phys. **79** (2007) 733 [arXiv:hep-th/0610102].

[44] H. L. Verlinde, "Holography and compactification," Nucl. Phys. B **580** (2000) 264 [arXiv:hep-th/9906182].

[45] S. Gukov, C. Vafa and E. Witten, "CFT's from Calabi-Yau four-folds," Nucl. Phys. B **584** (2000) 69 [Erratum-ibid. B **608** (2001) 477] [arXiv:hep-th/9906070].

[46] P. Candelas and X. de la Ossa, "Moduli space of Calabi-Yau manifolds," Nucl. Phys. B **355** (1991) 455.

[47] G. von Gersdorff and A. Hebecker, "Kaehler corrections for the volume modulus of flux compactifications," Phys. Lett. B **624** (2005) 270 [arXiv:hep-th/0507131].

[48] S. Kachru, R. Kallosh, A. Linde and S. P. Trivedi, "De Sitter vacua in string theory," Phys. Rev. D **68** (2003) 046005 [arXiv:hep-th/0301240].

[49] M. R. Douglas, "The statistics of string / M theory vacua," JHEP **0305** (2003) 046 [arXiv:hep-th/0303194].

[50] S. Ashok and M. R. Douglas, "Counting flux vacua," JHEP **0401** (2004) 060 [arXiv:hep-th/0307049].

[51] F. Denef and M. R. Douglas, "Distributions of flux vacua," JHEP **0405** (2004) 072 [arXiv:hep-th/0404116].

[52] G. R. Dvali and S. H. H. Tye, "Brane inflation," Phys. Lett. B **450** (1999) 72 [arXiv:hep-ph/9812483].

[53] S. H. S. Alexander, "Inflation from D - anti-D brane annihilation," Phys. Rev. D **65** (2002) 023507 [arXiv:hep-th/0105032].

[54] G. R. Dvali, Q. Shafi and S. Solganik, "D-brane inflation," arXiv:hep-th/0105203; C. P. Burgess, M. Majumdar, D. Nolte, F. Quevedo, G. Rajesh and R. J. Zhang, "The inflationary brane-antibrane universe," JHEP **0107** (2001) 047 [arXiv:hep-th/0105204].

[55] S. Kachru, R. Kallosh, A. Linde, J. M. Maldacena, L. P. McAllister and S. P. Trivedi, "Towards inflation in string theory," JCAP **0310** (2003) 013 [arXiv:hep-th/0308055].

[56] A. Sen, "Rolling tachyon," JHEP **0204** (2002) 048 [arXiv:hep-th/0203211];
A. Sen, "Tachyon matter," JHEP **0207** (2002) 065 [arXiv:hep-th/0203265];
A. Sen, "Field theory of tachyon matter," Mod. Phys. Lett. A **17** (2002) 1797 [arXiv:hep-th/0204143].

[57] N. D. Lambert, H. Liu and J. M. Maldacena, "Closed strings from decaying D-branes," JHEP **0703** (2007) 014 [arXiv:hep-th/0303139].

[58] N. Barnaby, C. P. Burgess and J. M. Cline, "Warped reheating in brane-antibrane inflation," JCAP **0504** (2005) 007 [arXiv:hep-th/0412040].

[59] D. Chialva, G. Shiu and B. Underwood, "Warped reheating in multi-throat brane inflation," JHEP **0601** (2006) 014 [arXiv:hep-th/0508229].

[60] L. Kofman and P. Yi, "Reheating the universe after string theory inflation," Phys. Rev. D **72** (2005) 106001 [arXiv:hep-th/0507257].

[61] A. R. Frey, A. Mazumdar and R. C. Myers, "Stringy effects during inflation and reheating," Phys. Rev. D **73** (2006) 026003 [arXiv:hep-th/0508139].

[62] X. Chen and S. H. Tye, "Heating in brane inflation and hidden dark matter," JCAP **0606**, 011 (2006) [arXiv:hep-th/0602136].

[63] S. Dimopoulos, S. Kachru, N. Kaloper, A. E. Lawrence and E. Silverstein, "Small numbers from tunneling between brane throats," Phys. Rev. D **64** (2001) 121702 [arXiv:hep-th/0104239];
S. Dimopoulos, S. Kachru, N. Kaloper, A. E. Lawrence and E. Silverstein, "Generating small numbers by tunneling in multi-throat compactifications," Int. J. Mod. Phys. A **19** (2004) 2657 [arXiv:hep-th/0106128].

[64] C. Csaki, J. Erlich, T. J. Hollowood and Y. Shirman, "Universal aspects of gravity localized on thick branes," Nucl. Phys. B **581** (2000) 309 [arXiv:hep-th/0001033].

[65] H. Firouzjahi and S. H. Tye, "The shape of gravity in a warped deformed conifold," JHEP **0601**, 136 (2006) [arXiv:hep-th/0512076].

[66] G. W. Gibbons and S. W. Hawking, "Action Integrals And Partition Functions In Quantum Gravity," Phys. Rev. D **15** (1977) 2752.

[67] H. A. Chamblin and H. S. Reall, "Dynamic dilatonic domain walls," Nucl. Phys. B **562** (1999) 133 [arXiv:hep-th/9903225].

[68] A. Hebecker and J. March-Russell, "Randall-Sundrum II cosmology, AdS/CFT, and the bulk black hole," Nucl. Phys. B **608**, 375 (2001) [arXiv:hep-ph/0103214].

[69] D. Langlois, L. Sorbo and M. Rodriguez-Martinez, "Cosmology of a brane radiating gravitons into the extra dimension," Phys. Rev. Lett. **89** (2002) 171301 [arXiv:hep-th/0206146];
D. Langlois and L. Sorbo, "Bulk gravitons from a cosmological brane," Phys. Rev. D **68** (2003) 084006 [arXiv:hep-th/0306281].

[70] P. Langfelder, "On tunnelling in two-throat warped reheating," JHEP **0606** (2006) 063 [arXiv:hep-th/0602296].

[71] K. Hosomichi, "Absorption of fermions by D3-branes," JHEP **9806** (1998) 009 [arXiv:hep-th/9806010].

[72] M. Srednicki, R. Watkins and K. A. Olive, "Calculations of relic densities in the early universe," Nucl. Phys. B **310** (1988) 693;
E. W. Kolb and M. S. Turner, "The Early Universe" *Redwood City, USA: Addison-Wesley (1990) 547 p. (Frontiers in physics, 69).*

[73] M. Krasnitz, "A two point function in a cascading N = 1 gauge theory from supergravity," arXiv:hep-th/0011179.

[74] E. Caceres and R. Hernandez, "Glueball masses for the deformed conifold theory," Phys. Lett. B **504** (2001) 64 [arXiv:hep-th/0011204].

[75] X. Amador and E. Caceres, "Spin two glueball mass and glueball Regge trajectory from supergravity," JHEP **0411** (2004) 022 [arXiv:hep-th/0402061].

[76] T. Noguchi, M. Yamaguchi and M. Yamashita, "Gravitational Kaluza-Klein modes in warped superstring compactification," Phys. Lett. B **636**, 221 (2006) [arXiv:hep-th/0512249].

[77] A. Y. Dymarsky and D. G. Melnikov, "On the glueball spectrum in the Klebanov-Strassler model," JETP Lett. **84** (2006) 368 [Pisma Zh. Eksp. Teor. Fiz. **84** (2006) 440].

[78] M. Berg, M. Haack and W. Mueck, "Glueballs vs. gluinoballs: Fluctuation spectra in non-AdS/non-CFT," arXiv:hep-th/0612224.

[79] A. Dymarsky and D. Melnikov, "Gravity Multiplet on KS and BB Backgrounds," arXiv:0710.4517 [hep-th].

[80] M. K. Benna, A. Dymarsky, I. R. Klebanov and A. Solovyov, "On Normal Modes of a Warped Throat," arXiv:0712.4404 [hep-th].

[81] L. Randall and R. Sundrum, "Out of this world supersymmetry breaking," Nucl. Phys. B **557** (1999) 79 [arXiv:hep-th/9810155].

[82] K. Choi and K. S. Jeong, "Supersymmetry breaking and moduli stabilization with anomalous U(1) gauge symmetry," JHEP **0608** (2006) 007 [arXiv:hep-th/0605108].

[83] F. Brümmer, A. Hebecker and M. Trapletti, "SUSY breaking mediation by throat fields," Nucl. Phys. B **755** (2006) 186 [arXiv:hep-th/0605232].

[84] S. Kachru, L. McAllister and R. Sundrum, "Sequestering in string theory," JHEP **0710** (2007) 013 [arXiv:hep-th/0703105].

[85] O. Aharony, Y. E. Antebi and M. Berkooz, "Open string moduli in KKLT compactifications," Phys. Rev. D **72** (2005) 106009 [arXiv:hep-th/0508080].

[86] A. Berndsen, J. M. Cline and H. Stoica, "Kaluza-Klein relics from warped reheating," arXiv:0710.1299 [hep-th].

[87] J. F. Dufaux, L. Kofman and M. Peloso, "Dangerous Angular KK/Glueball Relics in String Theory Cosmology," arXiv:0802.2958 [hep-th].

[88] B. Batell and T. Gherghetta, "Holographic Mixing Quantified," Phys. Rev. D **76** (2007) 045017 [arXiv:0706.0890 [hep-th]].

[89] S. B. Giddings and A. Maharana, "Dynamics of warped compactifications and the shape of the warped landscape," Phys. Rev. D **73** (2006) 126003 [arXiv:hep-th/0507158].

[90] A. R. Frey and A. Maharana, "Warped spectroscopy: Localization of frozen bulk modes," JHEP **0608** (2006) 021 [arXiv:hep-th/0603233].

[91] K. Ghoroku and A. Nakamura, "Stability of Randall-Sundrum brane-world and tachyonic scalar," Phys. Rev. D **64** (2001) 084028 [arXiv:hep-th/0103071];
A. Delgado and M. Redi, "Tachyons in a slice of AdS," Phys. Lett. B **562** (2003) 127 [arXiv:hep-th/0301151].

[92] A. Ceresole, G. Dall'Agata, R. D'Auria and S. Ferrara, "Spectrum of type IIB supergravity on AdS(5) x T(11): Predictions on N =1 SCFT's," Phys. Rev. D **61** (2000) 066001 [arXiv:hep-th/9905226];
A. Ceresole, G. Dall'Agata and R. D'Auria, "KK spectroscopy of type IIB supergravity on AdS(5) x T(11)," JHEP **9911** (1999) 009 [arXiv:hep-th/9907216].

[93] K. Benakli and A. Y. Smirnov, "Neutrino-modulino mixing," Phys. Rev. Lett. **79** (1997) 4314 [arXiv:hep-ph/9703465].

[94] E. W. Kolb, D. Seckel and M. S. Turner, "The Shadow World," Nature **314** (1985) 415;
J. R. Ellis, J. L. Lopez and D. V. Nanopoulos, "Confinement of fractional charges yields integer charged relics in string models," Phys. Lett. B **247** (1990) 257;
A. E. Faraggi and M. Pospelov, "Self-interacting dark matter from the hidden heterotic-string sector," Astropart. Phys. **16** (2002) 451 [arXiv:hep-ph/0008223];
J. A. R. Cembranos, A. Dobado and A. L. Maroto, "Brane-world dark matter," Phys. Rev. Lett. **90** (2003) 241301 [arXiv:hep-ph/0302041];
G. Shiu and L. T. Wang, "D-matter," Phys. Rev. D **69** (2004) 126007 [arXiv:hep-ph/0311228];
J. R. Ellis, V. E. Mayes and D. V. Nanopoulos, "Flipped cryptons and the UHECRs," Phys. Rev. D **70** (2004) 075015 [arXiv:hep-ph/0403144].

[95] W. Buchmüller, L. Covi, K. Hamaguchi, A. Ibarra and T. Yanagida, "Gravitino dark matter in R-parity breaking vacua," JHEP **0703** (2007) 037 [arXiv:hep-ph/0702184];

G. Bertone, W. Buchmüller, L. Covi and A. Ibarra, "Gamma-Rays from Decaying Dark Matter," arXiv:0709.2299 [astro-ph].

[96] F. Takayama and M. Yamaguchi, "Gravitino dark matter without R-parity," Phys. Lett. B **485** (2000) 388 [arXiv:hep-ph/0005214];
A. Ibarra and D. Tran, "Gamma Ray Spectrum from Gravitino Dark Matter Decay," arXiv:0709.4593 [astro-ph];
K. Ishiwata, S. Matsumoto and T. Moroi, "High Energy Cosmic Rays from the Decay of Gravitino Dark Matter," arXiv:0805.1133 [hep-ph].

[97] O. Aharony, S. Minwalla and T. Wiseman, "Plasma-balls in large N gauge theories and localized black holes," Class. Quant. Grav. **23** (2006) 2171 [arXiv:hep-th/0507219].

[98] D. M. Hofman and J. Maldacena, "Conformal collider physics: Energy and charge correlations," JHEP **0805** (2008) 012 [arXiv:0803.1467 [hep-th]].

[99] Y. Hatta, E. Iancu and A. H. Mueller, "Jet evolution in the N=4 SYM plasma at strong coupling," JHEP **0805** (2008) 037 [arXiv:0803.2481 [hep-th]].

[100] Y. Hatta and T. Matsuo, "Jet fragmentation and gauge/string duality," arXiv:0804.4733 [hep-th].

[101] M. J. Strassler, "Why Unparticle Models with Mass Gaps are Examples of Hidden Valleys," arXiv:0801.0629 [hep-ph].

[102] G. D. Kribs and I. Z. Rothstein, "Bounds on long-lived relics from diffuse gamma ray observations," Phys. Rev. D **55** (1997) 4435 [Erratum-ibid. D **56** (1997) 1822] [arXiv:hep-ph/9610468].

[103] J. R. Ellis, G. B. Gelmini, J. L. Lopez, D. V. Nanopoulos and S. Sarkar, "Astrophysical Constraints On Massive Unstable Neutral Relic Particles," Nucl. Phys. B **373** (1992) 399.

[104] J. A. R. Cembranos, J. L. Feng and L. E. Strigari, "Resolving Cosmic Gamma Ray Anomalies with Dark Matter Decaying Now," Phys. Rev. Lett. **99** (2007) 191301 [arXiv:0704.1658 [astro-ph]];
H. Yuksel and M. D. Kistler, "Dark Matter Might Decay... Just Not Today!," arXiv:0711.2906 [astro-ph];
S. Palomares-Ruiz, "Model-Independent Bound on the Dark Matter Lifetime," arXiv:0712.1937 [astro-ph];
J. A. R. Cembranos and L. E. Strigari, "Diffuse MeV Gamma-rays and Galactic 511 keV Line from Decaying WIMP Dark Matter," Phys. Rev. D **77** (2008) 123519 [arXiv:0801.0630 [astro-ph]].

[105] J. R. Hörandel, "The composition of cosmic rays at the knee," Nuovo Cim. B **120** (2005) 825 [arXiv:astro-ph/0407554].

[106] J. P. Conlon, F. Quevedo and K. Suruliz, "Large-volume flux compactifications: Moduli spectrum and D3/D7 soft supersymmetry breaking," JHEP **0508** (2005) 007 [arXiv:hep-th/0505076];
J. P. Conlon, S. S. Abdussalam, F. Quevedo and K. Suruliz, "Soft SUSY breaking terms for chiral matter in IIB string compactifications," JHEP **0701** (2007) 032 [arXiv:hep-th/0610129];
J. P. Conlon and F. Quevedo, "Astrophysical and Cosmological Implications of Large Volume String Compactifications," JCAP **0708** (2007) 019 [arXiv:0705.3460 [hep-ph]].

[107] M. Birkel and S. Sarkar, "Extremely high energy cosmic rays from relic particle decays," Astropart. Phys. **9** (1998) 297 [arXiv:hep-ph/9804285];
S. Sarkar and R. Toldra, "The high energy cosmic ray spectrum from massive particle decay," Nucl. Phys. B **621**, 495 (2002) [arXiv:hep-ph/0108098].

[108] A. Klemm, B. Lian, S. S. Roan and S. T. Yau, "Calabi-Yau fourfolds for M- and F-theory compactifications," Nucl. Phys. B **518** (1998) 515 [arXiv:hep-th/9701023].

[109] P. Candelas, A. Font, S. H. Katz and D. R. Morrison, "Mirror symmetry for two parameter models. 2," Nucl. Phys. B **429** (1994) 626 [arXiv:hep-th/9403187];
A. C. Avram, M. Kreuzer, M. Mandelberg and H. Skarke, "Searching for K3 fibrations," Nucl. Phys. B **494** (1997) 567 [arXiv:hep-th/9610154];
F. Denef, M. R. Douglas and B. Florea, "Building a better racetrack," JHEP **0406** (2004) 034 [arXiv:hep-th/0404257].

[110] M. Y. Khlopov and A. D. Linde, "Is It Easy To Save The Gravitino?," Phys. Lett. B **138** (1984) 265;
I. V. Falomkin, G. B. Pontecorvo, M. G. Sapozhnikov, M. Y. Khlopov, F. Balestra and G. Piragino, "Low-Energy Anti-P He-4 Annihilation And Problems Of The Modern Cosmology, GUT And Susy Models," Nuovo Cim. A **79** (1984) 193 [Yad. Fiz. **39** (1984) 990];
M. Y. Khlopov, Yu. L. Levitan, E. V. Sedelnikov and I. M. Sobol, "Nonequilibrium cosmological nucleosynthesis of light elements: Calculations by the Monte Carlo method," Phys. Atom. Nucl. **57** (1994) 1393 [Yad. Fiz. **57** (1994) 1466];
R. H. Cyburt, J. R. Ellis, B. D. Fields and K. A. Olive, "Updated nucleosynthesis constraints on unstable relic particles," Phys. Rev. D **67** (2003) 103521 [arXiv:astro-ph/0211258].

[111] M. Kawasaki, K. Kohri and T. Moroi, "Big-bang nucleosynthesis and hadronic decay of long-lived massive particles," Phys. Rev. D **71** (2005) 083502 [arXiv:astro-ph/0408426].

[112] H. Davoudiasl, J. L. Hewett and T. G. Rizzo, "Phenomenology of the Randall-Sundrum gauge hierarchy model," Phys. Rev. Lett. **84** (2000) 2080 [arXiv:hep-ph/9909255].

[113] D. J. H. Chung, L. L. Everett and H. Davoudiasl, "Experimental probes of the Randall-Sundrum infinite extra dimension," Phys. Rev. D **64** (2001) 065002 [arXiv:hep-ph/0010103].

[114] I. S. Gradshteyn, I. M. Ryzhik and A. Jeffrey (ed.), "Table of Integrals, Series, and Products" (Fifth edition) *San Diego, USA: Academic Press (1994) 1204 p.*

[115] M. Abramowitz and I. A. Stegun (eds.), "Handbook of Mathematical Functions" *New York USA: Dover Publ. (1965) 1064 p. (National Bureau of Standards Applied Mathematics Series - 55).*